PHENOMENOLOGICAL IMPLICATIONS OF CALCULATIONS IN NONPERTURBATIVE QCD

by

Sergiu Sanielevici

A thesis submitted to the Faculty of Graduate Studies and Research
in partial fulfillment of the requirements for the
Ph. D. degree.

Department of Physics
McGill University
Montreal, Quebec
Canada.

September 1985

PHENOMENOLOGICAL IMPLICATIONS OF CALCULATIONS IN NONPERTURBATIVE QCD

ABSTRACT

We interpret a body of results in nonperturbative Quantum Chromodynamics (QCD) as an indication that hadron structure is governed by two effective, dynamically generated mass scales: the chiral-symmetry breaking (χSB) scale Λ_χ and the confinement scale Λ_c. These scales must satisfy the inequality $\Lambda_c \ll \Lambda_\chi$. We propose that χSB determines the universal distribution of partons in constituent quarks. To test this hypothesis, we use an analytic description of χSB in the framework of a successful phenomenological model based on the two-scale idea. This gives a good approximation to hadronic charge form factors and to the pion decay constant. We then generalize the model in order to analyze elastic hadron-hadron scattering at high energies. Our two-scale picture is shown to offer a natural explanation of the behavior of scattering observables. In order to discriminate between two basic alternatives for the confinement mechanism, we propose an interquark potential which incorporates the requirements of the two-scale picture. This model of confinement gives rise to color Van der Waals forces which should be detectable in forthcoming high-precision search experiments. Nondetection of such forces would thus suggest that potential-models cannot adequately describe confinement, whereas a positive result would rule out "rigid" confinement.

RESUME

Nous interprétons de nombreux résultats en Chromodynamique Quantique (QCD) nonperturbative comme une indication que la structure des hadrons est régie par deux échelles énergétiques générées dynamiquement: l'échelle Λ_{χ} de la brisure de la symetrie chirale (BSχ) et l'échelle du confinement, Λ_c. Ces échelles doivent satisfaire à l'inégalité $\Lambda_c \leqslant \Lambda_{\chi}$. Nous suggérons que c'est la BSχ qui détermine la distribution universelle des partons dans les quarks constituants. Pour vérifier cette hypothèse, nous intégrons une description analytique de la BSχ dans un modèle phénoménologique basé sur l'idée des deux échelles. Ceci donne une bonne approximation aux facteurs de forme de charge des hadrons ainsi qu'à la constante de désintegration du pion. Ensuite, nous généralisons le modèle afin d'analyser les collisions élastiques hadron-hadron à haute énergie. Nous sommes conduits à une explication naturelle du comportement des observables de ces collisions. Dans le but de discriminer entre deux alternatives fondamentales pour le mécanisme du confinement, nous formulons un potentiel entre quarks qui tient compte de la structure à deux échelles. Ce potentiel implique l'existence des forces colorées de Van der Waals qui devraient être détectables dans les prochaines expériences de haute précision. Ainsi, un résultat négatif de ces expériences suggérerait que le concept même d'un potentiel entre quarks est inadéquat pour décrire le confinement. Par contre, un resultat positif éliminerait le confinement "rigide".

ACKNOWLEDGEMENTS

I wish to thank my thesis supervisor, Professor Roland Henzi, for encouraging me to work independently and for his firm but discreet guidance. This work is the result of a most pleasant collaboration with Prof. Henzi and with Dr. Pierre Valin. It would not have been possible without their constant willingness to discuss and to share new ideas. At various stages of this research, I have greatly benefitted from discussions or correspondence with P. Hasenfratz, R.C. Hwa, C.S. Lam, B. Margolis, M. Peskin and N. De Takacsy.

STATEMENT OF ORIGINALITY

This thesis is an original attempt to correlate concepts and results in nonperturbative QCD with phenomenological information about hadron structure. Chapter 2 is a review of the literature on nonperturbative QCD, written from the original point of view of our attempt. There we collect all the concepts and results which we apply to phenomenological problems in the subsequent chapters. Chapters 3 and 4 are based upon our paper [94]. They are rendered more pedagogical by a more extensive review of related work by other authors than was possible in the original article. Chapter 5 is based on our papers [108,109] and contains a more complete summary of the impact-parameter formalism, based on Valin's exposition [119]. Chapter 6 is based on our paper [140]. An earlier version of a unified presentation of our work can be found in the conference talk [137].

Any views and interpretations or other statements not literally contained in the original papers quoted above are the exclusive responsibility of the present author and do not necessarily express the views of his co-authors in those papers.

TABLE OF CONTENTS

CHAPTER 1: INTRODUCTION

1.1. EFFECTIVE THEORIES AND NONPERTURBATIVE METHODS

Research efforts in contemporary theoretical high energy physics are mainly concentrated in two areas:

A. Extending the Standard Model;

B. Nonperturbative QCD.

The so-called "Standard Model" of strong, weak and electromagnetic interactions provides an adequate description of elementary particles with masses up to roughly that of the W boson [1]. At such energy scales ($M_W \cong 80$ GeV) the gauge group of the model factors into a direct product of gauge subgroups, $SU(3)_c \times (SU(2) \times U(1))_{EW}$, which means that strong and electroweak interaction dynamics are independent. For aesthetic as well as practical reasons one believes, however, that the standard model must derive from a more fundamental, unified theory valid at higher energies [2]. At energy scales of the order of the Planck mass ($M_{Pl} \cong 10^{19}$ GeV) this unification should include gravitation as well.

Problem A consists in finding this fundamental super-high energy theory and in calculating phenomena at lower energies from it. By analogy with known statistical and field-theoretic models, one expects that the system specified by the fundamental Lagrangian written in terms of fields defined at superhigh energies will undergo various phase transitions as the energy decreases. These transitions would be driven by the dynamical breakdown of various symmetries of the original Lagrangian. Each phase would be characterized by a specific set of degrees of freedom, in general composites of the elementary fields in the fundamental Lagrangian. Phenomenology in each phase would thus be calculable from an "effective theory" written in terms of the degrees of freedom active in that phase. In particular, the standard model must be shown to be an effective theory describing physics at energies of the order M_W. The precise nature of the fundamental theory and the exact pattern by which it evolves to low energies will determine phenomenology between M_{Pl} and M_W.

The difficulties involved in solving this problem are daunting. At the present time there is a profusion of candidate extensions of the standard model, such as various grand unified theories, composite models, supersymmetries and supergravities. They propose fundamental Lagrangians and symmetries defined at totally inaccessible energy scales. They result in diverse phenomenological predictions for the world beyond M_W none of which is amenable to experimental verification at the present time (some of the predictions should, however, be verifiable at the next generation of colliders). From the theoretical viewpoint, the main problem is that there are as yet no rigorous, systematic methods for constructing effective theories from a given fundamental quantum field theory. The only reliable method for calculating quantum field theories is the perturbation expansion which depends upon the existence of a small parameter (such as the interaction strength) in which the observables of the theory are analytic. This is a very special situation which is not expected to hold true for all energies in any of the proposed extensions of the Standard Model. In general, transitions from one phase of a system to the next involve the breakdown of the perturbation expansion which may have been valid in the original phase. Even if perturbative techniques are applicable at the fundamental super-high energy level, they cannot describe the chain of symmetry-breakings which leads to lower-energy phenomenology. Constructing effective theories thus requires systematic, efficient and powerful nonperturbative methods of calculation.

1.2. QCD AS A THEORETICAL LABORATORY

Now consider Problem B. Quantum Chromodynamics (QCD) is believed to be the fundamental theory of the strong interactions. Its elementary fields are fermionic "quarks" coupled to the gauge fields ("gluons") of the nonabelian gauge group $SU(3)_c$ (the first factor of the Standard Model gauge group) by means of a charge called "color". The validity of QCD as the fundamental theory can be tested in high momentum-transfer scattering processes involving hadrons. This is because the interaction strength decreases as the colored particles approach each other, so that perturbation theory becomes applicable in the high momentum-transfer limit. Hard hadronic processes can therefore be systematically calculated from the QCD Lagrangian and the results reproduce experimental data encouragingly well.

However, by the same token, the coupling strength must become large at low momentum transfer, so that the perturbation expansion cannot be used to calculate the bulk of hadronic phenomenology ("soft" scattering processes and static properties) from the QCD Lagrangian. Most conspicuously, the "confinement" of color fields (the fact that observed hadrons do not carry color) cannot be proved by perturbative methods. The problem thus consists in devising nonperturbative schemes to accomplish this task.

Of course, Problem B is far easier to solve than Problem A. Indeed, in the case of QCD we have experimental control over all scales of the theory. Both the high-energy and low-energy limits are well known; all experimental information relevant to intermediate scales either exists or can be "readily" obtained in today's or tomorrow's labs. This information can eliminate ideas, models and calculation methods which fail to reproduce the totality of hadronic phenomenology. In this way, the final theory will be extremely reliable.

From the theoretical side, the confidence we have in the validity of the basic QCD Lagrangian pinpoints the symmetry which characterizes the phases of the system of interacting quarks and gluons. It is "chiral symmetry", a global symmetry of the QCD Lagrangian written for massless quarks. Chiral symmetry is very nearly exact at large momentum-transfer (the quark masses in the fundamental Lagrangian are determined by electroweak dynamics and are thus irrelevant for color dynamics) but it must be broken in the static limit in order to account for well-established phenomenology. The breaking of chiral symmetry does not interfere with the local gauge invariance under $SU(3)_c$, which remains unbroken. By contrast, most extensions of the Standard Model involve several local and global symmetries whose breakings intertwine.

Consequently, the fundamental historic significance of QCD lies in its being a theoretical laboratory destined to produce the first rigorous, nonperturbative derivation of effective theories from a given fundamental Lagrangian. With the successful theory of hadron physics as a prototype, one will be in a much better position to extract the phenomenological, accessible-energy consequences of a given candidate Planck-energy theory.

1.3. PURPOSE OF THIS WORK

The above arguments show how essential it is to be able to confront calculations in nonperturbative QCD with experimental data. It is necessary to extract the phenomenological implications of all results obtained in nonperturbative QCD and to see whether or not they yield sensible descriptions of hadronic properties.

Over the past few years, a substantial body of results has been obtained by various nonperturbative techniques. Many of these results ~~are~~ consistent with each other and have thus acquired a measure of reliability. Some calculations yield directly measurable quantities, such as hadron masses, decay widths and magnetic moments. However, many of the more elaborate calculations regarding, in particular, the mechanisms of confinement and chiral-symmetry breaking, are not as straightforward to interpret.

In this work we propose to fill this gap. Our main idea is that the dynamical mechanism of chiral-symmetry breaking determines the internal structure of hadrons in terms of color fields, as explorable by means of lepton-hadron and hadron-hadron scattering. We shall argue that existing results on this nonperturbative mechanism suggest a certain picture of hadron structure which seems to explain experimental data quite nicely. This picture also enables us to propose an experimental test of the essential features of the confinement mechanism.

Chapter 2 presents the problems, methods and results of nonperturbative QCD in more detail. It defines the specific questions we set out to answer. Chapter 3 contains the arguments leading to our model of hadron structure as well as a detailed description of the proposed picture. Its confrontation with elastic lepton-hadron scattering data takes place in Chapter 4 whereas Chapter 5 presents the confrontation with high-energy hadron-hadron scattering data. In Chapter 6 we use our picture to set up a new model of the large-distance interquark potential and show how it can shed light on the confinement mechanism. The final chapter offers our conclusions and some opinions on future progress in this field.

CHAPTER 2: HADRON PHYSICS AND QCD

2.1. FACTS AND MODELS

a) Quarks and partons.

The constituent quark model was originally motivated by a successful classification scheme for the hadrons which were known in the early sixties. Independently, Gell-Mann and Ne'eman [3] recognized that the eight spin-1/2 baryons of the proton family could be considered as members of an octet representation of the global symmetry group SU(3). Two other octet representations of the same group were used to accomodate the low-lying pseudoscalar and vector mesons. However, SU(3) also possesses a complex triplet representation, the so-called fundamental representation, out of which all higher-dimensional representations can be built. This suggested that all hadrons are combinations of three basic building blocks which were dubbed "quarks" [4]. Hadrons were assumed to be built out of constituent quarks just as nuclei are built out of protons and neutrons. Each of the three quarks had to be given a name, corresponding to a value of the quantum number we now call "flavor": Up (U), Down (D) and Strange (S). They had to be assigned fractional charges (2e/3 for the U and -e/3 for the D and S, e being the charge of the proton) and baryon numbers (1/3 each) as well as spin 1/2. Thus the proton is built out of two U's and one D and the neutron out of one U and two D's. Being Dirac fermions, the quarks must have antiparticles associated with them: the $\bar{U}$, $\bar{D}$, $\bar{S}$ antiquarks which form a SU(3) triplet of their own. The octet mesons are combinations of quarks and antiquarks: for instance, the π^+ is a $U\bar{D}$ state.

Along these lines, all the known meson and baryon resonances could be classified according to the constituent quark model. Hadron masses, decay widths and electromagnetic properties were generally well reproduced. Conclusions regarding the masses of the constituent quarks could be drawn: thus, the masses of the U and D were found to be approximately 350 MeV [5]. As new particles were discovered, the model was able to incorporate them either as higher angular momentum excitations of known quark combinations or by increasing the number of quark flavors. We now have reason to believe there are six quark flavors, with the three new constituent quarks being called C (Charm), B (Bottom or Beauty) and T (Top or Truth) [6].

However, it soon became clear that the binding of constituent quarks into hadrons is in no way analogous to the binding of nucleons into nuclei: so far, it has not been possible to liberate fractionally charged particles even in the highest-energy collisions specifically designed to break up hadrons. For some dynamical reason, constituent quarks seem to be "permanently confined" in their host hadrons. On the other hand, high energy lepton-hadron inelastic scattering does lend support to the hypothesis of hadronic substructure, albeit in a rather unexpected way. As seen by a high-energy virtual photon, a proton appears to contain not only three "valence" quarks whose flavors coincide with those of the constituent quarks, but also an infinite "ocean" of quark-antiquark pairs of various flavors (the higher the photon energy, the more flavors are active in the ocean). These constituents are collectively known as "partons" [7]. Most strikingly, partons are pointlike, relativistic particles which interact with the very-high-energy photon as if they were free and independent of each other.

b) QCD.

To make a theory out of the model, one must describe these apparently contradictory extremes in terms of interactions between partons. It was another serious flaw in the naive model which indicated what we now hope to be the correct path towards the solution of this problem. The spin-3/2 resonance called Δ^{++} is made from three U quarks with parallel spins. The quark model wants them to be in a relative orbital symmetric S-state whereas Fermi statistics requires the orbital wavefunction to be antisymmetric. To resolve this paradox one introduces a new quantum number called "color" in which the wavefunction can be antisymmetrized so that it is symmetric in orbital angular momentum. There is evidence that each quark flavor must come in three colors (call them red, yellow and blue): this hypothesis allows one to explain the results of measurements of the ratio $R=\sigma(e^+e^- \rightarrow \text{hadrons})/\sigma(e^+e^- \rightarrow \mu^+\mu^-)$ [8] and of the π^0 decay rate [9]. Since observed hadrons do not carry color, confinement must be a consequence of the interactions between colored quarks. These must result in the formation of colorless bound states of colored constituents.

Once we accept the need for colored quarks we must make the forces which bind them color-dependent. The color-exchange quanta are called "gluons". The simplest way to explain why a quark and antiquark are strongly bound into a meson while two quarks are not is to attribute spin 1 to the gluon field. Indeed, fields with even spin couple in the same way to particles and antiparticles; spin one is the simplest odd-spin possibility and the only one which yields a renormalizable theory.

But this reminds us of a familiar situation: quantum electrodynamics (QED) describes the exchange of spin-1 photons between spin-1/2 electrically charged leptons. The way in which the photon couples to charged leptons is uniquely determined by the requirement that the QED Lagrangian be invariant under local U(1) gauge transformations [Appendix B]. The photon is called the "gauge boson" of electromagnetism.

QED is the best verified physical theory we know. The generalization of the gauge principle from local $U(1)_{em}$ to the gauge group $[SU(2)_L \times U(1)]_{ew}$ of the electroweak interaction has produced two Nobel prizes- one for the theoretical prediction of the existence and properties of the gauge bosons W and Z and one for the experimental confirmation of these predictions [1]. This suggests that we should build the fundamental theory of the strong interactions using the same mould: couple the three colors of quarks to the eight gauge bosons (identified with the gluons) of the local gauge group $SU(3)_C$ (three colors!) just as electrons are coupled to photons. As outlined in Appendix B, this requirement defines the Lagrangian of Quantum Chromodynamics (QCD), which is postulated to be the fundamental dynamical theory in terms of which all strong interaction physics must be explainable.

Let us rewrite the chromodynamic Lagrangian density(see App.B) as

$$L_{CD} = -\frac{1}{4}\vec{F}_{\mu\nu}\cdot\vec{F}^{\mu\nu} - g\bar{\Psi}\gamma^{\mu}(\vec{T}\cdot\vec{A}_{\mu})\Psi + \bar{\Psi}(i\not{\partial} - m)\Psi \qquad (2\text{-}1)$$

This implies that the gluon field satisfies Maxwell-like equations of motion

$$\partial_{\mu}\vec{F}^{\mu\nu} = -2g\bar{\Psi}\gamma^{\nu}\vec{T}\Psi + 2g\vec{A}_{\mu}\times\vec{F}^{\mu\nu} = \vec{J}^{\nu} \qquad (2\text{-}2)$$

while the quarks and antiquarks obey Dirac equations with the ordinary derivative replaced by the covariant derivative. It is easy to check that the fermionic and gauge field contributions to the current density $\vec{J}^{\nu}$ are not conserved separately due to the non-abelian character of the gauge group, but that the anomalies cancel to ensure that the total current density is divergenceless. Therefore, the gluon selfcoupling embodied in the term $g\vec{A}_{\mu}x\vec{F}^{\mu\nu}$ is essential for the theory to make sense. At the quantum level, three-and four-gluon couplings ensure the unitarity of the theory [10].

As a consequence of the nonlinearity of the gluon field equations, any color source will be surrounded by a cloud of self-interacting gluons which amplifies the effect of the source. The gluon cloud which surrounds a red quark will on the average also be red. Therefore, a colored test particle that penetrates the cloud will sense a smaller interaction if it comes close to the bare quark at the center of the cloud than if it passes at large impact parameter. This "antiscreening" effect due to gluon selfinteraction competes with the usual screening effect of fermionic vacuum polarization which is familiar from QED. As long as there are less than 17 quark flavors, antiscreening is more important and the effective color charge increases with the distance from the bare source.

The weakening of the QCD coupling at small distances is called "asymptotic freedom" and it explains the success of the parton model. Photons which come in with high energy probe the hadron at small distances at which the interactions between colored particles are faint. This suggests that one may identify Feynman's partons with the fundamental fields in the QCD Lagrangian: "current" quarks and antiquarks along with electrically neutral gluons. In fact, the need for neutral partons was obvious ever since the first attempts to interpret quarks as partons [11], since the fraction of proton momentum carried by charged fermions was uncomfortably small even when the ocean quarks and antiquarks were taken into account. Today we know that glue-partons carry about half the proton's momentum [12].

"Infrared slavery" is the counterpart of (ultraviolet) asymptotic freedom: colored particles interact more strongly as they are pulled apart so the large-distance structure of a hadron should be described in terms of collective motions of partons. On the other hand, it seems intuitively clear that this same qualitative behavior ought to explain confinement. However, it is by no means clear how constituent quarks are related to the partons which appear directly in the QCD Lagrangian. In order to relate infrared slavery to the confinement of constituent quarks, one must thus show explicitly how color field dynamics generates the constituent quark model as an "effective theory", in the language of Chapter 1.

c) Chiral symmetry.

Consider the relationship between the gauge theories of the strong and the electroweak interactions. The Standard Model [1] postulates that the gauge groups of these interactions are orthogonal. This hypothesis allows one to describe the strong and electroweak properties of hadrons in a way which naturally conserves parity and strangeness to order G_F (G_F is the coupling constant of the effective low-energy Fermi theory of the weak interaction) [13].

The color quantum number of quarks thus plays no role in their electroweak interactions, just as flavor is not active in chromodynamics. It is, however, important to recognize the indirect effect of Quantum Flavordynamics (QFD, the gauge theory of $[SU(2)_L \times U(1)]_{ew}$) on the QCD Lagrangian. This stems from the fact that the gauge group SU(2) must be spontaneously broken: whereas the Lagrangian of QCD+QFD is invariant under the direct product of gauge groups $SU(3)_c \times [SU(2)_L \times U(1)]_{ew}$, the vacuum state of the theory (the observed physical world) can be invariant only under $SU(3)_c \times U(1)_{em}$. If $SU(2)_L$ were not spontaneously broken, just as in a ferromagnetic system the symmetry under rotations is lost in the spontaneously magnetized ground state, the W and Z gauge bosons would have to be massless instead of acquiring their celebrated masses. Indeed, unbroken local gauge symmetries have massless gauge bosons, like the QCD gluons and the QED photon. Physically, a W moving through the asymmetric vacuum of QFD experiences "friction" and its velocity must be v<c.

In the Glashow-Salam-Weinberg theory [1] the leptons and quarks acquire their masses by the same token as the W and Z. Since $SU(2)_L$ only affects left-handed fermions, fermion mass terms which produce left-right transitions are forbidden unless $SU(2)_L$ is spontaneously broken.

It is an empirical fact that quarks and leptons come in various "generations": sets of two leptons and two quark flavors. To date, we have evidence of three distinct generations: (e,ν,u,d), (μ,ν_μ,s,c) and (τ,ν_τ,b,t) (we denote the quark flavors with lower-case letters to indicate that these are the current quarks in the QCD Lagrangian rather than the constituent quarks). The Standard Model does not explain spontaneous gauge-symmetry breaking dynamically and is therefore not able to account for the origin of generations, nor for the observed mass differences between the leptons within one generation. This is one of the main motivations for wanting to go beyond the Standard Model [2].

As far as QCD is concerned, however, orthogonality to QFD means that these questions are irrelevant. The only important point is that the current quark masses in the QCD Lagrangian are to be considered of extraneous origin and will only play a passive role in color dynamics. The essential features of chromodynamics can thus be studied, without any loss of generality, by neglecting the mass terms in the Lagrangian (2.1).

Like any gauge theory with massless fermions, massless QCD enjoys a set of global symmetries known as "chiral symmetry". On a formal level, the absence of mass terms which would mix left-handed and right-handed quarks means that the fermion numbers of q_R and q_L are separately conserved. For N_f flavors, the chiral symmetry of QCD should be $U(N_f)xU(N_f)$. As a consequence, Noether's theorem demands the conservation of the N_f^2 vector currents v_μ^i and of the N_f^2 axial-vector currents a_μ^i which can be formed as bilinear combinations of current quark fields. At the quantum level, however, an analysis of the Ward identities satisfied by these currents reveals that the flavor-singlet axial current has an anomaly and fails to be conserved (see Section 2.4c). The true chiral symmetry of the massless quark-gluon Lagrangian for N_f flavors (apart from baryon number conservation) is $SU(N_f)xSU(N_f)$. There are N_f^2 conserved vector charges

$$Q_V^i = \int d^3x \, v_0^i(x) \qquad ; \quad [Q_V^i, H_{QCD}] = 0 \qquad (2.3)$$

and $N_f^2 - 1$ conserved axial-vector charges

$$z_a^i = \int d^3x\, a_0^i(x) \quad ; \qquad [z_a^i, H_{QCD}] = 0 \qquad (2.4)$$

These are symmetries of the current quarks in the QCD Lagrangian. Assume they are also obeyed by the constituent quarks of the same flavors. Then we can construct conserved charges Z_V^i , Z_a^i with the same properties as z_V^i , z_a^i . This would have the following consequences for the hadron spectrum: since $[Z_V^i, H_{QCD}] = 0$, the state $Z_V^i |\chi\rangle$ would have the same energy as the state $|\chi\rangle$. For $N_f = 2$ this is a very good approximation (isospin symmetry of the strong interactions!) and for $N_f = 3$ it reproduces the original global SU(3) of Gell-Mann and Ne'eman. For the three heavy flavors ($N_f = 4,5,6$) the electroweak masses in the QCD Lagrangian are so large that it does not make sense to compare the predictions of chiral symmetry with hadron spectroscopy.

However, if the axial constituent charges were also conserved, then $Z_a^i |\chi\rangle$ should also be degenerate with $|\chi\rangle$. Since the axial charges carry negative parity, there should be a opposite-parity hadron mass-degenerate with any given "ordinary" hadron! Evidently, there is no trace of this symmetry in the spectrum of baryons and mesons. The current quarks in the QCD Lagrangian enjoy $SU(N_f)_L \times SU(N_f)_R$ chiral symmetry but constituent quarks only have the $SU(N_f')_{L+R}$ which classifies hadrons into multiplets ($N_f' = 2$ or 3). QCD must spontaneously break chiral symmetry as it gives rise to the long-distance physics described by constituent quark models. Since the vacuum of QCD is not symmetric under Z_a^i , we must have

$$Z_a^i |0\rangle \neq 0 \qquad (2.5)$$

This implies there exist $N_f^2 - 1$ states with the quantum numbers of $Z_a^i |0\rangle$: no energy, no momentum, no angular momentum and negative parity. These massless spin-0 bosons are called "Goldstone bosons" [14]. For $N_f' = 2$, the pion triplet is the natural candidate for the Goldstone bosons of chiral-symmetry breaking. By postulating this identification, one implies that the finiteness of the pion masses is due to the electroweak masses of the u,d current quarks. For $N_f' = 3$, one identifies the pseudoscalar octet (π, K, η) as Goldstone bosons and attributes their finite and unequal masses to the existence of the finite and unequal QFD masses of valence current quarks.

The study of the consequences of chiral-symmetry breaking was a classic subject in particle physics long before the emergence of QCD (one realized chiral symmetry had to be broken at low energy scales before one knew that it was unbroken in the high-energy limit). Effective Lagrangians based on the breaking of chiral symmetry and on the existence of Goldstone bosons have led to an extremely successful phenomenological theory of the interactions of soft pions with hadrons [15,16] and such methods are still among the most important analytic nonperturbative tools in the study of dynamical symmetry-breaking [17,18].

d) Summary.

To sum up the situation emerging from our review, the facts of hadron physics are well described by relatively simple models in two opposite limits. Static hadron spectroscopy and the low-energy interactions of hadrons are well described by models based on the existence of constituent quarks and on the breaking of chiral symmetry.

Constituent quark models fall into two main categories: potential models [5,19], in which hadron radii have probabilistic, quantum-mechanical interpretations, and bag models [20] in which confinement is explicitly imposed by means of a cutoff on possible hadron radii. At any rate, the lightest flavors of constituent quarks must have masses of around 350 MeV. The unification of constituent quark models with models based on chiral-symmetry breaking (sigma-models [16,17], Skyrmion models [18]) is an open problem: how is the Goldstone character of the pion to be reconciled with its status as an ordinary hadron, a bound state of a constituent quark and antiquark? Attempts to solve this problem are taking place within the bag model (cloudy-bag models [21], chiral bag models [22]), in constituent quark models without explicit confinement [23] and in the Skyrmion framework [24]. In all these investigations, the crucial issue is the evolution of hadron structure as one increases the resolution away from the static limit.

In the extreme of very high resolution of hadron structure, as achieved in deep inelastic lepton-hadron scattering and other hard scattering processes, the model which reproduces experimental data is the parton model interpreted in the framework of perturbative QCD. The partons are the current quarks and the gluons of the QCD Lagrangian: they are asymptotically free and interact according to the QCD Feynman rules. Gluons are exactly massless because they are the gauge fields of unbroken $SU(3)_c$; the masses of current quarks are determined by their electroweak properties. For the lightest flavors, the current quark masses are of the order of a few MeV. Chiral symmetry is an intrinsic property of the purely chromodynamic sector of the theory. Partons are field-theoretical quanta: they can be grouped into "valence quarks" which have the flavor of the constituent quarks defining the host hadron, "ocean" quark-antiquark pairs and gluons. Again, the main open theoretical and phenomenological questions have to do with the extrapolation of the model and of QCD to lower resolutions, at which perturbative calculations are beset by large higher-order corrections and eventually become inadequate.

We conclude that the fundamental problem in hadron physics is to describe the transition from the parton regime to the constituent quark regime by means of QCD. In the remainder of this chapter we shall introduce several perturbative and nonperturbative approaches to this problem, discuss their results and formulate the questions which we attempt to answer in this thesis.

2.2. PERTURBATIVE QCD

a) Soft singularities.

Covariant perturbation theory takes the quantum Lagrangian of a relativistic field theory and derives the corresponding Feynman rules. The simplest calculation with direct physical significance one can do based on the Feynman rules for QCD is to compute the cross-section for the process $e^+e^- \rightarrow$ hadrons. Let E^2 be the c.m. energy squared of the e^+e^- annihilation: it is equal to Q^2, the time-like four-momentum transfer squared imparted to its target by the created virtual photon (see Fig. 2.1). For $Q^2 \rightarrow \infty$ the photon will annihilate into a current quark-antiquark pair. Fig. 2.1 shows the diagrams required to calculate $e^+e^- \rightarrow \bar{q}q$ to first order in the "strong fine-structure constant" $\alpha_s = g^2/4\pi$. Setting all quark masses to zero and keeping the quark momenta squared $p^2 = p'^2 \neq 0$ one finds the following result for the cross-section of this process [25]:

$$\sigma_{q\bar{q}} = \sigma_0 \left\{ 1 + \frac{4\alpha_s}{3\pi} \left[-\frac{1}{2} \ln^2\left(\frac{Q^2}{p^2}\right) + \frac{3}{2} \ln\left(\frac{Q^2}{p^2}\right) - \frac{7}{4} + \frac{\pi^2}{6} \right] \right\} \qquad (2.6)$$

where $\sigma_0 = 4\pi\alpha_s^2 \sum_f e_f^2 / E^2$ is the Born (tree) approximation result corresponding to the first graph in Fig. 2.1. We see that $\sigma_{q\bar{q}}$ given by Eq. (2.6) diverges in the infrared limit p--> 0. If this divergence cannot be removed, QCD corrections to the free parton model result are infinite and perturbative QCD can never be used.

We recognize, however, that $e^+e^- \to q\bar{q}$ is but one of several possible parton subprocesses contributing to $e^+e^- \to$ hadrons. By analogy with the infrared problem in quantum elecrodynamics, we expect that a quark alone can never be distinguished from a quark radiating any number of soft or collinear gluons. Therefore the contribution of the diagrams in Fig. 2.2 should be added to Eq. (2.6). This contribution is [25]

$$\sigma_{q\bar{q}g} = \frac{4\alpha_s}{3\pi} \sigma_0 \left\{ \frac{1}{2} \ln^2\left(\frac{Q^2}{p^2}\right) - \frac{3}{2} \ln\left(\frac{Q^2}{p^2}\right) - \frac{\pi^2}{6} + \frac{10}{4} \right\} \qquad (2.7)$$

so that the total, observable cross-section to order α_s is free of infrared "mass singularities":

$$\sigma_{tot} = \sigma_0 \left(1 + \frac{\alpha_s}{\pi} \right) \qquad (2.8)$$

This miraculous cancellation of soft singularities has been shown to persist to all orders in perturbation theory, for cross-sections summed over all possible final states involving quarks and gluons. ("Kinoshita-Lee-Nauenberg theorem").

b) Renormalization.

Second-order diagrams in α_s such as the ones depicted in Fig. 2.3

give rise, however, to ultraviolet ($p \longrightarrow \infty$) divergences. Just as in QED, these must be removed by renormalization: they will be absorbed into redefinitions of the coupling constant, the quark masses and the scale of the fields. QCD, like all gauge theories, is "renormalizable" in the sense that once this has been done no new divergences arise in higher orders and all quantities are finite and calculable. There are many ways to actually carry out renormalization: the choice of renormalization scheme is not allowed to have observable consequences but one choice or the other may be more convenient for a given problem. The point we need to make here is that any renormalization scheme in QCD introduces a new parameter with dimensions of mass into the theory.

Consider, for instance, the "minimal subtraction" (MS) scheme [26] as applied to the quark self-energy graph of Fig. 2.4 in the Feynman- 't Hooft gauge (corresponding to a particular choice of the gauge-fixing term in the QCD Lagrangian). The quark momentum integral in the corresponding Green's function is UV-divergent in four dimensions but it would be finite in n<4 dimensions (n integer). The unrenormalized Green's function in n dimensions is

$$G_n^u(p) = \not{p} + K \frac{g_n^2}{(2\pi)^n} \int d^n k \, \frac{\gamma_\nu (\not{k} + \not{p}) \gamma^\nu}{k^2 (k+p)^2} \qquad (2.9)$$

where K contains group-theoretical factors. In four dimensions, the renormalizability of QCD is expressed by the fact that g is dimensionless. To keep the coupling dimensionless in n<4 dimensions we must define

$$g_n^2 = g^2 \Lambda^{4-n} \qquad (2.10)$$

where the "renormalization scale" Λ has dimensions of mass. Performing the integration we find

$$G_n^u(p) = \not{p} + ic\not{p}\,\frac{g_\mu^2}{(4\pi)^{n/2}}\,\frac{\Gamma(\epsilon/2)}{(-p^2)^{\epsilon/2}}(\epsilon-2)B(2-\tfrac{\epsilon}{2},1-\tfrac{\epsilon}{2}) \qquad (2.11)$$

where ϵ=4-n and B denotes Euler's Beta-function. This can be analytically continued from integer to complex ϵ and in the limit ϵ-->0 we have

$$G_n^u(p) = \not{p}\left\{1 - ic\frac{\alpha_s}{4\pi}\left[\frac{2}{\epsilon} + 1 + \ln(4\pi) - \gamma_E - \ln\left(-\frac{p^2}{\Lambda^2}\right)\right]\right\} \quad (2.12)$$

where γ_E is Euler's constant. Now a counter-term may be added to cancel the pole in Eq. (2.12) but the renormalized Green's function will explicitly depend upon the renormalization scale Λ.

Having thus removed all the singularities, one finds σ_{tot} to second order in α_s:

$$\sigma_{tot} = \sigma_0\left[1 + \frac{\alpha_s}{\pi} - b_0\frac{\alpha_s^2}{4\pi^2}\ln\left(\frac{Q^2}{\Lambda^2}\right)\right] + O\left(\alpha_s^2, \alpha_s^3 \ln^2\left(\frac{Q^2}{\Lambda^2}\right)\right) \qquad (2.13)$$

where

$$b_0 = 11 - \frac{2}{3}n \qquad (2.14)$$

n is the number of quark flavors which contribute to the vacuum polarization subgraph (third diagram in Fig. 2.3). n is a function of the gluon energy and is bounded above by N_f.

We now see a new problem for perturbative QCD: Λ^2 appears in new log terms which become large as Q^2 grows so that the corrections overwhelm the lower-order terms. It turns out, however, that the leading logs in Eq. (2.13) can be resummed so that σ_{tot} can be cast into the familiar form

$$\sigma_{tot} = \sigma_0 \left[1 + \frac{\bar{\alpha}_s(Q^2/\Lambda^2)}{\pi} \right] + O\left(\alpha_s^2, \alpha_s^3 \ln(Q^2/\Lambda^2)\right) \qquad (2.15)$$

("leading-log approximation" (LLA)). The effective, Q^2-dependent "running" coupling $\bar{\alpha}_s$ has the form

$$\bar{\alpha}_s(Q^2/\Lambda^2) = \frac{\alpha_s}{1 + b_0 \frac{\alpha_s}{4\pi} \ln(Q^2/\Lambda^2)} \qquad (2.16)$$

to second order in perturbation theory. This expresses the asymptotic freedom of QCD: the effective coupling decreases as Q^2 increases and partons become free as $Q^2 \to \infty$.

The resummation of leading and also of nonleading logs can be done in a systematic way by using the "renormalization group" (RG) [27]. The observable cross-section cannot depend on the value of the renormalization scale Λ:

$$\Lambda \frac{d}{d\Lambda} \sigma_{tot} = 0 \qquad (2.17)$$

or

$$\left\{ \Lambda \frac{\partial}{\partial \Lambda} + \beta(g) \frac{\partial}{\partial g} \right\} \sigma_{tot}(g, \Lambda) = 0 \qquad (2.18)$$

(strictly speaking, σ_{tot} also depends on the gauge-fixing parameter ξ defining the gauge-fixing term in the QCD Lagrangian: Eq. (2.18) can be considered as written in the Landau gauge where $\xi=0$). The Callan-Symanzik "beta-function" $\beta(g)$ is defined by

$$\beta(g) = \Lambda \frac{\partial g}{\partial \lambda} \tag{2.19}$$

Eqs. (2.18) and (2.19) may be solved to give

$$\sigma_{tot}(Q^2, \Lambda, g) = \sigma_{tot}\left(1, \bar{g}\left(Q^2/\Lambda^2\right)\right) \tag{2.20}$$

where

$$\begin{aligned} \Lambda \frac{\partial \bar{g}}{\partial \lambda} &= \beta(\bar{g}) \\ \bar{g}(1) &= g \end{aligned} \tag{2.21}$$

To leading order, $\beta(g)$ can be calculated from the sum of the UV-divergent subgraphs of α_s^1 Feynman diagrams [28]:

$$\beta(g) = -b_0 \frac{g^3}{16\pi^2} \tag{2.22}$$

Solving Eqs. (2.21) and (2.22) gives:

$$\bar{g}^2(Q^2/\Lambda^2) = \frac{g^2}{1 + b_0 \frac{g^2}{16\pi^2} \ln(Q^2/\Lambda^2)} \tag{2.23}$$

We see that keeping the leading-order contribution to the beta-function and solving the RG equations automatically sums the leading logs. By calculating the beta-function to higher order one can sum nonleading logs as well. To the next order [29]:

$$\begin{aligned} \beta(g) &= -b_0 \frac{g^3}{16\pi^2} - b_1 \frac{g^5}{(16\pi^2)^2} \\ \sigma_{tot} &= \sigma_0\left(1 + \bar{\alpha}_s(Q^2)/\pi + C\bar{\alpha}_s^2(Q^2)\right) \end{aligned} \tag{2.24}$$

where

$$\frac{\bar{\alpha}_s(Q^2)}{4\pi} = \frac{1}{b_0 \ln(Q^2/\Lambda^2)} - \frac{b_1}{b_0^3}\frac{\ln\ln(Q^2/\Lambda^2)}{\ln^2(Q^2/\Lambda^2)}$$
$$b_1 = 102 - \frac{38}{3}n \qquad (2.25)$$

Here Λ has been chosen so that there are no terms of order $(\ln Q^2/\Lambda^2)^{-2}$. Note that there is some ambiguity in Eq. (2.24): changing the arbitrary renormalization scale to Λ' changes the effective coupling. To keep σ_{tot} invariant under such changes, which amount to changing the renormalization prescription, c must depend on the renormalization scheme. For instance, $c_{\overline{MS}}=5.6/\pi^2$ while $c_{MOM}=-1.7/\pi^2$ for another popular (the "momentum-subtraction") scheme.

c) DIS and factorization.

Armed with this essential knowledge, which reproduces $e^+e^- \rightarrow H$ phenomenology very well [30], let us now consider a more involved physical process: deep inelastic lepton-hadron scattering $lH \rightarrow l'X$ (DIS, see Fig. 2.5). The lepton-hadron cross-section has the form [10]

$$\sigma = L^{\mu\nu} W_{\mu\nu} \qquad (2.26)$$

with the leptonic part

$$L^{\mu\nu} = 4\left\{k'^{\mu}k^{\nu} + k'^{\nu}k^{\mu} - g^{\mu\nu}k\cdot k' - i\epsilon^{\mu\nu\alpha\beta}k_{\alpha}k'_{\beta}\right\} \qquad (2.27)$$

and the hadronic part

$$W_{\mu\nu} = \int d^4\xi\, e^{iq\xi}\langle p|[J_{\mu}(\xi), J_{\nu}(0)]|p\rangle_{\text{spin ave}} \equiv \frac{1}{2}\,\mathrm{Im}\,T_{\mu\nu} \qquad (2.28)$$

where

$$T_{\mu\nu} = i\int d^4\xi\, e^{iq\xi} \langle p|T(J_\mu(\xi)J_\nu^+(0))|p\rangle \qquad (2.28')$$

is defined using hadronic currents (no constituents of hadrons at this stage). The tensor $T_{\mu\nu}$ may be expanded in terms of Lorentz invariants which also satisfy current conservation

$$\begin{aligned} T_{\mu\nu}(Q^2,\nu) = {} & \left(g_{\mu\nu} - \frac{q_\mu q_\nu}{q^2}\right) T_1(Q^2,\nu) + \\ & + \left[-g_{\mu\nu} + \frac{p_\mu q_\nu + p_\nu q_\mu}{p\cdot q} - \frac{p_\mu q_\nu}{(p\cdot q)^2}\right] T_2(Q^2,\nu) - \\ & - i e_{\mu\nu\alpha\beta} \frac{p_\alpha p_\beta}{\nu} T_3(Q^2,\nu) \end{aligned} \qquad (2.29)$$

where $Q^2 = -q^2$ (q^2 is spacelike) and $\nu = p.q$ (in this section we set the proton mass to unity). Further defining

$$W_i = \frac{1}{2\pi} \operatorname{Im} T_i \qquad (i=1,2,3) \qquad (2.30)$$

one finds

$$\frac{d^2\sigma}{dx\,dy} \approx \frac{G_F^2 E}{\pi}\left[(1-y)\nu W_2 + xy^2 W_1 + y\left(1-\frac{y}{2}\right)x\nu W_3\right] \quad (2.31)$$

where G_F is the Fermi coupling constant, $x=Q^2/2\nu$ and $y=\nu/E$.

The parton model was originally introduced by studying this cross-section in the "Bjorken limit" $Q^2 \rightarrow \infty, \nu \rightarrow \infty$, x fixed. Perturbative QCD must reproduce naive parton model "scaling" (Q^2-independence of the cross-section) in leading order and then compute higher-order corrections ("scaling- violations", Q^2-dependence). Fig. 2.6 shows the parton model form for Fig. 2.5 and Fig. 2.7 shows the leading-order QCD flavor non-singlet contribution to the structure function $F_2^q(Q^2,x) = \nu W_2(Q^2,\nu)$. Computing these gives [25]:

$$\frac{F_2^q(Q^2,x)}{x} = \delta(1-x) - \frac{\alpha_s}{2\pi} P_{qq}(x) \ln\left(Q^2/p^2\right) + \dots \tag{2.32}$$

where

$$P_{qq}(x) = \frac{4}{3}\left[\frac{1+x^2}{(1-x)_+} + \frac{3}{2}\delta(1-x)\right] \tag{2.33}$$

The distribution denoted by a + is defined as

$$\int_0^1 dx \frac{h(x)}{(1-x)_+} = \int_0^1 dx \frac{h(x)-h(1)}{1-x} \tag{2.33'}$$

(h(x) is a suitable test function). Eq. (2.32) is in double trouble: despite the fact that all quark+gluon final states have been summed over in deriving this result, there still are mass singularities; on the other hand, there is the $\ln Q^2$ term threatening perturbation theory as Q^2 grows. The hint to the solution of both problems lies in recognizing that the Kinoshita–Lee–Nauenberg theorem does not work because one has not summed over all the quark+soft gluon initial states which are possible in this process (as opposed to e^+e^- annihilation, a hadron is now present in the initial state). We shall now show that perturbative QCD can study DIS only at the price of explicitly admitting it cannot calculate the large-distance distribution of partons within the host hadron.

Let us take moments of Eq. (2.32):

$$\begin{aligned}\int_0^1 x^{n-2} F_2^q(Q^2,x)\,dx &= \\ &= 1 - \frac{g^2}{16\pi^2}\left(\frac{4}{3}\right)\left[1 - \frac{2}{n(n+1)} + 4\sum_{j=2}^{n}\frac{1}{j}\right]\ln\left(Q^2/p^2\right) + o(g^2) \\ &\equiv M_n(Q^2,p^2,g) \equiv 1 - g^2 a_n \ln\left(Q^2/p^2\right) + o(g^2)\end{aligned} \tag{2.34}$$

To obtain the observable moments of the proton's structure function F_2, this M_n must be convoluted with the n^{th} moment of the probability that a quark of type k has a fraction ζ of the proton's momentum:

$$\int_0^1 dx\, x^{n-2} F_2(x,Q^2) = \sum_k \int_0^1 dy\, y^{n-2} F_2^{q_k}(y,Q^2) \int_0^1 \zeta^{n-1} f_k(\zeta)\, d\zeta$$
$$\equiv \sum_k \left[1 - a_n^k g^2 \ln(Q^2/\rho^2) + \ldots\right] b_n^k \tag{2.35}$$

where the b_n are effective, perturbatively uncalculable coefficients representing the initial "preparation" of the quark's wavefunction inside the proton at a large space-time scale which is irrelevant for $Q^2 \to \infty$ parton physics. The leading-order expression (2.35) can be trivially rewritten as

$$\int_0^1 dx\, x^{n-2} F_2(x,Q^2) = \sum_k \left[1 - a_n^k g^2 \ln(Q^2/\mu^2) + \ldots\right]\left[1 - a_n^k g^2 \ln\left(\frac{\mu^2}{\rho^2}\right) + \ldots\right] b_n^k$$
$$\equiv \sum_k \left[1 - a_n^k g^2 \ln(Q^2/\mu^2) + \ldots\right] b'^k_n \tag{2.36}$$

Postulating the existence of the nonperturbative moments b_n has thus provided a refuge for the infrared singularities and perturbative QCD has found an excuse for concentrating solely on the ultraviolet problem. As we saw above, such UV problems are solved by resumming $\log Q^2$-terms using the renormalization group. However, the buried soft singularity has left a trace in the guise of the new mass scale μ, the "factorization scale", which modifies the renormalization group analysis. Furthermore, the factorization step, trivial to leading order in α_s, requires proof for higher orders.

There is a more learned justification of factorization which is applicable to any order in perturbation theory and which also permits a transparent discussion of the effects of factorization on the RG: Wilson's famous "operator product expansion" (OPE) [31]. Wilson postulates that, for $\xi \to 0$, one can write

$$iT(J(\xi)J(0)) = \sum_{i=2}^{\infty} \sum_{n=0}^{\infty} \xi^{\mu_1} \cdots \xi^{\mu_n} C_{i,n}(\xi^2) O^i_{\mu_1 \cdots \mu_n}(0) \qquad (2.37)$$

for the case of spinless currents. $O^i_{\mu_1 \cdots \mu_n}(0)$ are local operators formed out of the fields available in a given theory and $C_{i,n}(\xi^2)$ are c-number coefficient functions. To illustrate this expansion and to clarify the meaning of the index i, consider free scalar currents. In this case, we can write the left-hand side of Eq. (2.37) as

$$iT(J(\xi)J(0)) = -2[\Delta(\xi, m^2)]^2 + 4i\Delta(\xi, m^2) : \phi(\xi)\phi(0) : + \\ + : \phi^2(\xi)\phi^2(0) : \qquad (2.38)$$

In the right-hand side of Eq. (2.38) all light-cone singularities reside in the propagator functions

$$\Delta(\xi, m^2) \underset{\xi \to 0}{\sim} \frac{i}{4\pi^2} \frac{1}{-\xi^2 + i\epsilon} \qquad (2.39)$$

$:\phi(\xi)\phi(0):$ has no singularities and can thus be expanded in a Taylor series:

$$:\phi(\xi)\phi(0): = \sum_{n=0}^{\infty} \frac{1}{2^n} \xi^{\mu_1} \cdots \xi^{\mu_n} \phi(0) \overleftrightarrow{\partial}_{\mu_1} \cdots \overleftrightarrow{\partial}_{\mu_n} \phi(0) \qquad (2.40)$$

We see that the OPE is identically true for Klein-Gordon theory in the limit $\xi \to 0$ with

$$O_{\mu_1 \cdots \mu_n}(0) = \phi(0) \overleftrightarrow{\partial}_{\mu_1} \cdots \overleftrightarrow{\partial}_{\mu_n} \phi(0) \qquad (2.41)$$

The coefficient functions have singularities

$$C_i(\xi) \sim (1/\xi^2)^{d_{c_i}} \qquad (2.42)$$

where the dimension d_{C_i} is defined in terms of the "twist" i as

$$d_{C_i} = 2 d_J - i \qquad (2.43)$$

(d_J is the dimension of the current J; in [31] twist is defined as the difference between the dimension D_{O_i} and the spin S_{O_i} which characterize an operator O_i). The most singular terms, and the ones which dominate in the small-distance limit $\xi \to 0$, are those with lowest ("leading") twist i=2. As ξ becomes larger (Q^2 smaller) the effect of higher twist i>2 may become larger but the validity of the OPE itself becomes questionable at such distances.

With spin-1/2 fields we may form the twist-two operator

$$O^F_{\mu_1 \cdots \mu_n}(0) = \frac{1}{n}\left[\bar{\Psi}(0)\gamma_{\mu_1}\overleftrightarrow{\partial}_{\mu_2}\cdots\overleftrightarrow{\partial}_{\mu_n}\Psi(0) + perm\right] \qquad (2.44)$$

The OPE has further been shown to be valid for renormalizable interactions to all orders of perturbation theory [31], provided Q^2 is large enough. Let us therefore insert Eq. (2.37) into Eq. (2.28'):

$$T(x,Q^2) = \sum_{i,n}\left(-\frac{1}{Q^2}\right)^{i+n-3} \langle p|O^i_{\mu_1 \cdots \mu_n}(0)|p\rangle q^{\mu_1} \cdots q^{\mu_n}\,\bar{C}_{i,n}(Q^2) \qquad (2.45)$$

In the limit $Q^2 \to \infty$ the proton mass can be neglected so that $\langle p|O_{\mu_1 \cdots \mu_n}(0)|p\rangle = \bar{O}_n p_{\mu_1} \cdots p_{\mu_n}$ and finally

$$T(x,Q^2) \underset{Q^2\to\infty}{\sim} \sum_{i,n}\left(-\frac{1}{Q^2}\right)^{i-3} \bar{C}_{i,n}(Q^2)\bar{O}^i_n(-2x)^{-n} \qquad (2.46)$$

By integrating along the contour shown in Fig. 2.8 we obtain

$$\frac{1}{2\pi i}\oint_C dx\, x^{n-1}\, T(x,Q^2) \underset{Q^2\to\infty}{\sim} \left(\frac{1}{Q^2}\right)\left(-\frac{1}{2}\right)^n \bar{C}_{2,n}(Q^2)\bar{O}^2_n + \cdots \qquad (2.47)$$

where we have displayed the twist-two contribution. The discontinuity of

Eq. (2.47) is just $W(x,Q^2)$, so

$$\int_0^1 dx\, x^{n-1} W(x,Q^2) \underset{Q^2\to\infty}{\sim} \frac{1}{Q^2}\left(-\frac{1}{2}\right)^{n-2} \bar{O}_n^2\, \bar{C}_{2,n}(Q^2) \qquad (2.48)$$

We see that the moments of W in the Bjorken limit are related to the large-Q^2 behavior of the OPE coefficient functions, which should therefore be observable in DIS and must obey RG equations:

$$\left(\Lambda\frac{\partial}{\partial\Lambda} + \beta\frac{\partial}{\partial g} - \gamma_{O_n^i}\right)\bar{C}_{i,n}(Q^2) = 0 \qquad (2.49)$$

where the "anomalous dimension" $\gamma_{O_n^i}$ arises because the OPE operators must also be renormalized:

$$O_n^{i\,R} = Z_{O_n^i}\, O_n^{i\,u}$$
$$\gamma_{O_n^i} = \Lambda\frac{\partial}{\partial\Lambda} Z_{O_n^i} \qquad (2.50)$$

The solution to Eq. (2.49) is

$$\bar{C}_n^i(Q^2/\Lambda^2, g) = \bar{C}_n^i(1, \bar{g}(Q^2/\Lambda^2)) \exp\left[-\int_1^{Q^2/\Lambda^2} \gamma_{O_n^i}(\bar{g}(\tau))\frac{d\tau}{\tau}\right] \qquad (2.51)$$

Comparing Eqs. (2.48) and (2.36) we can identify the b_n^2's with the reduced operator matrix elements $\bar{O}_n^2$ and the twist-two coefficient functions with the M_n. In terms of the M_n, Eq. (2.51) reads

$$M_n(Q^2/\Lambda^2, g, \mu^2) = M_n(1, \bar{g}(Q^2/\Lambda^2), \mu^2) \exp\left[-\int_1^{Q^2/\Lambda^2} \gamma_0^n(\bar{g}(\tau))\frac{d\tau}{\tau}\right] \qquad (2.52)$$

where we have reintroduced the factorization scale whose existence is now justified by the OPE. The anomalous dimension can thus be calculated from Feynman diagrams: to leading order, $\gamma_0^n = a_n g^2$ and using Eq. (2.16) one finds [32]

$$M_n(Q^2/\Lambda^2, g, \mu^2) = \left[\frac{\bar{g}^2(Q^2)}{\bar{g}^2(\mu^2)}\right]^{-\gamma_0^n/2b_0} \cdot b_n^2 \qquad (2.53)$$

This is the result of summing leading logs; non-leading logs are summed by including higher-order terms in γ_0^n and $\bar{C}_n$.

The solution for moments of flavor-singlet combinations of structure functions involves gluon as well as quark (antiquark) constituents and can be written to leading order as [32]:

$$M_n^s(Q^2) = A_n\left[\bar{g}^2(Q^2)\right]^{\gamma_+^n/2b_0} + B_n\left[\bar{g}^2(Q^2)\right]^{\gamma_-^n/2b_0} \qquad (2.54)$$

where A and B are constants and the are eigenvalues of the lowest-order singlet anomalous dimension matrix

$$\Gamma_n^s = \begin{pmatrix} \frac{8}{3}\left[1-\frac{2}{n(n+1)}+4\sum_{j=2}^{n}\frac{1}{j}\right] & -4N_f\frac{n^2+n+2}{n(n+1)(n+2)} \\ -\frac{16}{3}\frac{n^2+n+2}{n(n^2-1)} & 6\left[\frac{1}{3}-\frac{4}{n(n-1)}-\frac{4}{(n+1)(n+2)}+4\sum_{j=2}^{n}\frac{1}{j}\right]+\frac{4}{3}N_f \end{pmatrix} \qquad (2.55)$$

This RG resummation procedure can be cast into parton model language in a way suggested by Altarelli and Parisi [33]. The non-singlet moments satisfy the equations

$$\frac{dM_n(u)}{du} = -\frac{\alpha_s(u)}{4\pi}\gamma_0^n M_n(u) \qquad (2.56)$$

where $u=\ln Q^2/\Lambda^2$. These authors define a function $P_{q\to q}(z)$ such that

$$\int_0^1 dz\, z^{n-1} P_{q\to q}(z) = -\frac{\gamma_0^n}{4} \qquad (2.57)$$

Inverting Eq. (2.56) we get

$$d\bar{f}(x,u)/du = \frac{\alpha_s(u)}{2\pi}\int_x^1 \frac{dy}{y}\bar{f}(y,u)P_{q\to q}(x/y) \qquad (2.58)$$

where $\tilde{f}(x,u)$ is a flavor non-singlet combination of quark distribution functions. So $P_{q\to q}(z)$ can be interpreted as the variation per unit u of the probability of having a given quark evolve into a quark which carries a fraction z of the original quark's momentum. Analogously we can use the singlet anomalous dimension matrix Γ^s_u to define evolution probabilities $P_{g\to q}$, $P_{q\to g}$ and $P_{g\to g}$. The flavor singlet combinations of ocean quark and of gluon distribution functions $Q_o(x,u)$ and $G(x,u)$ satisfy the following Altarelli-Parisi equations:

$$\frac{dQ_o}{du} = \frac{\alpha_s(u)}{2\pi}\int_x^1 \frac{dy}{y}\left[Q_o(y,u)P_{q\to q}(x/y) + G(y,u)P_{g\to q}(x/y)\right]$$

$$\frac{dG}{du} = \frac{\alpha_s(u)}{2\pi}\int_x^1 \frac{dy}{y}\left[Q_o(y,u)P_{q\to g}(x/y) + G(y,u)P_{g\to g}(x/y)\right] \qquad (2.59)$$

Confrontations between QCD and deep inelastic leptoproduction phenomenology are based upon this formalism. Although the leading-twist predictions are in remarkable agreement with the data on the Q^2-dependence of the structure functions, a sizable contribution of higher-twist terms to the observed scaling deviations cannot be ruled out at presently accessible values of Q^2 [12,34]

d) Summary.

Perturbative QCD gives an encouraging description of high-Q^2 hadron structure in terms of partons identified with the fundamental quark, antiquark and gluon fields appearing in the QCD Lagrangian while burying large-distance effects in constants it cannot compute. Nonperturbative QCD is called upon to calculate this large-scale structure while connecting smoothly with the perturbative formalism in the high-Q^2 limit.

2.3. NONPERTURBATIVE METHODS

a) Vacuum condensates.

Let us pin down more details on the operator matrix elements $\bar{O}_\kappa$ which represent nonperturbative physics at large Q^2. We have seen that they are to be taken with respect to the "true" physical vacuum out of which the observed hadrons are excited by the action of the appropriate currents (Eqs. (2.28) and (2.45)). This must also be the exact ground state of QCD. It follows that the OPE operators must be composites of current quark and of gluon fields and that they must be $SU(3)_c$-gauge-invariant. Furthermore, they must carry vacuum quantum numbers. A given operator's contribution to the OPE is determined by its canonical dimension: the contribution from an operator with higher dimension falls off more rapidly with Q^2 than from a lower-dimensional operator. Apart from the identity operator, the operators $\bar{\Psi}\Psi$ (dimension 3) and $\vec{F}_{\mu\nu}.\vec{F}^{\mu\nu}$ (dimension 4) are the lowest-dimensional gauge-invariant operators one can form in QCD. We must therefore expect that the first nonperturbative effects one feels as one decreases Q^2 are due to the "vacuum condensates" $\langle\bar{\Psi}\Psi\rangle$ and $\langle\vec{F}_{\mu\nu}.\vec{F}^{\mu\nu}\rangle$. According to the OPE, any time-ordered current-current correlation function can thus be represented as

$$\Omega^\alpha(Q^2) = C_I^\alpha I + C_{\bar{\Psi}\Psi}^\alpha \langle 0|\bar{\Psi}\Psi|0\rangle + C_{FF}^\alpha \langle 0|\vec{F}_{\mu\nu}\cdot\vec{F}^{\mu\nu}|0\rangle + \cdots \qquad (2.60)$$

for sufficiently high Q^2. α stands for a set of quantum numbers pertaining to the currents in question. Higher-dimensional operators would become more important for lower Q^2.

Assuming that such higher-dimensional contributions can be expressed in terms of products of $\langle\bar{\psi}\psi\rangle$ and $\langle\vec{F}_{\mu\nu}.\vec{F}^{\mu\nu}\rangle$ and that the cofficients can be calculated from perturbative QCD in conjunction with high-Q^2 DIS data, the famous "ITEP sum rules" [35] allow estimates of the numerical values of the vacuum condensates. Indeed, consider the vacuum polarization induced by a hadronic current J_α:

$$\Omega^\alpha(Q^2) \rightarrow \Pi(Q^2)$$

$$T^{\mu\nu\cdots}\,\Pi(Q^2) = i\int d^4x\, e^{iqx}\langle 0|T(J^\alpha(x)J^+_\alpha(0))|0\rangle\Big|_{q^2=-Q^2} \tag{2.61}$$

where $T^{\mu\nu\cdots}$ is a space-time tensor dependent on the chosen current. In general, the function $\Pi(Q^2)$ obeys an n-times subtracted dispersion relation:

$$\Pi(Q^2) = \frac{(q^2)^n}{\pi}\int\frac{Im\,\Pi(s)\,ds}{s^n(s-q^2)} + \sum_{k=0}^{n-1} a_k (q^2)^k \tag{2.62}$$

The subtraction constants a_k can be removed by taking an appropriate number of derivatives with respect to Q^2. In turn, the imaginary part of Π is related to an observable cross section. In particular, for a vector current we have

$$Im\,\Pi^V(s) = \frac{9}{64\pi^2\alpha_s^2}\, s\,\sigma(e^+e^- \rightarrow \text{HADRONS}) \tag{2.63}$$

The created particles will be resonances plus a continuum above the respective production threshold. In a narrow-resonance approximation (appropriate mainly in the case of heavy quarkonia- the Ψ and Υ families) one can represent $Im\,\Pi$ for the vector current as

$$Im\,\Pi^V(s) = \frac{\pi}{e_q^2}\sum_{Res.}\frac{m_R^2}{g_R^2}\,\delta(s-m_R^2) + \frac{1}{4\pi}\left(1+\frac{\alpha_s}{\pi}\right)\theta(s-s_0) \tag{2.64}$$

where g_R is related to the electronic width of the resonance and the θ-function stands for the continuum.

Now we have two representations of $\Pi(Q^2)$: the high-Q^2 OPE in terms of QCD parameters and the equations (2.62) and (2.64) in terms of known hadron masses and decay widths. By equating the derivatives of these representations with respect to Q^2 (of sufficiently high order to eliminate all subtraction constants) one can thus evaluate the vacuum condensates. Currently accepted results are [35]:

$$\begin{aligned}
&\langle \bar{u}u \rangle = \langle \bar{d}d \rangle = -(.225 \pm .025)^3 \ \mathrm{GeV}^3 \\
&\langle \bar{s}s \rangle = (0.8 \pm 0.1) \langle \bar{u}u \rangle \\
&\langle \frac{\alpha_s}{\pi} \vec{F}_{\mu\nu} \cdot \vec{F}^{\mu\nu} \rangle \simeq +0.012 \ \mathrm{GeV}^4
\end{aligned} \qquad (2.65)$$

(with $\alpha_s \sim 1$ and $\Lambda = 0.1 \cdot \mathrm{GeV}$). Once one knows these constants, one can predict hadronic properties corresponding to other currents. The method works quite well [35,36].

b) The effective action.

Nonperturbative QCD thus empirically appears to be characterized by nonvanishing vacuum condensates. Would it be possible to compute these values and to understand their physical implications directly from the QCD Lagrangian, without having to resort to perturbative nor to phenomenological considerations? Let us go back to the general path-integral formulation of quantum field theory, which underlies Feynman diagramatics in the first place [37], and try to find a different way to calculate with it.

The sum of all connected Feynman diagrams of a quantum field theory which have n>1 external lines terminating at the Minkowski space-time points $x_1, \ldots, x_n$ is the connected n-point Green's function $G_n(x_1, \ldots x_n)$. Let us define the functional W[J] as the "generating functional for connected Green's functions"

$$\frac{i}{\hbar} W[J] = \sum_{n=0}^{\infty} \left(\frac{i}{\hbar}\right)^n \frac{1}{n!} \int d^4x_1 \ldots d^4x_n G_n(x_1, \ldots x_n) J(x_1) \ldots J(x_n) \tag{2.66}$$

where J is an auxiliary c-number valued function ("current") and we have explicitly exhibited h. Defining the functional Z[J] as the vacuum-to-vacuum amplitude of the field theory in the presence of the sources J

$$\langle 0|0\rangle_J \equiv Z[J] \tag{2.67}$$

one can show that it is related to W[J] by

$$Z[J] = \exp\left[\frac{i}{\hbar} W[J]\right] \tag{2.67'}$$

Therefore, if the Minkowskian action of a generic field theory with field variables ϕ_α is

$$S[\phi_\alpha] = \int d^4x \, L(\phi_\alpha(x), \partial\phi_\alpha(x)) \tag{2.68}$$

then Z[J] can be calculated as

$$Z[J] = C \int [D\phi_\alpha] \exp\left\{\frac{i}{\hbar}\left(S[\phi_\alpha] + \int d^4x \, \phi_\alpha J^\alpha\right)\right\} \tag{2.69}$$

where $[D\phi_\alpha]$ is an "integration measure", that is, a certain prescription for adding up the contributions from all possible paths.

To gain some insight into the connection between generating functionals and vacuum condensates, consider for simplicity a real scalar field with Lagrangian density

$$L = \frac{1}{2}\partial_\mu \phi(x)\partial^\mu \phi(x) - V(\phi(x))$$

$$V(\phi) = \frac{\alpha_0}{4!}\phi^4 - \frac{\mu_0^2}{4}\phi^2 \qquad (2.70)$$

The vacuum expectation value of ϕ in the presence of an external source J is given by the functional derivative

$$\phi_c = \frac{\delta W[J]}{\delta J(x)} \qquad (2.71)$$

The "true physical" vacuum expectation value of the dynamical field is the limit of ϕ_c as J—>0. We now ask the question: what source function J will produce a given, prescribed ϕ_c? To answer this question, it is convenient to replace the independent variable J by ϕ_c as the independent variable. As in thermodynamics, this is achieved by a Legendre transformation:

$$\Gamma[\phi_c] = W[J] - \int J(x)\phi_c(x)\, d^4x \qquad (2.72)$$

$\Gamma[\phi_c]$ is called the "effective action" [38]. The Maxwell-like relations corresponding to (2.72) imply that

$$\frac{\delta \Gamma[\phi_c]}{\delta \phi_c(x)} = -J(x) \qquad (2.73)$$

To take the limit J—>0 we notice that for J=0 ϕ_c should be x-independent by translational invariance. So the functional derivative becomes a "straight" derivative and $\langle\phi\rangle$ must be among the roots of the equation

$$d\Gamma/d\phi_c = 0 \qquad (2.74)$$

We conclude that vacuum condensates can be calculated once the effective action is known. Of course, to compute Γ from the Lagrangian of a theory like QCD is a highly nontrivial matter.

Let us define the "effective potential" corresponding to Γ by $\Gamma[\rho]=-\Omega U(\rho)$, with $\rho=\phi_c=$ constant and Ω being the total volume of the space-time domain where the field is supported. We shall show that the evaluation of the effective potential can be a worthwhile shortcut to the essential quantum physics of vacuum condensates.

To proceed, we have to actually do the path-integral for $W[J]$. This requires that we specify the integration measure $[D\phi]$. Consider the standard Gaussian integral over one real variable x:

$$\int_{-\infty}^{+\infty} dx\, e^{-Q(x)} = \left(\frac{2\pi}{a}\right)^{1/2} \exp\left(b^2/2a\right)$$
$$Q(x) = \frac{1}{2}ax^2 - bx \qquad (2.75)$$

Next suppose we have a quadratic form $Q(u)=(u,Mu)/2-(u,v)$ where u is a n-component argument vector $(u_1,\ldots u_n)$, v a constant n-vector, M a nxn symmetric nonsingular matrix and (,) denotes the scalar product. Then (2.75) generalizes to

$$\int_{-\infty}^{+\infty} (2\pi)^{-n/2} du_1 \cdots du_n\, e^{-Q(u)} = (\det M)^{-1/2} \exp\left[\frac{1}{2}(v, M^{-1}v)\right] \qquad (2.75')$$

To date, the only known analytical method to do a functional integral for quantum fields ϕ is to use (2.75'). In order to get a quadratic form in the fields one expands the action around its saddle point and only keeps the term of order h. If one now defines $[D\phi]=C\prod_x d\phi(x)$, then one can take over the result (2.75'):

$$\int [D\phi] \exp\left[-\frac{1}{2}(\phi, M\phi) + (v,\phi)\right] = C(\det M)^{-1/2} e^{\frac{1}{2}(v, M^{-1}v)} \qquad (2.75'')$$

In using this analogy, we have thus discretized the space-time support of ϕ: x is considered to be a discrete variable. It is implicitly assumed that the final result remains true as the continuum limit is taken at the end of the calculation. We may also imagine that we have enclosed the field in a large but finite space-time box, integrated over each of the independent Fourier components of ϕ and finally taken the infinite-volume limit (hoping nothing dramatic happens as we do so).

In applying this procedure to our example, it is convenient to evaluate the scalar product in Euclidean rather than in Minkowski space-time [Appendix A]. The result is [39]:

$$\mathcal{U}(\rho) = V(\rho) + \hbar V_1(\rho) + o(\hbar^2)$$
$$V_1(\rho) = \int \frac{d^4k_E}{(2\pi)^n} \ln\left(\frac{k_E^2 + V''(\rho)}{k_E^2}\right) \qquad (2.76)$$

where V_1 contains the leading-order ("one-loop") quantum corrections to the classical potential V, and is given by a divergent integral over Euclidean momentum space. We must therefore renormalize the "bare" parameters appearing in Eq. (2.70) in terms of fixed and finite values α_1 and μ_1

$$\alpha_0 = \alpha_1 + \delta\alpha$$
$$\mu_0 = \mu_1 + \delta\mu$$

and of a renormalization mass scale Λ (in favor of which $\delta\alpha$ and $\delta\mu$ are eliminated by the subtraction procedure, as discussed in Section 2.2). The result for the effective potential to one-loop order is

$$\mathcal{U}(\rho) = V(\rho) + \frac{\hbar}{64\pi^2}\left[V''(\rho)\right]^2\left(-\frac{1}{2} + \ln\frac{V''(\rho)}{\Lambda^2}\right) \qquad (2.77)$$

where V is now written in terms of α_1 and μ_1. The expectation value of ϕ with respect to the true vacuum must correspond to an absolute minimum of the function $U(\langle\phi\rangle)$:

$$U'(\langle\phi\rangle) = 0 \tag{2.78}$$

An extremum of U which is not an absolute minimum indicates a metastable vacuum. The renormalized mass and coupling strength can be evaluated as

$$\begin{aligned} \mu^2 &= U''(\rho = \langle\phi\rangle) \\ \alpha &= U'''(\rho = \langle\phi\rangle) \end{aligned} \tag{2.79}$$

It is obvious that $\langle\phi\rangle=0$ is always an extremum of U in this approximation. If $\mu_1^2<0$, this is a unique stable vacuum. The effective potential then has the shape shown in Fig. 2.9a. On the other hand, the situation depicted in Fig. 2.9b corresponds to spontaneous symmetry breakdown. As we have repeatedly stressed, the latter case is often preferred by physics.

Consider the famous linear sigma-model in its original formulation by Gell-Mann and Lévy [15]. It describes the interaction of nucleons (an SU(2)-isodoublet of fermion fields) with pions (a pseudoscalar isotriplet) and with the scalar 0^+ sigma-meson:

$$\begin{aligned} L = \bar{\psi} i \not{\partial} \psi + g \bar{\psi}(\sigma' + i\vec{\tau}\cdot\vec{\pi}\gamma_5)\psi - \tfrac{1}{2}\left[(\partial_\mu\sigma')^2 + (\partial_\mu\vec{\pi})^2\right] - \\ - B^2(\sigma'^2 + \vec{\pi}^2 - A^2)^2 \end{aligned} \tag{2.80}$$

If A^2 were negative, the corresponding effective potential would have its only minimum at $\langle\sigma'\rangle=\langle\vec{\pi}\rangle=0$. Then the $\vec{\pi}$ and σ' would have equal masses given by $(-4A^2B^2)^{1/2}$ but the nucleons would be massless! So physics forces us to take $A^2>0$. In this case we have the situation of Fig. 2.9b, the true vacuum is characterized by a nonvanishing vacuum condensate for the sigma, $\langle\sigma'\rangle \neq 0$, and is no longer invariant under the chiral SU(2)xSU(2) of the Lagrangian but only under SU(2). Redefining the field σ as

$$\sigma = \sigma' - \langle\sigma'\rangle \tag{2.81}$$

we find that the pions are now massless, as becomes the Goldstone bosons of chiral-symmetry breaking. The nucleons and the sigma meson have their correct, observed masses. It is customary to express the vacuum condensate which signals chiral-symmetry breaking in terms of the "pion decay constant" f_π which has the empirical value ≈ 93 MeV (in the normalization we shall use throughout our work):

$$f_\pi = -\langle\sigma'\rangle \tag{2.82}$$

The Goldberger-Treiman relation

$$m_N = g f_\pi / g_A \tag{2.83}$$

then results from the model, to all orders in the πN interaction. $g_A \simeq 1.24$ is the renormalized axial-vector coupling ($g_A = 1$ to lowest order, where $m_N = gf_\pi$).

Let us now return to the Lagrangian (2.70) and assume $\mu_1 = 0$ (massless neutral scalar field with quartic coupling). The apparent root of the equation $U' = 0$

$$\hbar\alpha \ln \frac{\langle\phi\rangle^2}{\Lambda^2} = -\frac{32\pi^2}{3} \tag{2.84}$$

must be rejected because we are not allowed to equate a quantity of order h in the loop expansion to a quantity of order 1. $\langle\phi\rangle = 0$ is the only solution in this case.

Consider, however, massless scalar electrodynamics [40]:

$$L = -\frac{1}{4} F_{\mu\nu} F^{\mu\nu} + \left[(\partial_\mu - ieA_\mu)\phi^* \right] \left[(\partial_\mu + ieA_\mu)\phi \right] - \frac{\lambda_0}{6} (\phi^* \phi)^2 \tag{2.85}$$

This Lagrangian density has been obtained using the general principle of U(1)-gauge-invariant minimal coupling [Appendix B]. The self-coupling is necessary in order to renormalize the scalar-scalar scattering amplitude. The phase of ϕ can be eliminated by going to unitary gauge; the vector field is subjected to the auxiliary condition $\partial_\mu A^\mu = 0$; e is considered to be the renormalized charge whereas λ_0 is to be renormalized by radiative corrections. Under these conditions, the action of the theory is:

$$S[A,\phi] = \int d^4x \left[\frac{1}{2} A^\mu (D^2 + e^2\phi^2) A_\mu - \frac{1}{2} \phi D^2 \phi - \frac{\lambda_0}{4!} \phi^4 \right] \tag{2.86}$$

One integrates out the vector field to obtain an action for ϕ alone:

$$S[\phi] = -\int d^4x \left(\frac{1}{2} \phi D^2 \phi + \frac{\lambda_0}{4!} \phi^4 \right) - \frac{3}{2} \operatorname{Tr} \ln (D^2 + e^2\phi^2) \tag{2.87}$$

The corresponding one-loop effective potential is

$$U(\rho) = \rho^4 \left[\frac{\lambda_0}{4!} + \frac{3e^4}{64\pi^2} \left(-\frac{1}{2} + \ln \frac{e^2\rho^2}{\Lambda^2} \right) \right] \tag{2.88}$$

Now the equation $U' = 0$ has a legitimate nonzero root $\langle\phi\rangle$ which satisfies

$$\frac{3e^4}{64\pi^2} \ln \left(e^2 \langle\phi\rangle / \Lambda^2 \right) = -\frac{\lambda_0}{4!} \tag{2.89}$$

This relation can be used to eliminate Λ in favor of $\langle\phi\rangle$:

$$U(\rho) = \frac{3e^4\rho^4}{64\pi^2} \left(-\frac{1}{2} + \ln \frac{\rho^2}{\langle\phi\rangle^2} \right) \tag{2.90}$$

The initially massless scalar field has acquired a mass

$$m^2 = U''(\rho)\big|_{\rho=\langle\phi\rangle} = \frac{3e^4}{8\pi^2} \langle\phi\rangle^2 \tag{2.91}$$

which is entirely due to its interaction with the gauge field. We thus see that a nonzero vacuum condensate need not be explicitly generated by a term in the Lagrangian but can also appear dynamically, as a result of the "dimensional transmutation" mechanism we have just described. Its scale is set, in this case, not by a parameter like f_π but by the renormalization scale Λ.

By Eq. (2.86), the vector field has also acquired mass by the same token:

$$m_A^2 = e^2 \langle\phi\rangle^2 \qquad (2.92)$$

Thus, a dynamical Higgs phenomenon has taken place. It is not known whether the electroweak Higgs is of explicit or of dynamical origin. The model (2.85) is the relativistic generalization of the Ginzburg-Landau phenomenological theory of supercorductivity. It has many tantalizing features which we would also expect of QCD (purely dynamical generation of quantities not present in the fundamental Lagrangian; a finite range for the gauge field configuration). We shall now review the indications that this similarity might not be accidental.

c) $\langle \vec{F}_{\mu\nu} \cdot \vec{F}^{\mu\nu} \rangle$ and confinement in QCD.

The effective-action formalism has been applied to $SU(2)_c$ Yang-Mills theory without fermions [41], with the result that a minimum occurs at a nonzero value of $Tr(\vec{F}_{\mu\nu}^{\,2})$:

$$g^2\, Tr(\vec{F}_{\mu\nu}^{\,2}) = 2\Lambda^4 \qquad (2.93)$$

One may think of this condition as being realized by a constant, homogenous color-magnetic field $\vec{B}$ pointing in a fixed direction of

3-space (let us choose the z-direction for definiteness). Its magnitude is $B=\Lambda^2/g$. It turns out, however, that this minimum cannot be absolute [42]: the energy of the state develops an imaginary part for distances larger than $d_c \sim 1/\sqrt{gB}$. The gauge field must have an unstable mode W to cause the decay of this false vacuum.

In the presence of the fields W and B, the only nonvanishing field strength is [42]:

$$F_{12}^{3} = B - 2g|W|^2 \tag{2.94}$$

The classical energy is therefore

$$\frac{1}{2}\,\mathrm{Tr}\,\vec{F}_{\mu\nu}^{\,2} = \int d^3x \left[\frac{1}{2}B^2 - 2gB|W|^2 + 2g^2|W|^4\right] \tag{2.95}$$

The decay of the false vacuum (2.93) can thus be described as a dynamical Higgs phenomenon and the unstable mode W can be thought of as a Higgs field of mass

$$m^2 = gB/2\pi \tag{2.96}$$

This analysis can be generalized to $SU(N)_c$ gauge theory [42] and, in particular, the result is valid for N=3. The physical implication is that in the true vacuum of QCD, the color-magnetic field cannot be homogenous over distances larger than $d_c \sim \Lambda^{-1}$. The Copenhagen school has extensively pursued this clue [42,43], using in particular the isomorphism of the Higgs model (2.86) to the relativistic superconductor. It now appears [43] that the vacuum of pure glue QCD is a condensate of vortices of characteristic dimension d_c. With respect to this vacuum:

$$\langle \vec{F}_{\mu\nu} \rangle = 0 \;;\; \langle \vec{F}_{\mu\nu}\cdot\vec{F}^{\mu\nu} \rangle \neq 0 \tag{2.97}$$

Confinement can be thought of as a chromomagnetic Meissner effect and the confinement scale d_c corresponds to the Ginzburg-Landau coherence length.

This picture of confinement implies that chromomagnetic flux must be quantized according to the group Z(3), the center of the gauge group $SU(3)_c$. Z(3) is thus identified as the dynamical symmetry which characterizes the confining phase of QCD. Z(3)-invariance can be shown to imply that the vacuum expectation value of the "Wilson loop" operator

$$\tilde{W} = \langle \exp\left(ig \oint d\vec{x}_\mu \cdot d\vec{A}^\mu\right) \rangle \qquad (2.98)$$

obeys an "area law":

$$\tilde{W} = \exp\left[-\frac{k}{2} g^2 d_c^2 \langle \vec{F}_{\mu\nu} \cdot \vec{F}^{\mu\nu} \rangle\right] \qquad (2.99)$$

(k=0,1,2) [44]. This behavior is commonly used as an indicator of confinement in nonperturbative calculations of QCD.

In solid state physics there are two distinct types of superconductors: type I is characterized by positive surface energy at its interface with normal material, whereas type II has negative surface energy. Nair and Rosenzweig [45] have shown that, as naively expected from the requirement that the domain shape should minimize the total energy, type I corresponds to bag-like spherical vacuum domains and type II to stringlike domains. However, domain walls could have violent long-wavelength fluctuations and even become delocalized as a consequence of quantum corrections which cannot be seen in the semiclassical analysis. By the same token, the field strengths could present large dispersions about the mean values (2.97).

We have seen that the nonvanishing of the vacuum condensate $\langle \vec{F}_{\mu\nu} \cdot \vec{F}^{\mu\nu} \rangle$ is consistent with some of the main features nonperturbative QCD must demonstrate. The effective-action formalism is, however, unable to produce a quantitative derivation of such behavior from the chromodynamic Lagrangian without introducing a large number of ad-hoc approximations. Another problem is the interplay with the quark fields, to which we now turn.

d) $\langle \bar{\psi}\psi \rangle$ and chiral-symmetry breaking in QCD.

The nonvanishing vacuum expectation value $\langle \bar{\psi}\psi \rangle$ mixes left-handed and right-handed quarks and thus confirms the breaking of chiral symmetry by QCD. Cornwall, Jackiw and Tomboulis [46] have generalized the effective-action formalism to study $\langle \bar{\psi}\psi \rangle$. Consider a theory of massless fermions in Euclidean space-time:

$$Z[\psi, A] = \int [D\psi][DA] \exp\left\{ -\int d^4x \left(\tfrac{1}{4} F^2 + \bar{\psi} \not{D} \psi \right) \right\} \qquad (2.100)$$

(see Appendix A for the transition from the Minkowskian to the Euclidean action; we now set $\hbar=1$). Discard the pure gauge field Lagrangian in order to concentrate on the specific effects of the fermions. Turning on the source function $J(x,y)$ we have

$$Z[J] = \int [D\psi] \exp\left\{ -\int d^4x \left(\bar{\psi} \not{D} \psi - \bar{\psi} J(x,y) \psi(y) \right) \right\} \qquad (2.101)$$

We can again define an effective action by a Legendre transformation to the independent variable $\Delta = \langle \bar{\psi}\psi \rangle$. The condensate with respect to the true vacuum is then again among the roots of the equation $d\Gamma/d\Delta = 0$. Eq. (2.101) can be rewritten as

$$\begin{aligned} \exp(-W[J]) &= \int [D\psi] \exp\left\{ -\int d^4x \left(\bar{\psi} \Delta^{-1} \psi + \bar{\psi} (\not{D} - \Delta^{-1}) \psi + J \bar{\psi}\psi \right) \right\} \\ &= \exp\left\{ -\mathrm{Tr} \ln \Delta^{-1} + \mathrm{Tr} (\Delta^{-1} - \not{D}) \Delta + D \right\} \qquad (2.102) \end{aligned}$$

where D stands for the sum of all vacuum diagrams with at least one gluon vertex. In performing the functional integration over fermion fields, (2.75") has been generalized by representing the spinor fields $\Psi(x)$, $\bar{\Psi}(x)$ as anticommuting c-numbers ("Grassmann variables") η, $\bar{\eta}$ defined at each discrete space-time point, then using the theory of Grassmann integration to find [47]:

$$\int (D\eta)(D\bar{\eta}) \exp(\bar{\eta} M \eta - \bar{\nu}\bar{\eta} - \nu\eta) = = (\det M) e^{-\bar{\nu} M^{-1} \nu} \qquad (2.75''')$$

So the effective action is

$$\Gamma[\Delta] = -\operatorname{Tr} \ln \Delta^{-1} + \operatorname{Tr}(\Delta^{-1} - \mathcal{D})\Delta + D \qquad (2.103)$$

Now the source term J must be adjusted such as to cancel all corrections to the prescribed propagator Δ. For example, the two diagrams in Fig. 2.10 must cancel exactly. Therefore, the only diagrams contributing to (generated by) $\Gamma[\Delta]$ are 2-particle irreducible (2PI), see Fig. 2.11. The final expression

$$\Gamma[\Delta] = -\operatorname{Tr} \ln \Delta^{-1} + \operatorname{Tr}(\Delta^{-1} - \mathcal{D})\Delta - (2PI) \qquad (2.104)$$

is thus independent of J and involves only Δ.

We are again faced with the generic problem of having to sum an infinite series of diagrams. To obtain any results at all one must truncate the series somehow. Keeping only the first diagram in Fig. 2.11 leads to

$$\begin{aligned} 0 = \frac{d\Gamma}{d\Delta} &\approx \frac{d}{d\Delta}\left[\operatorname{Tr} \ln \Delta + \operatorname{Tr}(\Delta^{-1} - \mathcal{D})\Delta - \bigodot\right] = \\ &= \Delta^{-1} - \Delta^{-1}\Delta\Delta^{-1} + (\Delta^{-1} - \mathcal{D}) + \frown \\ &\Rightarrow \Delta^{-1} = \mathcal{D} - \frown \end{aligned} \qquad (2.105)$$

This is precisely the Hartree-Fock approximation to the equations of motion, obtained after integrating out the gauge fields. If the gluon propagator is denoted by $D_{\mu\nu}(x-y)$, the equation of motion for $\psi(x)$ may be written as

$$\gamma^\mu (\partial_\mu - igA_\mu)\psi(x) = 0$$

$$\therefore \gamma^\mu \left[\partial_\mu + g^2 \int d^4y\, D_{\mu\nu}(x-y)\bar{\psi}(y)\gamma^\nu\psi(y)\right]\psi(x) = 0 \qquad (2.106)$$

In the Hartree-Fock approximation this becomes

$$\not\partial\psi(x) + g^2\left(\int d^4y\, \gamma^\mu D_{\mu\nu}(x-y)\Delta\right)\gamma^\nu\psi(x) \approx 0 \qquad (2.107)$$

which is indeed equivalent to (2.105). This fact reassures us as to the validity of simply neglecting the gauge field Lagrangian in writing down Eq. (2.101) - the result is the same as that obtained, to the same degree of approximation, by properly integrating out the gauge field. One can again draw an analogy to superconductivity, this time to the microscopic BCS theory which leads to an equation analogous to (2.105) (the "gap equation").

The effective-action formalism for the evaluation of $\langle\bar{\psi}\psi\rangle$ has several conceptual problems even after one cures the lack of manifest gauge-invariance in the above simplified presentation. In particular, examples are known where $\Gamma[\Delta]$ is not bounded below. Nevertheless, one justifiably hopes that even the approximation (2.105) contains much of the right physics, for it leads to results which are qualitatively confirmed by more reliable computations. For future reference, let us quote a calculation by Peskin [48] which indicates a major difference between chiral-symmetry breaking in QCD and superconductivity in BCS theory.

Upon inserting the Landau-gauge trial form for the propagator

$$\Delta = \frac{1}{-i\not{p} + \Sigma(p)} \tag{2.108}$$

into Eq. (2.105) and neglecting coupling strength renormalization, he finds that the chiral-symmetric vacuum described by $\Sigma=0$ is unstable as soon as

$$\alpha_s > \frac{\pi}{4} \tag{2.109}$$

In BCS theory, an arbitrarily small attractive force due to phonon exchange can bring about the condensation of Cooper pairs. In QCD, gluon exchange can bring about condensation of quark-antiquark pairs only when the coupling strength exceeds a certain critical value.

d) Summary.

The success of the ITEP (or "SVZ") sum rules suggests that nonperturbative chromodynamics is characterized by nonvanishing vacuum expectation values for the operators $\vec{F}^{\mu\nu}\cdot\vec{F}_{\mu\nu}$ and $\bar{\psi}\psi$. Such objects are central in the effective-action approach to the semiclassical solution of quantum field theories. Qualitatively, effective-action studies do produce encouraging results, linking the gluon condensate to confinement and the pair condensate to chiral-symmetry breaking. However, the approximation schemes they are forced to employ in order to actually calculate are not systematic enough to yield truly dependable results. A more systematic approach to the calculation of Z[J] is thus required.

2.4. LATTICE QCD

a) Latticization.

Recall, at this point, equations (2.75'') and (2.75'''). In defining the integration measure which was used to evaluate the bosonic and fermionic functional integrals in the Gaussian approximation, space-time had to be discretised as an intermediate step. The other tactical device which simplified the calculation of Z[J] was to do the integration in Euclidean space-time. Let us take Euclideanization and subsequent discretization more seriously and write down the corresponding Z-functional for the scalar field ϕ:

$$Z = \int d\phi_1 \cdots d\phi_n \exp\left[-\frac{1}{\hbar} S_E(\phi_1, \cdots \phi_n)\right] \qquad (2.110)$$

where $\phi_i = \phi(x_i)$ and we have temporarily reintroduced h. But this looks exactly like the partition function for a statistical system of n atoms with velocity-independent interactions at a temperature $\hbar$! Thus we have mapped the original problem in quantum field theory onto a four-dimensional problem in classical equilibrium statistical mechanics.

Since statistical mechanics has a rich technology of analytical and numerical methods, one tries to solve QCD in its statistical formulation and then translate the results back into quantum field theoretical language and into the attendant phenomenology. The discrete set of space-time points on which the matter fields are supported is called a "lattice" and the Euclidean discretized version of QCD is called "lattice QCD".

It is customary to latticize on a "hypercubic" regular lattice with constant "lattice spacing" a (see Fig. 2.12 for d=2). The fundamental length scale a introduces an ultraviolet momentum cutoff Λ . So latticization is a regularization prescription (note that a statistical model like (2.110) always is finite). While it is natural to implement gauge-invariance on the lattice (see below) this regularization scheme is not O(4) rotation invariant as long as $a\neq 0$. O(4) rotation invariance had better be restored when the continuum limit $a \to 0$ is taken at the end of the calculation, otherwise the original quantum field theory in Minkowski space has lost its Lorentz invariance.

Now consider a d=1 Euclideanized scalar field theory

$$S_E = \int dx \left[(\partial_x \phi)^2 + m^2 \phi^2 \right] \qquad (2.111)$$

and let us discretize the derivative in a naive way:

$$\partial_x \phi \to \frac{\phi(x_i + a) - \phi(x_i)}{a} \qquad (2.112)$$

Since $\int dx \to a \sum_i$,

$$S_E \to S_L = a \sum_i \left(\frac{\phi_{i+1} - \phi_i}{a} \right)^2 + a m^2 \sum_i \phi_i^2 \qquad (2.113)$$

Setting h=1, we scale all dimensional quantities with respect to a:

$$\begin{aligned} \phi_L &= a^{-1/2}\, \phi \\ m_L &= a m \end{aligned} \qquad (2.114)$$

Hence, dropping the subscript L from the field variables,

$$Z = \int d\phi_1 \cdots d\phi_n\, e^{-(2+m_L^2) \sum_i \phi_i^2}\, e^{+2 \sum_i \phi_i \phi_{i+1}} \qquad (2.115)$$

This is the partition function of a one-dimensional spin chain at temperature $1/T = 1/2$ with nearest-neighbor interaction. This problem is exactly solvable in statistical mechanics. But we notice that by the act of scaling the lattice spacing has disappeared from the partition function. How are we then to take the continuum limit $a \to 0$?

Measuring all lengths in units of a means that any fixed physical length L will appear larger on a finer lattice (a is small) than on a coarser lattice (a is large), see Fig. 2.13. In a statistical system of spins, the spin-spin correlation length depends on the inverse temperature β. This correlation length diverges at a phase transition of order ≥ 2, and only if such a transition is present. Therefore, a given lattice version of a quantum field system only stands chances of having a sensible continuum limit if it has a phase transition of order two or higher when viewed as a statistical system. As mentioned above, all physical symmetries of the continuum should be restored in this transition (and any unphysical lattice symmetries should disappear). Furthermore, different choices of the lattice, of the discrete derivative or of irrelevant terms in the Lagrangian (such as total derivatives) should lead to the same continuum limit; however, they do give rise to widely different statistical systems. Thus we must expect that all statistical models one can obtain from a given quantum field system should be in the same "universality class" as far as the transition to the continuum is concerned: their critical behavior should be governed by the same critical exponents.

Mathematically, an observable of dimension mass should behave as

$$M = a^{-1} f(\beta) \tag{2.116}$$

If it is to be unaffected by our taking the continuum limit $a \to 0$, then there must exist a critical point β_c such that $f(\beta_c) = 0$. For a quantity of mass dimension d we must have

$$M^d = a^{-d} F^{(d)}(\beta) \; ; \; F^{(d)}(\beta) = C \left[f(\beta) \right]^d \tag{2.117}$$

The last relation is the "scaling hypothesis". To transcribe these requirements for QCD we need to identify β. Let us therefore construct the lattice action for pure-glue QCD.

b)· Glue on the lattice.

In many respects, it is more natural to state the idea of local gauge-invariance on the lattice than in the continuum. Consider a four-dimensional hypercubic lattice and place on each link connecting site n to site $n+\mu$ ($\mu=1,2,3,4$) an $SU(3)_c$ matrix

$$U_\mu(n) = \exp\left(iga\vec{A}_\mu \cdot \vec{T}\right) \tag{2.118}$$

With a link in the backward direction one can associate the matrix $U_\mu^{-1}(n) = U_{-\mu}(n+\mu)$. If we imagine a local color frame at each site, then the orientation of these frames in color space should be locally arbitrary [49,50]. So if a local rotation in color space is accomplished by the matrix

$$G(\vec{\beta}(n)) = e^{-i\vec{T}\cdot\vec{\beta}(n)} \tag{2.119}$$

then local gauge-invariance means that $U_\mu(n)$ must transform as

$$U_\mu(n) \to G(n)U_\mu(n)G^{-1}(n+\mu) \tag{2.220}$$

The action of pure $SU(3)_c$ theory on the lattice should thus be built out of U's much as the continuum action was built out of A's. A simple way to achieve a gauge-invariant action is to form the product of U matrices taken around a closed path, because this will cause all $SU(3)_c$ group indices to contract. The smallest (most local) closed paths are elementary squares or "plaquettes" (Fig. (2.12)). This leads to the original Wilson-Polyakov-Wegner action [50-52]:

$$S_G = -\frac{1}{2g^2}\sum_{n,\mu,\nu} \mathrm{Tr}\left[U_\mu(n)U_\nu(n+\mu)U_{-\mu}(n+\mu+\nu)U_{-\nu}(n+\nu) + H.C.\right]$$
$$= \frac{6}{g^2}\sum_{\Box}\left(1-\frac{1}{3}\mathrm{Re}\,\mathrm{Tr}\,U_\Box\right) \qquad (2.121)$$

where $\Box$ stands for plaquette.

The classical (g = constant) limit of this action as a—>0 is just the standard continuum Euclidean action $S = (1/4)\int d^4x\, \vec{F}_{\mu\nu}\cdot\vec{F}^{\mu\nu}$ and O(4) rotation invariance is properly restored in this limit. The difference between the hypercubic and the O(4)-invariant theory can explicitly be seen to disappear into higher-order terms in a.

The quantum continuum limit must be obtained as outlined in our general presentation on latticization: the lattice theory should be calculated at weaker and weaker color coupling (since $\beta = 6/g^2$) and scaling should set in at some β. The significance of going from strong to weak coupling is depicted in Fig. 2.13. Weak coupling lattice QCD should be equivalent to perturbative continuum QCD. So setting $\Lambda = a^{-1}$, the approach to the continuum limit should be governed by the solution to the renormalization group equation (2.18) for an observable with dimension mass. To two-loop order we have (see Eq. (2.25))

$$m = C_1 \Lambda \left(b_0 g^2\right)^{-b_1/(2b_0)^2} \exp\left(-\frac{1}{2b_0 g^2}\right)\left[1+o(g^2)\right] \qquad (2.122)$$

Neglecting the $o(g^2)$ correction in (2.122) is called "asymptotic scaling" [53]. For mass ratios, we expect

$$m_1/m_2 = C_{12} + o\left[(Q^2/\Lambda^2)\cdot \ln(Q/\Lambda)\right] \qquad (2.123)$$

This is called "pre-asymptotic scaling" [53] because the correction terms are exponentially small in g so (2.123) should be seen at lower than (2.122). Pre-asymptotic scaling is generally deemed a sufficient signal for the continuum transition.

In the opposite limit of strong coupling, or high temperature in the statistical model, one can consider the question of confinement. The equivalent of the Wilson loop (2.98) taken around a closed contour of lattice links is

$$\langle \prod_C U_\mu(n) \rangle = \left[\int \prod_{n,\mu} [DU_\mu(n)] \prod_C U_\mu(n) e^{-S} \right] Z^{-1} \qquad (2.124)$$

because, by the interpretation of Z as a partition function, the expectation value of any observable 0 must be given by

$$\langle O \rangle = \int \prod_{n,\mu} [DU_\mu(n)]\, O(U) e^{-S} / Z \qquad (2.124')$$

In a compact group like $SU(3)_c$, the integration measure [dU] is the invariant "Haar measure" defined by the properties [50-52]

$$\int [dU] = 1$$
$$\int [dU] f(U) = \int [dU] f(U_0 U) \qquad (2.125)$$

where U_0 is an arbitrary element of the group and f an arbitrary but sensible function. For $\beta \ll 1$ we can write

$$e^{-S} \approx \prod_\square e^{-\beta \, Tr \, U_\square} \qquad (2.126)$$

and the properties of the Haar measure yield the leading-order strong coupling result

$$\langle \prod_C U_\mu(n) \rangle \sim \exp[N(C) \ln g^2] \qquad (2.127)$$

where N is the number of plaquettes enclosed in the minimal surface determined by the contour C. This is just the loop area measured in dimensionless units, so we conclude that the strong-coupling limit of the Wilson action does exhibit confinement.

The "heavy quark potential" V(r) which acts between a static color source (infinitely massive quark) and a static color sink (infinitely massive antiquark) can be defined on the lattice as [51]

$$V(r) = \lim_{T \to \infty} \ln \langle \prod_c U_\mu(n) \rangle \qquad (2.128)$$

where C(r,T) is the Euclidean "world line" of the static $Q\bar{Q}$ pair configuration held apart at a distance r for a time T (see Fig. 2.14). The leading-order strong coupling result (2.127) implies

$$\begin{aligned} V(r) &= \varkappa |r| \\ \varkappa &= \ln g^2 + \cdots \end{aligned} \qquad (2.129)$$

In this limit, V(r) is linearly confining and the "string tension" $\varkappa$ is defined. Sophisticated calculational methods based on high-temperature techniques in statistical mechanics improve this calculation and push it to higher orders, that is, to weaker coupling [54].

The Wilson action thus appears to contain the right physics in both extreme limits ($g \to 0$, $g \to \infty$). If confinement is to survive the transition to the continuum, the extrapolation from strong to weak coupling must be smooth. However, even the most involved analytical strong-coupling calculations have so far been unable to match up smoothly with analytical weak-coupling calculations [55]. The only known successful way to interpolate between strong and weak coupling is to evaluate the partition function numerically, using the Monte Carlo method [56] or ramifications thereof.

This situation can be described by an analogy to the Riemann integral: we recall that it too is defined in terms of finite differences. In the 18^{th} century the only way to evaluate integrals was to develop the calculus, but nowadays one may use fast computers to calculate any integral directly from its discrete definition (even integrals which are not solvable by the calculus). For the nonperturbative evaluation of functional integrals we have been illustrating the fact that an advanced calculus does not even exist. One therefore tries (not without success) to evaluate functional integrals numerically on the lattice. Analytical calculations remain of course necessary in order to guide, interpret and check numerical computations. In particular, Monte Carlo calculations of the average plaquette energy $1-\mathrm{ReTr}U_{\square}/3$ and of the string tension reproduce all reliable analytical results at strong and weak coupling while interpolating smoothly between them [55].

More generally, Monte Carlo methods have been applied to the study of the phase structure of the Wilson action. Subject to the ubiquitous computer-power related limitations of such calculations, all indications are that for $SU(N)_c$, $N \geq 2$ pure gauge theories there is no phase transition at any finite β but that there is a higher-order continuum restoration transition at $\beta \rightarrow \infty$ [55]. This is exactly what is necessary for lattice QCD to make sense: a phase transition at finite β would mean strong-coupling confinement could not be a property of the continuum, but a higher-order transition must occur as $a \rightarrow 0$. Restoration of O(4) symmetry in this transition has been demonstrated for both $SU(2)_c$ and for $SU(3)_c$ [57]. In the latter case, rotation -

invariance seems to be approximately restored at $\beta = 5.7$.

Obviously, the inclusion of quark fields into lattice QCD is mandatory before any confrontations with experiment can be attempted. There are, however, certain quantities specifically associated with the pure glue sector whose study on the lattice may already be phenomenologically significant. Of these, we shall be mainly interested in the gluonic vacuum condensate $\langle \vec{F}_{\mu\nu} \cdot \vec{F}^{\mu\nu} \rangle$, the heavy quark potential V(r) and the fate of confinement in finite-temperature lattice QCD.

Present calculations of the gluon condensate, as reported in [58], are consistent with the SVZ value (2.65). The Copenhagen group is attempting to test their picture of the vacuum using numerical lattice methods [59]. We have seen that the naive strong-coupling analysis of the Wilson partition function indeed suggests the existence of thin flux tubes ("strings") between a heavy quark and antiquark. The same conclusion is reached in the Hamiltonian formulation of pure glue lattice QCD [60]. In going beyond the Gaussian approximation, lattice QCD can analyze the effect of string fluctuations. Let us show in more detail how string fluctuations show up in recent calculations of V(r) and of the string tension.

Motivated by the phase structure of lattice QCD, let us assume that the glue configuration between static color poles is a fluctuating thin flux tube even in the continuum. Let the ends of the tube be pinned down at x=0 and x=r. "Thin" means that the width w of the tube is small compared to r. The string is allowed to fluctuate in a transverse dimension y so the fluctuating string can be described by a two-component vector field $\vec{\xi}(x,y)$. At the ends of the string,

$\vec{\xi}(0,y)=\vec{\xi}(r,y)=0$. All relevant physics should be contained in a long-wavelength ($\lambda \gg w$) effective Lagrangian which should be built out of $\vec{\xi}$ and its derivatives. One requires [61] that this effective Lagrangian density be invariant under Poincaré transformations in the (x,y) plane and under O(2) translations and rotations of the vector $\vec{\xi}$. The latter requirement precludes mass terms for the fluctuation field. Therefore L must be made up of derivatives only:

$$L = \partial_i \vec{\xi}\,\partial^i \vec{\xi} + b(\partial_i \partial^i \vec{\xi}\,\partial_j \partial^j \vec{\xi}) + c(\partial_i \vec{\xi}\,\partial^i \vec{\xi})^2 + \cdots \qquad (2.130)$$

By dimensional analysis, the terms proportional to the parameters b, c,... are of higher order in w/λ . So the effective Lagrangian density for long-wavelength modes reduces to

$$L_{eff} = \partial_i \vec{\xi}\,\partial^i \vec{\xi} \qquad (2.131)$$

Let us now enclose these massless vector bosons in a two-dimensional box of side r. The ground state of the system is the nonfluctuating straight string $\vec{\xi}=0$ and we know its energy is $E=V(r)=\chi r$. To compute the shift in the energy due to the leading-order long-wavelength fluctuations we have to do a sum over normal modes

$$\Delta E(r) = \frac{1}{2}\sum_n \varepsilon_n = \frac{\pi}{2r}\sum_n n \qquad (2.132)$$

which is divergent. We must first do the sum with a convergence factor $e^{-\eta n}$ and let $\eta \to 0$ at the end. We obtain

$$\Delta E(r;\eta) = \frac{\pi}{2r}\sum_n n e^{-\eta n} = \frac{\pi}{2r}\frac{d}{d\eta}\sum_n e^{-\eta n} =$$
$$= -\frac{\pi}{2r}\frac{d}{d\eta}\left(\frac{1}{e^{\eta}-1}\right) = -\frac{\pi}{2r}\sum_n B_n (n-1)\eta^{n-2}/n! \qquad (2.133)$$

where B_n are Bernoulli numbers. Only the n=2 term survives as $\eta \to 0$ so

$$\Delta E(r) = -\frac{\pi}{2r}\frac{B_2}{2} = -\frac{\pi}{24}\cdot\frac{1}{r} \qquad (2.134)$$

In d-2 transverse dimensions we must thus expect that the potential for sufficiently large quark-antiquark distances has the form

$$V(r) = -\frac{\alpha}{r} + \varkappa r$$

$$\alpha \to \frac{(d-2)\pi}{24} \qquad (2.135)$$

Stack [62] has used the parametrization (2.135) to fit his Monte Carlo measurements of the potential in pure glue $SU(2)_c$ and $SU(3)_c$ lattice QCD. As expected from the fact that a potential with the same functional form has been proposed for small r by perturbative arguments [63], one finds that α and $\varkappa$ are actually functions of r (different values for α and $\varkappa$ give the best fit to data taken in different regions of r). However, it is found that an effective global fit with "compound" r-independent parameter values gives an excellent account of all numerical data obtained from r=0.01 fm to r=1 fm. The corresponding $SU(3)_c$ string tension as reported by Otto and Stack [62] is $\Lambda/\sqrt{\varkappa}$ = $(9.4\pm 0.3)\times 10^{-3}$. By working with the same functional form but from the asymptotic-freedom side, the authors of [63] find $\Lambda/\sqrt{\varkappa} = 9.6\times 10^{-3}$. Their work also indicates that asymptotic scaling only holds for $\beta \gtrsim 6$ while preasymptotic scaling may hold for $\beta \gtrsim 5.6$ (compare this to $\beta \simeq 5.7$ for the restoration of O(4) invariance).

We have seen that the very act of latticization defines a temperature in the statistical analogue of a quantum field system. Varying this parameter means to study the system at various values of the hypercubic lattice spacing. On the other hand, assume that we start from a continuum scalar field which is supported not over all of Euclidean space-time but only over a slab of finite extension τ in the "time" direction. Since the final and initial states are identical in the Z-functional, we must have $\phi(x,0)=\phi(x,\tau)$. With this constraint, we can write

$$Z=\int[d\phi]\exp\left\{-\tau\int_0^{\tau}dt\int d\vec{x}\,L(\phi,\partial\phi)\right\} \qquad (2.136)$$

Upon latticization the factor τ which has thus been smuggled into the theory will give rise to a second temperature variable $T=1/\tau$ which will be present even if we decide to fix β to unity. Since numerical computations inevitably deal with finite lattices, all numerical results on the lattice will be affected not only by finite-volume effects but also by finite-temperature effects due to the finite number n_t of lattice sites in the time direction: $T=1/an_t$. One must therefore study such effects in order to correct for them in "ordinary" calculations.

Finite field-temperature lattice QCD is furthermore believed to be of physical interest in itself, the most often invoked potential applications being heavy-ion collisions, the early universe and astrophysical matter under extreme conditions [64]. The crucial parameter in finite field-temperature lattice QCD is the special Wilson loop defined in Fig. 2.14b [65]. It is the product of all link matrices for the links oriented in the temporal direction at a fixed space coordinate $\vec{x}$ and is closed by virtue of periodicity. It would correspond to the world line of a single static color charge placed at a fixed spatial position. Thus its expectation value measures the free energy required to produce such a configuration:

$$\langle L_{\vec{x}}\rangle = \exp(-\Delta F/T) \qquad (2.137)$$

A confining theory should be characterized by $\Delta F=\infty$ and hence by $\langle L_{\vec{x}} \rangle=0$. Svetitsky and Yaffe [66] have pointed out that the order parameter $\langle L_{\vec{x}} \rangle$ must be zero as long as the ground state of the theory is invariant under Z_3, the center of $SU(3)_c$. Indeed, it is easy to see that the Wilson action is invariant under the multiplication of all the link matrices with an element of the center but $L_{\vec{x}}$ is not, so its expectation value changes sign: $\langle L_{\vec{x}} \rangle \rightarrow -\langle L_{\vec{x}} \rangle$. Note that this is in agreement with the analogy to superconductivity (Section 2.3c). These authors point out, however, that one should expect Z_3 symmetry to be broken for sufficiently high field temperature, at least in the strong-coupling region.

This is precisely what one sees in Monte Carlo studies of the problem [67]. There is undoubtedly a strong first-order phase transition from a confinement phase at low temperature, where $\langle L_{\vec{x}} \rangle=0$, to a high-temperature "color plasma" phase with $\langle L_{\vec{x}} \rangle \neq 0$. The critical temperature T_c is estimated to be of the order 260 MeV if the string tension is used to set the scale (which is not an unambiguous procedure). Would this phenomenon still be present in full QCD with dynamical quarks?

c) Quarks on the lattice.

There is a fundamental problem with the latticization of the Dirac equation. This may be anticipated from the fact that Lorentz invariance, which is the guiding principle of the Dirac equation, is absent on the lattice. While it is natural to assign (vector) gauge fields to the links of the lattice, bosonic matter fields to the sites and tensors to the plaquettes, there is no obvious place for the fermions. If one places the fermions on the links all the same one runs into trouble.

To understand the origin of the trouble, let us briefly return to continuum QCD. If the current quark masses are set to zero, the chromodynamic Lagrangian will not only have its $SU(N_f)_L \times SU(N_f)_R$ chiral symmetry but will also be invariant under the axial U(1) transformation

$$\psi(x) \rightarrow e^{-i\gamma_5 \theta} \psi(x) \qquad (2.138)$$

This is due to the decoupling of left-and right-handed fermions. It is known, however, that any theory of massless fermions interacting with massless gauge fields is pathological due to infrared singularities (see Section 2.2). Therefore one may never simply set the quark mass to zero but must start with a massive theory and then take the limit m—> 0 (note that our argument in Section 2.1 was that the electroweak current quark masses are irrelevant for chromodynamics regardless of their values). Now, if one starts with a massive theory, then the fermions will have a definite helicity in the massless limit and will be able to make a transition to a virtual state of the opposite helicity by emitting an on-shell gauge boson. Therefore the radiative corrections must destroy the formal invariance under (2.138).

The current J^μ corresponding to the transformation (2.138) is indeed not divergenceless. Gauge-invariant, Lorentz-invariant continuum regularization of the "triangle graph" shown in Fig. 2.15 introduces an anomalous term:

$$\partial_\mu J^\mu \sim \frac{1}{2} \epsilon^{\mu\nu\alpha\beta} F^a_{\mu\nu} F^a_{\alpha\beta} \equiv \tilde{F}F \qquad (2.139)$$

(summation over color indices is implied). This is the well-known Adler-Bell-Jackiw (ABJ) anomaly [9,68].

At first sight it seems that the anomaly should vanish as $m \to 0$ since $\tilde{F}F$ can be written as a surface integral:

$$\tilde{F}F = \partial_\mu \left\{ 2\epsilon^{\mu\nu\alpha\beta} \left[\vec{A}_\nu \cdot \partial_\alpha \vec{A}_\beta + \frac{g}{3} \vec{A}_\nu (\vec{A}_\alpha \times \vec{A}_\beta) \right] \right\} \quad (2.140)$$

But if $\vec{F}_{\mu\nu}(x)$ is to vanish as $|x| \to \infty$, $A_\mu = \vec{A}_\mu \cdot \vec{T}$ must tend to a gauge transform of $A_\mu = 0$:

$$A_\mu(x) \to \frac{i}{g} U(x) \partial_\mu U^+(x) \qquad (|x| \to \infty) \qquad (2.141)$$

where the $SU(3)_c$ matrix U is a mapping of the three-dimensional sphere at $|x| = \infty$ into the gauge group. For a compact Lie group like SU(3), such mappings fall into homotopy classes each of which is characterized by an integer value of the Pontriyagin index n:

$$n = \int d^4x \frac{g^2}{32\pi^2} \tilde{F}F \qquad (2.142)$$

Therefore continuum Euclidean QCD must admit field configurations with $n \neq 0$ if the ABJ anomaly is to persist. The minimum-action solutions to the classical field equations with $n = +1$ are called "instantons" [69].

The effective-action analysis we sketched in Section 2.3 has been applied to fermions in a one-instanton gauge field configuration [48]. It is found that, aside from breaking the U(1) axial symmetry, instantons add a further term to the right-hand side of Eq. (2.105), a term which dynamically breaks $SU(N_f) \times SU(N_f)$ chiral symmetry for sufficiently large g (corresponding to sufficiently large instanton radii). The effects of pair condensate formation through one-gluon exchange and of instantons thus both destabilize the chirally symmetric vacuum.

Can the lattice method of regularization break the axial U(1) symmetry? Consider the massless free Dirac action

$$S_F = \sum_{x,x',\mu} \bar{\Psi}(x)\gamma^\mu \partial_\mu(x,x')\Psi(x') \qquad (2.143)$$

and "naively" define the lattice derivative as in Eq. (2.112), so that the momentum operator becomes $(\sin ap_\mu)/a$, $p_\mu \in (-\pi/a, \pi/a]$. Thus the inverse fermion propagator on the lattice will read

$$\Delta^{-1}(p) \rightarrow \sum_\mu \gamma^\mu \frac{\sin ap_\mu}{a}, \quad p_\mu \in \left(-\frac{\pi}{a}, \frac{\pi}{a}\right] \qquad (2.144)$$

This has 2^d zeros (each p_μ can be 0 or π/a) corresponding to 2^d fermions with $2^{d/2}$ components making a total of $2^{3d/2}$ degrees of freedom. Each of the 2^d fermion fields is afflicted by an anomaly in the weak-coupling limit, but the anomalies cancel between the $p_\mu=0$ and the $p_\mu=\pi/a$ modes [70]. Thus "species-doubling" is just a way of making the presence of U(1) axial invariance on the lattice compatible with its absence in the continuum.

The Susskind-Kogut approach to the fermion problem is to make the best out of this fact [71]. The essential point is that lattice fermions do not need to have $2^{d/2}$ components like their continuum counterparts which are ruled by Lorentz invariance. One can therefore diagonalize the naive action in spin space by making a so-called Kawamoto-Smit transformation [72] from $2^{d/2}$-component Ψ-spinors to one-component "staggered" spinors χ. For d=4,

$$\Psi(n) = (\gamma_1)^{n_1}(\gamma_2)^{n_2}(\gamma_3)^{n_3}(\gamma_4)^{n_4}\chi(n) \qquad (2.145)$$

The fermion degrees of freedom have been spread out over the lattice, with one component at each site. The sixteen species of quarks (per flavor) corresponding to Eq. (2.144) have been realized as four spinor components times four "odors" of χ's. The lattice can therefore be divided into "even" and "odd" sites, depending on whether $\sum_i n_i$ (i=1,4) is an even or an odd integer. One can define the following transformations:

$$\begin{aligned} \chi(n) &\to e^{i\alpha_e}\,\chi(n) \qquad (\text{even sites}) \\ \chi(n) &\to e^{i\alpha_o}\,\chi(n) \qquad (\text{odd sites}) \end{aligned} \tag{2.146}$$

In the massless limit, this is a continuous $U(1)_e \times U(1)_o$ symmetry which is broken if $\langle\bar{\chi}(n)\chi(n)\rangle \neq 0$ (in particular, by a fermion mass term). In the Susskind formulation there is thus a direct lattice analogue of chiral-symmetry, of its breaking and restoration. In the continuum limit, the spinor and odor degrees of freedom untangle, the odors collapse into a single flavor and continuum regularization creates the correct ABJ anomaly. Generalizing from the free Dirac action to QCD, the lattice fermion action according to Susskind and Kogut has the form

$$S_F^{KS} = \frac{1}{2}\sum_{n,\mu} \bar{\chi}(n)\eta_\mu\left[U(n,\mu)\chi(n+\mu) - U^\dagger(n-\mu,\mu)\chi(n-\mu)\right];$$

$$\eta_1 = 1\,,\quad \eta_2 = (-1)^{n_1}\,,\quad \eta_3 = (-1)^{n_1+n_2}\,,\quad \eta_4 = (-1)^{n_1+n_2+n_3} \tag{2.147}$$

Alternatively, one may explicitly break the axial U(1) on the lattice by adding an artificial mass term to the naive action [73]:

$$\begin{aligned} S_F^W &= \sum_n \bar{\psi}(n)\left[\not{D} + Ma\right]\psi(n) \\ \not{D}\psi(n) &= \sum_\mu\left[(\gamma_\mu - rI)U_\mu(n)\psi(n+\mu) - (\gamma_\mu + rI)U^\dagger(n-\mu)\psi(n-\mu)\right] \\ Ma &= ma + 8r \end{aligned} \tag{2.148}$$

This is the lattice fermion action according to Wilson. The presence of an explicit mass term even in the limit of massless quarks ($m \to 0$), removes the spurious poles: the inverse propagator for free massless quarks now reads

$$\Delta_L^{-1} = 2\sum_\mu \gamma_\mu \sin p^\mu - 2r\sum_\mu \cos p_\mu + 8r \qquad (2.149)$$

On the other hand, there is no longer any trace of the physically crucial continuum chiral symmetry and it is quite tricky to take the limit of zero quark mass in the interacting theory where the "critical mass" M must be renormalized from its free-field value 1/8.

Still another approach to the lattice fermion problem consists in constructing the action such as to make the axial U(1) current diverge in the continuum limit. This is the closest reproduction of the situation in the continuum but it requires the use of a nonlocal derivative operator on the lattice ("SLAC derivative" [74]). Such an action is quite inconvenient for the standard methods of numerical computation. The Nielsen-Ninomiya "no-go theorems" [75] rigorously state the conditions under which no further alternative of putting fermions on a lattice is possible.

The generic form of the lattice QCD action is thus

$$S = S_G + \sum_{n,m} \bar{\psi}(n)\, Q_{nm}(\{U\})\, \psi(m) \qquad (2.150)$$

where the matrix Q depends on the fermion scheme. For numerical simulation purposes, it is convenient to integrate out the fermion fields in the partition function. This is done analogously to the procedure for integrating out the photon field in the Coleman-Weinberg model (Section 2.3) but taking into account the rules of Grassmann integration. The result is

$$Z = \int \prod_{\mu} dU_{\mu} \det(Q\{U\})\, e^{-S_G} \qquad (2.151)$$

So the generalization of pure-glue calculations to full QCD with dynamical current quarks boils down to the calculation of the "fermion determinant" detQ.

Since this is a difficult numerical problem, the first historical attempts to include light fermions have been based on the so-called "quenched approximation", which consists in simply setting detQ=1 [76]. This amounts to neglecting all closed fermion loops in the Feynman diagram expansion of the theory's functionals (n =0 in the language of Eq. (2.14)). It has been shown that this rather drastic approximation does contain much of the right physics- in particular it permits the study of chiral-symmetry breaking [77]. It has mainly been used in hadron mass spectrum calculations [78], where the results can (as usual) be described as "encouraging". In this approximation, the finite field-temperature deconfining phase transition persists and remains strongly first order [79]. At the same time, the study of the order parameter $\langle\bar{\psi}\psi\rangle$ has revealed the existence of a chiral-symmetry restoration transition at a certain temperature T_χ: $\langle\bar{\psi}\psi\rangle \neq 0$ below T_χ (phase of broken chiral symmetry) and $\langle\bar{\psi}\psi\rangle = 0$ for $T \geq T_\chi$ [79]. Moreover, the transition appears to be first order and it seems that $T_\chi \simeq T_c$ [79]. This last relationship is not understood. Hamber and Parisi have observed asymptotic scaling for $\langle\bar{\psi}\psi\rangle$ in the quenched approximation [76,80].

What happens if one actually calculates the quark determinant? This is currently the main topic in lattice QCD and a lot of effort is being made, both numerically and analytically, to go beyond the quenched approximation. As was pointed out by several authors [81], the influence of dynamical light fermions on the d=4 gauge system is equivalent to that of an external magnetic field on a d=3 spin system. Indeed, the fermion term explicitly breaks the Z_3-invariance of the lattice QCD Lagrangian. The Wilson line $L_{\vec{x}}$ can no longer serve as an order parameter because it is nonzero for all values of T due to color screening by dynamical quarks. In the d=3 spin system without a magnetic field there is a second-order phase transition in temperature. It disappears if the external field is strong enough. Does the first-order deconfinement transition in QCD share a similar fate? In the context of numerical calculations this is a quantitative problem which depends crucially on the dependence of the mass parameter on the QCD coupling [82]. These simulations are also very vulnerable to finite-volume effects [83]. Results obtained so far [84] indicate that the deconfinement transition persists but it is not yet clear whether it remains first order. As far as the chiral-symmetry restoration transition is concerned, its existence in the presence of dynamical quarks has been rigorously established by analytical methods in the case of strong-coupling lattice $SU(2)_c$ [85] and it is argued to be second-order in strong-coupling $SU(3)_c$ [86]. Numerically, it seems to still occur at the same critical temperature as the deconfinement transition and to share its order [84].

The influence of the fermion determinant on the $Q\bar{Q}$ potential has been studied by Joos and Montvay [87] for the model system of $SU(2)_c$ with dynamical Wilson quarks. Physically, one expects that light quark-antiquark pairs would screen the color charges of the static pair from each other. Thus the Q and $\bar{Q}$ could experience each other's force field only up to a certain, finite distance which should set the scale of hadron radii. This suggests an analogy to the Schwinger model [88], (spinor electrodynamics in d=2), whose Lagrangian is made up of elementary fermions and of photons, while the observable, gauge-invariant particle spectrum only consists in bosonic bound states of mass m_s. The corresponding potential between two external charges is

$$V_s(r) = \sigma\left(1 - e^{-m_s r}\right) \tag{2.152}$$

Joos and Montvay put this ansatz together with Eq. (2.135) and fit their numerical data with the parametrization:

$$V(r) = -\frac{\alpha}{r} + \sigma\left(1 - e^{-mr}\right) \tag{2.153}$$

Note that for $r \ll m^{-1}$ the second term is $\propto \chi r$, which means that σm defines an effective string tension in the small-r region where screening is as yet remote. (2.153) gives a good description of their Monte Carlo data but the particular values of the best fit parameters have no physical meaning since they are obtained for $SU(2)_c$ and there is no corresponding hadron spectroscopy. Only few tentative attempts to include the fermion determinant into the direct calculation of hadron masses have been made so far [89].

d) Conclusions.

The numerical investigation of the lattice model of QCD is potentially the most systematic approximation scheme towards the solution of the functional-integral problem of the full theory. It relies heavily on advanced and advancing computer technology and has many quasi-experimental aspects. In particular, it needs a lot of guidance from analytical and numerical model calculations. We know, however, that a theory can only be tested and developed by making "hard" predictions for experiments whose results are not yet known or are at least unexplained. This is not the case for the static properties of hadrons which constitute the standard phenomenological "testing" ground for lattice QCD and other nonperturbative methods: the results are known in advance and the theory merely tries to reproduce them. On the other hand, it is natural to ask whether non-static properties of hadrons, as manifested for instance in scattering experiments, can in any way be related to the results of nonperturbative calculations.

2.5. RELATION TO HADRON STRUCTURE

Deep inelastic lepton-hadron scattering probes hadron structure at small distances between partons. Perturbative QCD expresses this structure by means of the Q^2-dependent Wilson coefficients. By going back to the functional-integral formulation of QCD, one gives up factorization in the hope of calculating hadron structure at all distance scales. This means that some nonperturbative quantities should explicitly depend upon Q^2.

The effective-action analysis reveals that the gluonic condensate is indicative of the structure of the QCD vacuum over distance scales of the order of Λ_c^{-1} . It is hence relevant for the confinement problem but does not relate directly to the internal structure of hadrons, as probed in scattering experiments at finite momentum-transfer. On the other hand, the pair condensate must depend explicitly upon the QCD coupling strength g. In the weak-coupling limit, we know how g depends in turn on Q^2. If one could extend this connection to the nonperturbative region, one could thus use the mechanism of chiral-symmetry breaking to calculate hadron structure.

Lattice QCD is well suited for the study of the g^2-dependence of measurable quantities. The β-dependence of lattice observables is usually investigated in connection with the continuum limit. Let us remark, however, that Fig. 2.13 can also be interpreted as a succession of images seen by a "microscope" with increasing resolution, that is, by a photon which communicates increasing four-momentum to the target hadron. In this context, the absence of phase transitions at finite β confirms that hadron structure evolves smoothly from high to low Q^2 and that QCD should be able to interpolate between asymptotic freedom and confinement. By identifying a suitable observable related to chiral-symmetry breaking and measuring its β-dependence, one could thus extract the nonperturbative dependence of hadron structure on g^2.

What is the physical meaning of the "field" temperature T? In relation to heavy-ion collisions it is argued [64] to be interpretable as a real, thermodynamic temperature variable which expresses the deposition of center-of-mass energy $\sqrt{s}$ into the system of colliding nucleons. Quasi-macroscopic equilibrium conditions may be realized in certain kinematical regions if the number of participating nucleons is high enough. Deposition of sufficient energy density can presumably destroy the structure of ordinary hadron matter, which we know to be characterized by confinement and chiral-symmetry breaking. The critical temperatures for deconfinement and chiral symmetry-breaking measure (by the Stefan-Boltzmann law) the necessary energy densities.

On the other hand, it is considered unlikely that "QCD plasma" could be obtained in any practically realizable hadron-hadron collisions. Furthermore, thermodynamical temperature can probably not be defined for just two colliding hadrons. But this situation also has certain advantages: colliding hadrons at high energies are still ordinary hadrons, so hadron-hadron scattering probes dynamical "excitations" of ordinary hadron structure. The point now is that finite T on the lattice is relevant for such excitations even if it is not physically realized in the system of colliding QCD fields. If β is held fixed, T is identical to the temperature variable of the statistical model of QCD. The conjugate thermodynamic potential is the free (Helmholtz) energy which maps onto the vacuum energy of the quantum field system [90]. Therefore finite lattice temperature at fixed g^2 is a measure of the c.m. energy $\sqrt{s}$ of the colliding hadron-hadron system.

It follows that any observable temperature measured in lattice calculations should depend on β. In particular, deconfinement and the restoration of chiral symmetry should occur at different values of n_t for different values of β. This point ought to be investigated numerically. Combined with the knowledge of the nonperturbative Callan-Symanzik function, this might permit the derivation of a "scaling" law between s and $t=-Q^2$, characteristic of hadron-hadron scattering.

Our work is a preliminary investigation of these points. We first identify a quantity which measures chiral-symmetry breaking and also provides us with a picture of hadron structure. Using the perturbative one-loop Callan-Symanzik beta-function as a crude first approximation to the relationship between color coupling and parton four-momentum, one can then calculate electromagnetic form factors of hadrons. Generalizing the model to the phenomenological analysis of hadron-hadron scattering data, we find an appealing physical interpretation of the most salient phenomenological trends. In particular, we empirically discover a relationship between an observable scale of Q^2 and the c.m. energy.

Once we have a picture of hadron structure which is consistent with nonperturbative QCD and with scattering phenomenology, we can address the detailed mechanism of confinement. Recall that the main question in this context is the effect of long-wavelength fluctuations on the vacuum domain structure. We have seen how this has been preliminarily investigated within the framework of lattice calculations of the heavy-quark potential. After correcting Eq. (2.153) according to our model of hadron structure, we can compare its predictions to heavy-quark spectroscopy and then propose a direct experimental test for the large-distance properties of the potential.

CHAPTER 3: THE TWO-SCALE PICTURE

3.1. DYNAMICAL QUARK MASS

Any quark mass term destroys the chiral symmetry of the chromodynamic Lagrangian. The flavordynamic masses which are inserted into QCD "by hand" provide an explicit breaking. We have seen, however, that nonperturbative QCD must break chiral symmetry even if explicit breaking is neglected. An obvious and popular [91-93] way to express this is to say that QCD generates a dynamical, nonperturbative mass term in addition to the flavor-dependent "bare" current quark mass. Both mass terms must depend on Q^2: dynamical chiral-symmetry breaking depends on the QCD coupling and any mass is subjected to renormalization. The mass of a colored fermion is thus

$$M_f(Q^2) = M_{dyn}(Q^2) + \hat{m}_f(Q^2) \qquad (3.1)$$

In particular, the spectroscopical mass of a constituent quark can be defined as $M_f = M_f(Q^2=0)$. In the following we shall concentrate on the purely chromodynamic term M_{dyn} and neglect the running current quark masses. Let us denote $M = M_{dyn}(Q^2=0)$. This must be of the order of the U and D mass (350 MeV).

Bearing in mind the conclusions of Chapter 2, the main question of relevance to hadron structure is the functional dependence of M_{dyn} on Q^2. This problem has a dynamical and a kinematical component, as can be illustrated in the short-distance limit where the OPE and perturbative QCD are applicable. Consider a current quark of four-momentum p. Its inverse propagator can be expressed in terms of a running normalization function N(p) and of a running self-energy $\Sigma(p)$:

$${}^{ab}_{\alpha\beta}S^{-1}(p) = \delta^{ab} N^{-1}(p)\left(-i\not{p} + \Sigma(p)\right)_{\alpha\beta} \qquad (3.2)$$

Here α, β are spinor indices and a,b are color indices. For $p \to \infty$ the inverse propagator can be expresed as an OPE, following Eq.(2.60):

$$ {}^{ab}_{\alpha\beta}S'(p) \underset{p\to\infty}{\sim} {}^{ab}_{\alpha\beta}C_I(p) + {}^{ab}_{\alpha\beta}C_{\bar\psi\psi}(p)\langle\bar\psi\psi\rangle + {}^{ab}_{\alpha\beta}C_{FF}(p)\langle\vec{F}_{\mu\nu}\cdot\vec{F}^{\mu\nu}\rangle \tag{3.3} $$

The coefficient functions can be calculated by perturbative QCD and the SVZ values (2.65) can be used for the condensates, therefore the functional dependence of Σ on p can be computed. The result is of the form

$$ \Sigma(p) = \frac{A}{p^2}(\ln p^2)^B \tag{3.4} $$

where the values of A and B are still research topics in perturbative QCD [91].

What is the physical interpretation of $\Sigma(p)$? In Eq.(3.2), the quark is treated like an electron in a crystal: it is described as a free particle even though it interacts with other color fields. All its interactions are absorbed into the p-dependence of its self-energy Σ. Graphically, Σ can be represented by the generalization of Fig. 2.4 to many-gluon exchange along the quark line (Fig. 3.1). For nonasymptotic four-momenta p, the summation over all possible gluon exchanges would have to be done nonperturbatively. This is the dynamical part of the calculation of $\Sigma(p)$. On the other hand, the quantity which one can hope to relate to experimental probes of hadron structure is $M_{dyn}(Q^2)$. There is thus the kinematical problem of relating the four-momenta Q (of the incident electroweak gauge boson) and p (of the struck quark) such that $\Sigma(p)$ gives rise to an expression for $M_{dyn}(Q^2)$ which in turn must have experimentally observable consequences.

The first step is to find a nonperturbative expression for $\Sigma(p)$. The only one we have encountered in the literature has been obtained by Peskin [48] for $M \ll p \ll \infty$, within the Hartree-Fock approximation (2.105). He studies the inverse quark propagator in the Landau gauge, where $N(p) \to 1$ for $p \gg M$. (It is assumed that S^{-1} is gauge-invariant so that we can pick any gauge convenient for calculations). Then S as given by Eq.(3.2) can be identified with Δ given by Eq.(2.108). Coupling strength renormalization is tentatively incorporated by using the one-loop result (2.23):

$$g^2(p) = \frac{g_c^2}{1 + b_0 \frac{g_c^2}{(4\pi)^2} \ln \frac{p^2}{p_c^2}} \qquad (3.5)$$

Peskin finds it convenient to define $g_c = g(p_c)$ where

$$\frac{3C_2 g_c^2}{4\pi^2} = 1 \qquad (3.6)$$

($C_2 = (N^2-1)/2N$ is the quadratic Casimir operator of $SU(N)_c$ in the fundamental representation). He further assumes that

$$B^3 = \frac{b_0}{6\pi C_2} \ll 1 \qquad (3.7)$$

The generalization of Eq. (2.14) to $SU(N)_c$ and n flavors

$$b_0 = \frac{11}{3} N - \frac{2}{3} n$$

implies that the validity of the condition (3.7) depends on the values of n and N: B^3 is $\cong 0.36$ for $N=n=3$ and $\cong 0.28$ for $N=3$, $n=6$.

Within these restrictions, Peskin finds an analytical solution to the gap equation satisfied by $\Sigma(p)$:

$$\Sigma(p) = \frac{D}{p} Ai\left(B \ln p/p_c\right) \tag{3.8}$$

where Ai stands for the Airy function and D is a constant. In Fig. 3.2 we show the shape of this function as compared to a Gaussian (the meaning of the p-scale and of the various parameter choices will be explained in Chapter 4). For $p \to \infty$,

$$\Sigma(p) \longrightarrow \frac{D'}{p} \frac{1}{(\ln p/p_c)^{1/4}} \exp\left[-\frac{2}{3} B^{3/2} (\ln p/p_c)^{3/2}\right] \tag{3.9}$$

This expression falls to zero faster than any inverse power of p and is thus inconsistent with the perturbative result (3.4). However, this rapid falloff also means that the approximation scheme which led to (3.8) breaks down at sufficiently high values of p [48], so that the "true" $\Sigma(p)$ (assuming it exists) would be well approximated by (3.8) for values of p of the order of the scale p_c but would revert to (3.4) as $p \to \infty$. Physically, one may argue that the solution (3.8) is valid at strong QCD coupling where the dynamics is essentially collective (Section 2.1) but that it is bound to break down at small distances where radiative processes can be described by perturbative QCD.

On the other hand, Peskin shows that not just (3.8), but indeed any Σ which solves Eq. (2.105), must tend to a constant $\Sigma(0)$ as $p \to 0$ [48]. This is precisely what one would expect of M_{dyn} and suggests that Σ might differ from M_{dyn} only by normalization. However, we must remember that this analysis is not valid for $p < M$. We may therefore not draw any conclusions before we obtain a quantitative estimate of the reference momentum p_c. Let us first investigate its physical meaning.

3.2. THE SCALE OF CHIRAL-SYMMETRY BREAKING

If quarks become massive, chiral symmetry will be broken. Clearly, dynamical fermion mass generation is a valid method for studying chiral-symmetry breaking only if the inverse implication is also true. We therefore ask [94]: does the breaking of chiral symmetry imply that constituent quarks are massive? We shall base our answer to this question upon a theorem first given by 't Hooft [95] and rigorously proven by Frishman et al. and by Coleman and Grossman [96].

Consider Fig. (2.15) as representing the vertex function of three symmetry currents of SU(3) . That is to say, this diagram can be computed at any energy scale, with currents formed out of the particles of the effective theory valid at that scale. Out of the three currents, two are conserved but the third (J_μ, say) is afflicted by the ABJ anomaly. The most general odd-parity amplitude which is symmetric under the interchange of J_ν and J_λ has the structure [96]

$$\Gamma_{\mu\nu\lambda} = A_1(q^2)\epsilon_{\mu\nu\lambda\alpha}(k-p)^\alpha + A_2(q^2)q_\mu\epsilon_{\nu\lambda\alpha\beta}k^\alpha p^\beta + A_3(q^2)\left(k_\nu\epsilon_{\mu\lambda\alpha\beta} - p_\lambda\epsilon_{\mu\nu\alpha\beta}\right)k^\alpha p^\beta + A_4(q^2)\left(k_\lambda\epsilon_{\mu\nu\alpha\beta} - p_\nu\epsilon_{\mu\lambda\alpha\beta}\right)k^\alpha p^\beta \tag{3.10}$$

In perturbation theory, $A_4(q^2)$ has a real constant value C determined by the anomaly [97]. Since $k^\nu\Gamma_{\mu\nu\lambda} = 0$ by current conservation at the vertex ν

$$-A_1(q^2) + \frac{q^2}{2}A_4(q^2) = 0 \tag{3.11}$$

which can further be written as a dispersion relation for A :

$$A_1(q^2) = \frac{q^2}{2\pi}\int ds\,\frac{\mathrm{disc}\,A_4(s)}{s-q^2} \tag{3.12}$$

Since $A_1(q^2)$ is real,

$$\text{disc}\, A_1(q^2) = \frac{q^2}{2\pi}\, \text{disc}\, A_4(q^2) = 0 \qquad (3.13)$$

The only solution to these equations is

$$\text{disc}\, A_4(q^2) = -2\pi C\, \delta(q^2) \qquad (3.14)$$

In perturbative QCD, there are two possible explanations for Eq. (3.14): either there is a two-quark intermediate state or the theory contains physical zero-mass states [97]. However, if we apply the result to energy scales lower than or equal to the confinement scale Λ_c, the first possibility is ruled out. The theory of color-singlet mesons and baryons must contain zero-mass bound states of the massless elementary quarks. Two different types of massless bound states could give rise to Eq. (3.14): a single pseudoscalar particle created by J_μ, with C given by the product of the couplings to the axial and to the vector currents, or a pair of massless fermions produced by J_μ. The first alternative clearly signals chiral-symmetry breaking; in the second case, chiral symmetry is unbroken but the composite massless fermions must satisfy the same anomaly equations as the original elementary quarks ("'t Hooft anomaly matching conditions" [95,96]).

When applied to scales below Λ_c, this analysis thus agrees with Goldstone's theorem in the context of broken chiral symmetry, massless pions and massive baryons. In fact, it can be shown that the anomaly matching conditions cannot be fulfilled in QCD with more than two massless flavors [95,96]. We are, however, not interested in massive baryons but in massive constituent quarks. Phenomenology tells us that chiral symmetry is broken below Λ_c, but let us now assume that it is in fact already broken at some higher, independent scale $\Lambda_\chi \gg \Lambda_c$. Then Eq. (3.14) forbids massless constituent quarks: an effective theory valid between Λ_χ and Λ_c contains massive colored fermions and massless Goldstone bosons.

We conclude that the description of chiral-symmetry breaking by dynamical fermion mass generation is only consistent if one postulates the existence of a distinct scale Λ_χ, independent of the confinement scale and satisfying $\Lambda_\chi \gg \Lambda_c$. Baryons would thus become massive in two stages: massless partons bind into massive constituent quarks which, in turn, bind into color-singlet baryons. Pions would be massless bound states of massive constituents, where the binding energy cancels the sum of the masses (Section 3.3).

Various forms of such a "two-scale picture" have been proposed in the literature [22,23,98]. In realising that the concept of two scales is intimately linked with fermion mass generation, we have, however, gained a substantial advantage over other approaches. The fact that $\Sigma(p)$ can be explicitly calculated allows us to go beyond the rough "step-function" picture of hadron structure which is characteristic of all other two-region models. Consider Eq. (3.8). Colored fermions pick up dynamical mass as they smoothly evolve from quark-partons to full-fledged constituent quarks. Let us define p_0 as the momentum at which $\Sigma(p_0)=\Sigma(0)$. Impose that $\Sigma(p)$ reach its maximum at p_0 and normalize $\Sigma(0)=1$ for convenience:

$$\Sigma(p_0) = 1 \qquad d\Sigma/dp\big|_{p=p_0} = 0 \tag{3.15}$$

The following relationships between p_o, p_c and D follow:

$$\begin{cases} p_c \gtrsim p_o\, e^{u_o/B} \\ D = \dfrac{p_o}{Ai(-u_o)} \end{cases} \qquad (3.16)$$

where u_o is the unique root of the equation

$$Ai(-u_o) = B\,Ai'(-u_o) \qquad (3.17)$$

($u_o \cong 1.775$ for n=N=3).

In this picture, chiral symmetry is thus gradually approached as $p \rightarrow \infty$. It is completely broken for $p \lesssim p_o$. Eq. (3.8) is characterized by the fact that p_o (which uniquely determines p_c, according to Eq. (3.16)) is the only parameter governing the smooth evolution from current quark to constituent quark. More generally, the existence of a momentum scale where constituent quarks are fully grown is determined by the Hartree-Fock approximation, provided p_o>M. If this condition is true, it is natural to associate the fundamental scale Λ_χ with p_o.

3.3. COLOR FIELD CONFIGURATIONS

Cornwall [99] has proposed that dynamical mass generation in QCD also applies to gluons. As in the analogous case of the 2d-Schwinger model, dynamical generation of a gluon mass does not violate $SU(3)_c$-invariance. Massive gauge-invariant QCD has vortex solutions and Cornwall conjectures that it is this color field configuration which is responsible for confinement. In other words, the vacuum structure of pure-glue QCD, as described in Section 2.3, would be due to dynamical gluon mass generation. It is interesting that the mechanism is reasonable only if the gluon mass depends on the four-momentum and vanishes as $p \to \infty$.

Even though no nonperturbative expression for the p-dependence of this dynamical gluon mass has yet been found, let us accept Cornwall's argument and associate the confinement scale Λ_c with gluon mass generation by analogy to the association of Λ_χ with quark mass generation [94]. In full QCD one would expect an interplay between the two mechanisms. Recall that both $\langle\bar{\psi}\psi\rangle$ and $\langle\vec{F}_{\mu\nu}\cdot\vec{F}^{\mu\nu}\rangle$ contribute to $\Sigma(p)$ in the framework of the OPE enhanced by SVZ sum rules. These vacuum condensates are each characterized by an independent distance scale (the range of the bilinear condensate is shorter because it has canonical dimension 3) which it seems natural to associate with our ordered set of momentum scales $\Lambda_\chi \gg \Lambda_c$. In our nonperturbative example for $\Sigma(p)$, the Hartree-Fock approximation, which is an assumption about the gluon field, determines the structure of constituent quarks.

We now have a unified picture of the internal structure of hadrons in terms of momentum-dependent quark and gluon "masses". In physical terms, these "masses" are seen to correspond to color field configurations which can be observed by suitable probes exploring the hadron at various distance scales (resolutions). Since quarks and gluons interact at all momentum scales, there is only one hadronic configuration embodying both confinement (gluon mass) and chiral-symmetry breaking (quark mass) along with asymptotic freedom. We have thus found quantities which are calculable in nonperturbative QCD and which directly describe hadron structure. How would one relate them to experiment?

We have pointed out that the natural experimental tool for observing the quark configuration in a hadron is a γ (or W,Z) microscope. Let us train it on a proton. By varying Q^2 from 0 to ∞ we resolve smaller and smaller distance scales inside the proton. If the scale Λ_χ characterizes the "full growth" of the massive constituent quark, there must exist a corresponding resolution scale Q_0^2 such that we observe the following succession of images (see Fig. 3.3): for $Q^2 \in [0,Q_0^2)$ we shall see three structureless, massive, confined constituent quarks U,U,D. For $Q^2 \geqslant Q_0^2$, we start seeing into a constituent quark. The picture becomes complicated. It might be visualized in terms of a certain distribution of partons. The existence of other constituent quarks and of confinement would not be apparent at this scale. At very high Q^2, we would see uncorrelated partons (valence, sea, glue).

Obviously, if we are to explain the flavor of the constituent quark U, one of the "u" current quarks within it must play a special role. Let us imagine that a certain "u" quark is created at high Q^2 in some production process (Fig. 3.4). If Q^2 is high enough, this quark will be noninteracting at the tree level but it must undergo radiative processes, thereby evolving to lower Q^2 and creating pairs and gluons. In the perturbative QCD region, its evolution will be governed by the Altarelli-Parisi equations. The computation of $\Sigma(p)$ can be done by solving the gap equation perturbatively. Thus our "valence" u quark has a "cloud" of partons of which it is the "parent" (it has radiated them) and which can be assumed to be flavor-neutral (they are pairs and gluons).

At still lower Q^2, g has become large enough that collective pair creation (instability of the chirally symmetric vacuum) dominates over perturbative radiative processes. This would be the region of validity of the approximations leading to (3.8). The result will be a constituent U quark which consists of the parent u quark and of a flavor-neutral cloud of ocean pairs and gluons.

It is interesting to examine the consequences of this two-scale picture for the Goldstone bosons of chiral-symmetry breaking. By virtue of the continuous character of chiral-symmetry breaking in our model, these must exist at any finite Q^2 (however large it may be). This means that a fraction of the pairs radiated by the valence quark bind together in the strongly attractive s-wave color-singlet channel. Such a "proto-pion" is of course tachyonic because its constituents are massless while the binding energy E is large. Now downward Q^2-evolution sets in. It seems reasonable to assume that the binding energy is independent of the evolution process (Fig. 3.5). Hence, when the constituent quark and antiquark are fully grown, the pion ceases to be tachyonic and reaches its on-shell mass (zero in this approximation).

Our model thus implies there must be real pions in the "rim" of any hadron. That is, an effective theory of hadron structure valid for resolutions between Λ_L and Λ_χ should describe the interaction of constituent quarks with pions. In this we agree with references [21-23]. Note, however, that pions don't seem to be good degrees of freedom for the description of the interior of a constituent quark because there they are tachyonic. We do not therefore favor models which admit pions throughout the hadron. It is better to consider off-shell color singlets as part of the flavor-neutral parton cloud of the constituent quark.

The preceding discussion raises an obvious question. The notion that "recombination" of colored partons into color singlets can take place at high Q^2 and thus precede evolution seems to contradict our arguments that confinement should act upon fully formed constituent quarks. In fact, confinement is not equivalent to color-singlet formation: it is characteristic of on-shell hadrons only. Our version of the two-scale picture thus provides a natural reconciliation of the Goldstone character of the pion with its status as an ordinary hadron.

Electroweak gauge boson microscopy has the disadvantage of being blind to gluons. To test the gluonic component of a proton we need gluon microscopy. But a gluonic probe can be carried into its target only by another hadron, so we must do hadron-hadron scattering. Now, a hadron-hadron scattering process is characterized by two independent Mandelstam variables: let us choose $t=-Q^2$ as in lH scattering along with s, the c.m. energy squared. In Section 2.5 we have argued that s determines the degree of excitation of hadron structure in a hadron-hadron collision. The dependence of hadron-hadron scattering observables upon s and t thus reflects the internal structure of the colliding hadrons at various energies. The temperatures T_c and T_χ are independent of the Q^2-scales Λ_c and Λ_χ. They measure the energy densities needed to break up the ordinary structure of hadrons.

To clarify these points, let us assume first-order deconfinement and chiral-symmetry restoration phase transitions. Then the two-scale picture seen by the electroweak microscope would be valid below the value of s which corresponds to T_c, but the parameter Q_0^2 would now have to depend on s. If $T_\chi > T_c$, a phase of deconfined massive constituent quarks would follow between the two corresponding values of s; above the energy corresponding to T_χ there would be no more constituent quarks, either. Note that our inequality $\Lambda_\chi \gg \Lambda_c$ in no way implies a similar inequality for T_c and T_χ; in fact, if we believe that chiral-symmetry breaking and confinement result from the same dynamics it is reasonable to expect $T_c = T_\chi$ as suggested by finite-temperature lattice QCD. In our interpretation, this would confirm that the chiral-symmetry breaking configuration is just the confining color field configuration seen at a smaller distance scale (at higher resolution). This discussion would be only slightly modified in the case of "rapid-crossover' second order transitions, in that ordinary hadron structure would "melt" over a small, finite range of s.

3.4. VALONS

The "Valon Model" has been proposed by Hwa and coworkers [100] following various earlier attempts at a phenomenological implementation of the two-scale idea [101]. We have chosen it as the bridge between our version of the two-scale picture and scattering experiments because it expresses the same physics and can be successfully applied to a wide variety of hard and soft hadronic processes. These include hadronization [100], deep inelastic scattering (study of DIS structure functions [102] and of DIS fragmentation [103]), low-p_T fragmentation [104], electromagnetic form factors of hadrons [105,106,94] and high-energy elastic hadron-hadron scattering [107,108,109]. We consider this "universality" of the model to be especially important, because it is a necessary feature of any serious attempt to describe hadron structure.

In the language of this model, fully grown constituent quarks are called "valons" to indicate that they are clusters of sea and glue partons around the parent valence quark, of which they inherit the flavor. Although they are spin-1/2 color triplets, their color and their spin projection perpetually fluctuate due to absorbtion and emission of "wee" infrared soft gluons [103] of which there always is a cloud surrounding any partonic Fock state.

Let us write down such a state for, say, the proton P:

$$\Psi_p = \langle P | u u d \bar{q} q \cdots g \rangle \tag{3.18}$$

where u,u,d are valence current quarks, $\bar{q}q$ are ocean pairs and g are non-wee gluons. Our discussion up to this point can be summarized by inserting the "valon basis":

$$\Psi_p = \sum_{UUD} \langle P | UUD \rangle \langle UUD | u u d \bar{q} q \cdots g \rangle \tag{3.19}$$

where the sum indicates integration over all valon coordinates. To express the independence of the internal structure of a valon from the existence of other valons, one factorizes one step further:

$$\langle UUD | u u d \bar{q} q \cdots g \rangle = \langle U | u q \bar{q} \cdots g \rangle \langle U | u q \bar{q} \cdots g \rangle \langle D | d q \bar{q} \cdots g \rangle \tag{3.20}$$

Thus, the distribution of partons in a hadron is expressed as the convolution of the distribution of valons in the hadron ~~with~~ the distribution of partons in a valon.

As we saw in Section 2.2, deep inelastic scattering (DIS) probes the structure functions of hadrons in the parton basis, at some high value of Q^2 fixed by the c.m. energy of the lepton-lepton scattering experiment. One might try to transform these structure functions into the valon basis by writing

$$F_2^H(z, Q^2) = \sum_V \int_z^1 \frac{dx}{x} L_V^H(x, Q_V^2) F_2^V\left(\frac{z}{x}, Q^2\right) \tag{3.21}$$

Here $F_2^V(z/x,Q^2)$ is the structure function of a valon in the parton basis, which is calculable by perturbative QCD if Q^2 is high enough. The moment equation for (3.21) is obviously related to the OPE (Eq. (2.36)). Therefore Eq. (3.21) is formally independent of the valon model and is valid at all Q^2. In order to interpret the Q^2-independent factor as the distribution of valons in the host hadron, the calculation must take place at some low $Q^2=Q_V^2$ which satisfies

$$F_2^V(z,Q_V^2) = \sum_f e_f^2\,\delta(z-1)\,\delta_{Vf} \qquad (3.22)$$

expressing the existence of Λ_V (it corresponds to the Q_0^2 of our microscope in Section 3.3). Therefore one would need to know the exact function F_2^V at low Q^2 where perturbative QCD should no longer apply. However, the validity of the decomposition (3.21) at both low and high Q^2 hints at the possibility of using some sensible extrapolation of the perturbative evolution function to represent F_2^V.

Hwa and Zahir [102] have used the LLA of the perturbative evolution function in order to extrapolate down to Q_V^2, the value of which determines the evolution parameter

$$\xi = \ln\left[\ln(Q^2/\Lambda^2)/\ln(Q_V^2/\Lambda^2)\right] \qquad (3.23)$$

For the functional form of the longitudinal distribution of valons in the hadron they use an ansatz inspired by the shape of the wavefunctions calculated in the harmonic-oscillator model of confinement [110] as well as by the canonical form of the distribution of hadronic constituents:

$$L_V^H(x) = A_V^H\, x^{B_V^H}\,(1-x)^{C_V^H} \qquad (3.24)$$

The parameters are determined by fits to the data on DIS structure functions in various reactions and at various values of Q^2 [102]. For the proton, the resulting coefficients in Eq. (3.24) are listed in Table 3.1. The corresponding values for Q_v^2 and Λ are

$$Q_v^2 \approx 0.64\ \mathrm{GeV}^2\ ;\ \Lambda \cong 0.65\ \mathrm{GeV} \qquad (3.25)$$

These results are compatible with the solutions of the harmonic-oscillator model. Once the valon distributions are determined, one can use (3.21) to predict the structure functions at other values of Q^2. The results are very good [102].

Of course, these distributions must be regarded as "effective" in the sense that they depend upon the approximations used in their derivation. In particular, the numerical values for Q^2 and especially for Λ have no physical significance- they are the price one pays for obtaining a reasonable solution within the LLA. It is therefore important to check these solutions against distributions obtained by independent methods, preferably from low-Q^2 physics in order to avoid the extrapolation problem. This will be addressed in Chapters 4 and 5. We shall find that the validity of these solutions is confirmed, so that the x-distributions of valons within hadrons can be considered as known. In practice, they have been determined for nucleons and pions. For convenience, the coefficients obtained from DIS and from charge form factors are collected in Table 3.1.

On the other hand, Eq. (3.19) demands the existence of analogous distributions of partons in a valon. Given the flavor-independence of the internal structure of valons, there are two types of longitudinal distributions of charged partons in a valon: let L_1 represent the distribution of current quarks of the same flavor as the valon and L_2 the distribution of current quarks and antiquarks of a different flavor.

Instead of L_1 one uses the "flavor-nonsinglet" distribution

$$L_{NS}(z) = L_1(z) - L_2(z) \tag{3.26}$$

As far as gluons are concerned, the very small probability that hadronization will result in the production of a glueball indicates that it is a very good approximation to assume that gluons convert into ocean pairs ("saturation of gluons by the ocean", [104]). Thus the gluons would be included in the flavor-neutral distribution L_2. Also included in this distribution should be the off-shell pions and other color singlets which may form out of ocean pairs according to our discussion in Section 3.3.

In references [104], particle production data at low laboratory transverse momentum (p_T) were used to extract and to test the distributions L_{NS} and L_2. Consider inclusive pion production in hadron-hadron scattering. Partons with large longitudinal momentum-fraction ($z \gtrsim 0.2$) are widely separated in rapidity and will not interact effectively in the collision. Therefore they fly through the interaction region essentially unchanged in their z-distribution. This means that by observing the produced pions in the forward direction in the lab (at small p_T) we can learn about the original longitudinal distributions of partons in the initial valons. Recall that these distributions are defined to be independent of the flavor of the valon as well as of the host hadron. By the analysis of the reaction $K^+p \to \pi^- X$ at $p_{lab} = 70$ GeV/c with the pions in the proton fragmentation region, using the valon distribution from DIS, the results for L_{NS} and L_2 are

$$L_{NS}(z) = 0.41\, z^{1/2}(1-z)^{-0.27}$$
$$L_2(z) = 2n\left[0.61(1-z)^{5.13}\right] \tag{3.27}$$

where n is the number of flavors active in the ocean and gluons are assumed to be saturated by the ocean. For n = 3, these distributions satisfy the momentum constraint

$$\int_0^1 dz \left[L_{NS}(z) + L_2(z) \right] = 1 \qquad (3.28)$$

Once the L-distributions are known, they can be used to predict the distribution of π^+ in the same experiment. The results are good [104].

3.5. CONCLUSIONS

We have investigated the physical implications of the assumption that the formalism of dynamical quark mass generation can be used to compute chiral-symmetry breaking. We find that this approach is consistent only if the dynamical quark self-energy $\Sigma(p)$ describes the internal structure of hadrons in terms of color fields: this structure must be characterized by two independent effective momentum scales $\Lambda_\chi \gg \Lambda_c$. The shape of $\Sigma(p)$ is determined by the interaction of gluon and quark degrees of freedom. Perturbative QCD enhanced by ITEP sum rules, arguments about dynamical gluon mass generation and the Hartree-Fock approximation to the gap equation suggest that the confinement scale is associated with the vacuum structure of pure-glue QCD and Λ_χ with the momentum scale at which constituent quarks are fully grown. In Eq. (3.8) the parameter p_c signals the existence of Λ_χ. This interpretation only makes sense if we can show that $p_c \gg M \simeq 350$ MeV.

Exploring the interior of an ordinary hadron with a t-microscope does not reveal any phase transitions according to this picture: chiral-symmetry is broken smoothly, following the function $\Sigma(p)$, and is complete at the full-growth scale of the constituent quark. The constituent quark is viewed as a cloud of partons distributed around a "parent" valence quark. This distribution is just a local detail of the global hadron structure: Λ_c is associated with the size of a hadron and Λ_χ with the size of a constituent quark. Goldstone pions must exist below Λ_χ; above Λ_c they coexist with the massive constituent quarks with which they interact.

Assuming rapid-crossover "melting" of ordinary hadron structure upon deposition of sufficient center-of-mass energy into a system of colliding hadrons, the above picture should be valid below the threshold measured by $T_c = T_\chi$. Our interpretation in terms of color field configurations suggests that the latter equality should hold exactly.

We are now in a position to pursue our program outlined in Section 2.5. We consider the dynamical problem of calculating $\Sigma(p)$ to be solved by Eq. (3.8) and use the two-scale picture to solve the kinematical problem and to relate Eq. (3.8) to observable quantities. To this end, we use the "valon" model, which is a quantitative, phenomenologically applicable formulation of the two-scale picture. It transforms the wavefunction of a hadron from the parton basis into a representation spanned by valons (alias constituent quarks).

Simple parametrizations of the distributions of valons in hadrons and of partons in valons (in terms of the parton-model momentum-fraction variable x) are obtained from the study of deep inelastic scattering and of low-p_T fragmentation. The fact that one can use extrapolations of one-loop perturbative QCD to obtain satisfactory results for these distributions is grounded in the compatibility of the convolution property of valon model distributions with the OPE. In other words, the valon model can describe x-distributions by interpreting the nonperturbative Wilson operator matrix elements.

The Feynman x-variable does not, however, shed any light on the geometric distributions of constituents within hadrons and valons (for example, on the size of a valon). Such questions are traditionally addressed by measuring the electromagnetic form factors of the extended charge distribution. We shall see that the study of hadron and valon charge form factors connects the geometry of parton distributions to $\Sigma(p)$ and also permits a verification of the results on longitudinal distributions.

CHAPTER 4: HADRON AND VALON CHARGE FORM FACTORS

4.1. CHARGE FORM FACTORS IN THE TWO-SCALE PICTURE

The spatial distribution of charged constituents within a composite system is measured by the system's charge form factor (CFF), which is defined as the Fourier transform of the charge density. For the case of a hadron, we first need to specify a suitable set of kinematical variables in terms of which the charge distributions shall be expressed.

We shall use "transverse coordinates", a kinematical framework introduced by Soper [110] for the very purpose of relating the parton distribution in a hadron to scattering experiments. Let any four-vector a^μ be described by its components (a^1,a^2,a^+,a^-) with $a^\pm=(a^0\pm a^3)/\sqrt{2}$. The scalar product is $a_\mu b^\mu = a^+b^- + a^-b^+ - \vec{a}.\vec{b}$, where $\vec{a}=(a^1,a^2)$. As is customary in the parton model, consider a reference frame in which the hadron H moves in the z-direction close to the velocity of light. The wavefunction of the partons which are distributed in this hadron, when viewed from the rest frame of H, looks as if it had been determined by local measurements on a space-time surface of equation r^0+r^3=const.$\to 0$. Transverse coordinates in the rest frame of H are defined by treating r^+ as a "time" coordinate so that the distribution of partons in H is described at fixed r^+. This reduces the hadron to a system of nonrelativistic particles, because the subgroup of the Poincare group which leaves the surface r^+=const. invariant is isomorphic to the Galilei group in two dimensions [110]. Let R^μ, P^μ refer to the hadron and r^μ, p^μ to any component parton. P^+ plays the role of the total "mass" of the Galilean parton system and p^+ is the "mass" of parton "i". The center of P^+ is like the center of mass of the parton collection. By evaluating the invariant $p_\mu p^\mu$ we find that p^- plays the role of the total energy of a parton (P^- corresponds to the total energy of the hadron) so the motion of a parton in H is described only by $(\vec{r},\vec{p})$.

With respect to the center of P^+ in H consider parton "i" with $\vec{p}$ and position $\vec{r}$ and denote by $\vec{y}$ its position relative to the center of + momentum in the residual system $H\backslash\{i\}$. If the longitudinal momentum-fraction is defined as $x=p^+/P^+$ it follows that [105]

$$\vec{r} = (1-x)\,\vec{y} \qquad (4.1)$$

Let us then denote the probability distribution for striking a current quark of flavor "i" and of longitudinal momentum-fraction x and transverse position $\vec{r}$ in a hadron H with a virtual photon at Q^2 by $q_i^H(x,\vec{r},Q^2)$. The corresponding CFF is [105]

$$F_H(Q^2) = \sum_i e_i \int_0^1 dx \int d^2\vec{r}\, e^{i\vec{Q}\cdot\vec{r}}\, q_i^H(x,\vec{r},Q^2) \qquad (4.2)$$

As $Q^2 \to \infty$, the oscillatory factor in the Fourier transform selects the dominant contribution to F_H to come from the region $\vec{r}\to 0$. By Eq. (4.1), this means either $x\to 1$ or $\vec{y}\to 0$ or both. If $q_i^H(x,\vec{r},Q^2)$ does not vanish very fast as $x\to 1$, perturbative QCD leads to the Drell-Yan-West relation between the hadron's CFF F_H and the DIS structure function W_2 [111]:

$$F_H(Q^2) \underset{\substack{Q^2\to\infty \\ x\to 1}}{\sim} (Q^2)^{-p} \;;\quad \nu W_2(x) \underset{x\to 1}{\sim} (1-x)^{2p-1} \qquad (4.3)$$

It has been argued that, in the general case, QCD will cause q_i^H to vanish so fast as $x\to 1$ that Eq. (4.2) becomes invalid and the $\vec{y}\to 0$ region dominates at high Q^2 [112]. A schematic diagram for the pion electric form factor corresponding to this situation is shown in Fig. 4.1. There is large momentum transfer between the probed colored fermions (which can be considered as current quarks), mediated by hard gluon exchange. Perturbative QCD is directly applicable to this situation and leads to beautiful, clear-cut predictions [112]. Unfortunately, these would apply only at asymptotically large Q^2; it appears that they cannot be tested against presently existing CFF data [113] (the highest available Q^2 is 33 GeV^2 for the proton [114]).

Perturbative QCD thus does not seem to be applicable as a theoretical framework for the explanation of existing CFF data. These appear to be dominated by nonperturbative, "soft" contributions. The problem is ideal for the application of the two-scale picture. The basic valon-model equations (3.18-3.20) suggest the following representation for $q_i^H(x,\vec{r},Q^2)$:

$$q_i^H(x,\vec{r},Q^2) = \sum_j \int_x^1 \frac{dx'}{x'} \int d^2\vec{r}\,' V_j^H(x',\vec{r}\,') p_i^j\left(\frac{x}{x'}, \vec{r}-\vec{r}\,', Q^2\right) \qquad (4.4)$$

However, as opposed to the case of Eq. (3.21), Eq. (4.4) cannot be related to the OPE because of the $\vec{r}$-dependence of the integrand. This means that this representation, characteristic of the valon model, must break down before asymptotically large Q^2 are reached.

To explore the consequences of Eq. (4.4) for $F_H(Q^2)$, let us insert it into (4.2) [105]. Defining $z=x/x'$, $\vec{\rho}=\vec{r}-\vec{r}\,'$, we have

$$\begin{aligned} F_H(Q^2) &= \left[\sum_j e_j \int_0^1 dx \int d^2\vec{r}\, e^{i\vec{Q}\cdot\vec{r}} V_j^H(x,\vec{r})\right] \cdot \\ &\quad \cdot \left[\sum_i \frac{e_i}{e_j} \int_0^1 dz \int d^2\vec{\rho}\, e^{i\vec{\rho}\cdot\vec{Q}} p_i^j(z,\vec{\rho},\vec{Q})\right] \\ &\equiv K_H(Q^2)\cdot F_V(Q^2) \end{aligned} \qquad (4.5)$$

We see that the valon-model ansatz (4.4) predicts the factorization of the hadron's CFF into a factor due to the distribution of valons in H (K_H which is normalized to e_H at $Q^2=0$) and the CFF of the valon itself (F_v which is normalized to 1 at $Q^2=0$). The valon form factor must be universal apart from the overall charge e_j (independent of the valon's flavor and of the host hadron) because it expresses the internal structure of the valon in terms of its component partons. This factorizability clearly only makes sense in the impulse approximation for the interaction of the photon with the probed colored fermions (Fig. 4.2).

On the other hand, there is no multiplicative valon CFF in the limit depicted in Fig. 4.1. This suggests that the mechanism by which Eq. (4.4) breaks down as $Q^2 \to \infty$ has to do with the gluons exchanged between colored fermions becoming so hard that the impulse approximation fails and the very notion of a valon loses its meaning. Therefore, we cannot hope to calculate F_v by any downward extrapolation scheme from perturbative QCD. Before we address the problem of finding a nonperturbative calculation scheme for the valon's CFF, let us review the determination of valon distributions in hadrons from CFF's.

4.2. VALON DISTRIBUTIONS FROM CFF's

Hwa and Lam [105] postulate that the L-distribution of valon j in H shall be related to $V_j^H(x,\vec{r})$ by

$$L_j^H(x') = \int d^2\vec{r}\,' \, V_j^H(x',\vec{r}\,') \qquad (4.7)$$

so that V factorizes into an x-dependent and an $\vec{y}$-dependent part:

$$V_j^H(x,\vec{r}) = (1-x)^{-2} L_j^H(x) \hat{T}_j^H(\vec{y}) \qquad (4.8)$$

where

$$\int d^2\vec{y}\, \hat{T}_j^H(\vec{y}) = 1 \qquad (4.8).$$

Note that factorization in $\vec{x}$ and $\vec{y}$ is suggested by the form of Eq. (4.1). If one further defines the Fourier transform of $\hat{T}_j^H(\vec{y})$:

$$T_j^H(\vec{k}) = \int d^2\vec{y}\, e^{i\vec{k}\cdot\vec{y}}\, \hat{T}_j^H(\vec{y}) \qquad (4.9)$$

one can finally express $K_H(Q^2)$ as

$$K_H(Q^2) = \sum_j e_j \int_0^1 dx\, L_j^H(x)\, T_j^H(\vec{k})\Big|_{\vec{k}=(1-x)\vec{Q}} \qquad (4.10)$$

For Q^2 low enough that valons are structureless, F_v should be equal to one and K_H by itself should account for the measured CFF's. Hwa and Lam study the CFF data for p, n and the pion at $Q^2 \lesssim 1\ GeV^2$. The ansatz for the longitudinal distributions is the same as in Eq. (3.24) for DIS. As for the transverse distribution of valons in hadrons, we know that it is governed by confinement. Based on this observation, Ref. [105] uses a simple Gaussian ansatz for T(k):

$$T_j^H(\vec{k}) = e^{-D_j^H k^2} \qquad (4.11)$$

With the parameter values listed in the second column of Table 3.1, they obtain a good simultaneous fit to the data (see Fig. 2 in Ref. [105]).

Furthermore, they observe that the factorizability predicted by Eq. (4.5) can be checked by cancelling the universal valon CFF between the pion and the proton CFF:

$$F_\pi(Q^2) = \frac{K_\pi(Q^2)}{K_p(Q^2)}\, F_p(Q^2) \qquad (4.12)$$

For values of Q^2 up to 10 GeV^2, the pion CFF predicted from proton CFF data (parametrized by the dipole approximation

$$F_p(Q^2) = (1 + Q^2/0.71)^{-2} \qquad (4.13)$$

which is a good description of the data up to Q^2=33 GeV^2) agrees very well with the measured values (Fig.2 in Ref. [105]). therefore Eq. (4.4) is good at least up to 10 GeV^2.

In Ref. [106], Hwa goes on to build a "macroscopic" model for the valon CFF itself. Without reference to the dynamical mechanism which generates the parton distribution in a valon, he argues that the empirically striking universal 1-pole structure of hadronic CFFs must be an intrinsic property of the universal valon CFF. His effective expression for F_v reads

$$F_v(Q^2) = \frac{m_\rho^2}{m_\rho^2 + Q^2} \qquad (4.14)$$

To obtain the corresponding fit to nucleon and pion CFF's, Hwa uses the valon distributions as given by DIS along with

$$T_j^H(\vec{k}) = \frac{D_j^H}{D_j^H + k^2} \qquad (4.15)$$

to obtain essentially the same results as had been obtained in the paper [105] (compare Fig. 5 in [106] to Fig. 2 in [105]). This underlines the compatibility of the various parametrizations and shows that, regardless of the method used, the valon picture allows a good simultaneous description of DIS and of charge form factors. However, the I=1 channel has not been isolated in Hwa's analysis and the global fit to charge form factors also depends on the effective parametrizations used for the valon distributions. The fair quality of the fit implies that there must be some I=0 admixture in this effective, "macroscopic" description of the valon's CFF. We shall therefore seek a "microscopic", dynamical model of the internal structure of valons.

4.3. A MODEL OF VALON STRUCTURE [94]

We begin by expressing the valon's CFF in terms of longitudinal and transverse parton distributions, by analogy with Eq. (4.10):

$$F_v(\vec{q}^{\,2}) = \int_0^1 dz \left[L_{NS}(z) + L_2(z)\right] T(\vec{p})\Big|_{\vec{p}=(1-z)\vec{q}} \qquad (4.16)$$

Like Eq. (4.10), this is justified by the form of Eq. (4.1). Recall that the longitudinal distributions of charged partons in the valon are given by Eq. (3.27). We assume that gluons are saturated by the ocean and take n=3.

The difficult part is, of course, to find a dynamically motivated expression for $T(\vec{p})$. We know that this expression cannot be inferred from perturbative QCD, and we expect that it should be common to the flavor-singlet and non-singlet components because it describes the geometry of the entire valon and does not refer to individual partons. Now, since our two-scale picture is based upon the description of chiral-symmetry breaking by dynamical quark mass generation, it is natural to correlate valon structure with the momentum-dependence of the colored fermion's self-energy.

Specifically, let us use $\Sigma(p)$ as given by Eq. (3.8). In transverse coordinates, all structural information about the parton distribution is carried by the $\vec{p}$-dependence. We therefore interpret the argument of as $|\vec{p}|$ (also assuming that the parton distribution is isotropic in $\vec{p}$). According to the convention for form factors, we normalize $\Sigma(0)=1$. At this point, using Eqs. (3.15-3.17), we can write down an explicit model for the distribution $T(\vec{p})$:

$$T(\vec{p}) = \begin{cases} 1 & , \ |\vec{p}| \leq p_0 \\ \Sigma(p) & , \ |\vec{p}| \geq p_0 \end{cases} \qquad (p \equiv |\vec{p}|) \qquad (4.17)$$

We combine this with the longitudinal distributions (3.27), according to Eq. (4.16).

In order to use the longitudinal distributions consistently, we must work with a three-flavor ocean. If we take N=3 for the number of colors, the parameters B and u_0 in Equation (3.8) can be evaluated from their definitions (3.7) and (3.17):

$$B^3 \cong 0.36 \quad ; \ u_0 \cong 1.775 \qquad (4.18)$$

We conclude that (3.8) should indeed be applicable for not too large values of p.

To test our model and to determine the fundamental parameter p_0, we have calculated the proton's CFF by using Eq. (4.17) in Eq. (4.16). For K_p we have used the expressions given by Hwa and Lam [105] (the longitudinal valon distributions from low-Q^2 CFF's along with the Gaussian form of the transverse valon distribution). The result for p_0=600 MeV is compared to the dipole approximation (4.13) in Figure 4.3. Note that we have not attempted any systematic best fit in order to improve the determination of p_0, because we can already see that our one-parameter model is only a (good) first guess and because we have not compared to actual data but only to the dipole approximation.

We are now in a position to explain Figure 3.2: $\Sigma(p)$ is plotted for three values of p_o and its shape is compared to a Gaussian chosen to be numerically close to the curve parametrized by p_o=600 MeV. Since the $\sqrt{\langle \vec{p}_T^{\,2} \rangle}$ of this Gaussian would have to be $\approx$ 2.6 GeV, we see that our distribution differs significantly from a simple Gaussian representation. Its detailed shape critically determines the order of magnitude of the valon size parameter.

Another essential test of our model is the calculation of the pion decay constant f_π. In Ref. [105] Hwa and Lam have argued that one can relate f_π to the transverse-momentum distributions of valons in the pion and of partons in the valon, by the following formula:

$$f_\pi = \frac{\sqrt{3}}{2\pi^{3/2}} \left[\int d^2\vec{k}\, T_v^\pi(\vec{k})\, T(\vec{k}) \right]^{1/2} \qquad (4.19)$$

By using our expression for $T(\vec{p})$, we obtain $f_\pi \simeq 87.8$ MeV for p_o=600 MeV as compared to the experimental value of 93 MeV.

4.4. DISCUSSION

We conclude from these results that our model seems to be phenomenologically reasonable for p_o of the order of 600 MeV. Within the approximations which define our model, p_o is the only parameter governing the size of a valon. By Eq. (3.16), it is related to p_c which in turn corresponds to the critical QCD coupling for χSB. p_o is therefore an expression of the fundamental scale parameter $\Lambda_\chi \gg \Lambda_c$. Most importantly, note that p_o is of the order of 2M so that the two-scale picture based on the Hartree-Fock approximation does make sense (see Chapter 3). The numerical value for p_o is in rough agreement with Politzer's estimate that $M_{dyn} = M$ at a momentum scale of 2M (first reference under [91]) as well as with the usually employed value of the "primordial" average transverse momentum of partons participating in hard collisions (massive lepton-pair production; large-p_T reactions) [115].

By studying the CFF problem, we have also solved the problem of relating $\Sigma(p)$ to $M_{dyn}(Q^2)$. Indeed, since $F_v(Q^2)$ is generated by $\Sigma(p)$ and the same must be true, by definition, for $M_{dyn}(Q^2)$, these quantities should be proportional. The factor of proportionality must be M because $F_v(0)=1$ while $M_{dyn}(0)=M$:

$$M_{dyn}(Q^2) = M\,F_v(Q^2) \tag{4.20}$$

In this context, it is interesting to compare an expression used by Cornwall [92] to calculate f_π from the effective propagator of a confined constituent quark:

$$M_{dyn}(Q^2) = \frac{M\,m_\rho^2}{m_\rho^2 + Q^2} \tag{4.21}$$

with the effective expression of the valon's CFF written down by Hwa (Eq. (4.14)). Cornwall also sets the scale by the rho mass and obtains the experimental value for f_π for $M = 340$ MeV. This tends to confirm our conclusion that both M_{dyn} and F_v are generated by $\Sigma(p)$.

The main shortcoming of our one-parameter model (as well as of Hwa's effective fit in [106]) is that the CFFs go too high as Q^2

increases. To stay closer to the data we should decrease p_0- but then the CFF goes too low for low Q^2. On the other hand, if we wanted to improve our numerical value for f_π, we should increase p_0. We must conclude that our $T(\vec{p})$ needs improvement- one parameter is not enough beyond a good first approximation. In fact, this situation lends support to the idea that the mechanism which leads to the breakdown of the approximation (3.8) for $\Sigma(p)$ as $p \gg p_0$ must be identical to the one which makes the notion of a multiplicative valon form factor inadequate at high Q^2. What is needed is, of course, a rigorous calculation of $\Sigma(p)$ at all p, directly from the QCD Lagrangian. This could be done, for instance, by calculating the (appropriately defined) quark propagator in full lattice QCD with dynamical fermions as a function of the inverse coupling. In conjunction with the extraction of the nonperturbative Callan-Symanzik function from, say, Monte-Carlo renormalization group studies, this would amount to a calculation of $\Sigma(p)$ in lattice QCD.

CHAPTER 5: HADRON AND VALON MATTER FORM FACTORS

5.1. ELASTIC HADRON–HADRON SCATTERING AT HIGH ENERGIES

We pursue our program by turning to the study of the "gluon microscopy" of hadron structure, which we have argued to be revealed in hadron–hadron scattering. The elastic channel obviously contains the most direct information about the structure of the colliding hadrons. Elastic HH scattering is a field of the utmost historical importance in hadron physics [116], where a huge body of data and a wealth of phenomenological models have accumulated but which still awaits a successful connection to QCD. One of the fundamental facts which have been established in long years of study is that the relationship of the measured observables to hadron structure becomes simpler and clearer as s, the c.m. energy squared of the collision, increases [116,117].

Consequently, we shall be concerned with "high energies". More specifically, we shall analyze differential cross-section (dcs) data taken in pp scattering at the CERN ISR for $\sqrt{s}$ between 23 and 63 GeV and $-t=Q^2$ up to 10 GeV^2, in pp scattering at Fermilab (FNAL) for $\sqrt{s}\epsilon(19,28)$ GeV and $-t$ up to 14 GeV^2, in π^-p scattering at FNAL for $\sqrt{s}\simeq 19$ GeV and $-t$ up to 10 GeV^2 and in $\bar{p}p$ scattering at the CERN S$\bar{p}$pS for $\sqrt{s}= 546$ GeV and $-t$ (at present) up to 1.5 GeV^2. As an output of our study, predictions will emerge for the dcs to be measured at the S$\bar{p}$pS for larger Q^2 and for the s–dependence of elastic scattering observables.

In the energy range under study, the following assumptions are well justified by their results [118]:

1. Asymptotic Pomeron dominance is valid:

$$\left.\frac{d\sigma}{dt}\right|_{Hp} = \left.\frac{d\sigma}{dt}\right|_{\bar{H}p} \qquad (5.1)$$

where H will be p or π^- in our applications.

2. The analysis can be performed in terms of only one, predominantly imaginary (absorptive) spin non-flip scattering amplitude f(s,t). As we shall see in more detail below, the real part of f(s,t) is automatically generated from Im f by the even crossing symmetry of Eq. (5.1).

3. s is high enough that the impact-parameter formalism is a consequence of partial-wave analysis.

This formalism is the natural framework for connecting scattering observables (the amplitude f) to the structure of the colliding hadrons [117-126]. Let us collect the formulae relevant to our tasks. The elastic differential cross-section (dcs) is related to the elastic amplitude f(s,t) by

$$\frac{d\sigma}{dt} = \pi\,|f(s,t)|^2 \qquad (5.2)$$

f(s,t) can be represented as the Fourier-Bessel transform (two-dimensional Fourier transform) of a quantity h(s,b) called the "elastic profile":

$$f(s,t) = \{h(s,b)\} \equiv \int_0^\infty h(s,b)\,J_0(b\sqrt{-t})\,b\,db \qquad (5.3)$$

(this follows from partial-wave analysis if s is high enough: Assumption

3 above). The optical theorem reads:

$$\sigma_{tot}(s) = 4\pi \, \mathrm{Im} f(s,0) \tag{5.4}$$

By unitarity in b-space, we must have for any s:

$$\frac{d^2\sigma_{tot}}{d^2\vec{b}} = \frac{d^2\sigma_{el}}{d^2\vec{b}} + \frac{d^2\sigma_{inel}}{d^2\vec{b}} \tag{5.5}$$

which is equivalent to

$$2\,\mathrm{Im}\, h(s,b) = |h(s,b)|^2 + G(s,b) \tag{5.6}$$

The quantity G(s,b) defined by (5.6) is called the "inelastic overlap function". Assuming it to be purely imaginary, one can solve (5.6) for the elastic profile:

$$h_0(s,b) = i\left[1 - \sqrt{1 - G(s,b)}\right] \tag{5.7}$$

The subscript reminds us that this is an approximate solution, obtained by neglecting the real part of h. The positive root to the quadratic equation (5.6) is ruled out by the requirement that G be continuous and vanish at large b together with h(s,b). It is customary to define the "eikonal" $\Omega(s,b)$ from $h_0(s,b)$

$$\Omega(s,b) = -\ln\left[1 - h_0(s,b)\right] \tag{5.8}$$

In terms of G:

$$\Omega(s,b) = -\tfrac{1}{2}\ln\left[1 - G(s,b)\right] \tag{5.9}$$

The full complex amplitude can be obtained from $f_0 = \{h_0\}$ by imposing Assumption 1 above (crossing-even symmetry):

$$f(s,t) = i\,\mathrm{Im} f_0(se^{-i\pi/2}, t) \tag{5.10}$$

Equivalently, the relationship between the full elastic profile and h is:

$$h(s,b) = i\,\mathrm{Im}\, h_0(s e^{-i\pi/2}, b) \qquad (5.11)$$

5.2. HADRONIC MATTER FORM FACTORS

The classical connection between elastic scattering and the structure of the colliding hadrons, pioneered by Chou and Yang [117], consists in building models of the eikonal $\Omega(s,b)$, in principle starting from some quantity related to the intrahadronic matter distributions. In general, such "geometric" models assume that the eikonal of the reaction AB-->AB is a function of the electromagnetic form factors of the hadrons [117,120,121]:

$$\Omega_{AB}(s,b) = A(s)\,\phi(F_A(t), F_B(t)) \qquad (5.12)$$

Since electromagnetic form factors only depend on the variable t, the s-dependence must necessarily factorize in all such models. It turns out, however, that this factorizability condition is too strong to accomodate the observed dependences of quantities like the dcs, the total cross-section and the forward logarithmic slope on s and t [119]. In order to fit the data, the function ϕ in (5.12) must actually depend on s as well as on a host of ad-hoc parameters and factors [120-125].

To us, this failure of the simple connection (5.12) seems hardly surprising, because we see no reason why the dynamically excited matter distributions in the overlapping hadrons at high c.m. energies should be be identical to the static charge distributions. If lepton-hadron elastic scattering defines the electromagnetic form factor of the hadronic target, then hadron-hadron elastic scattering must be expected to define its own "matter form factor" which should, in principle, depend on the two hadrons involved as well as on the s-value of the collision. We define this matter form factor (MFF) as [108,109]

$$M_{AB}(s,t) = \{\Omega(s,b)\} \qquad (5.13)$$

and, without imposing any a priori theoretical constraints upon it, extract it from the differential cross-sections measured in the experiments quoted in Section 5.1. Concerning our definition Eq. (5.13), note that the so-called MFF actually has the dimensions of a scattering amplitude. By analogy with CFF's, one can normalize MFF's to unity at t=0 by redefining

$$\tilde{M}_{AB}(s,t) = \frac{\{\Omega(s,b)\}}{\{\Omega(s,0)\}} \equiv F^{-1}(s)\, M_{AB}(s,t) \qquad (5.14)$$

The two definitions should be physically equivalent at fixed s, but in order to analyze the s-dependence of MFF's one must use (5.13) because any factorizable contribution F(s) cancels out upon normalization.

We have used two methods to extract the (normalized) MFF from the differential cross-sections measured in pp elastic scattering in the ISR range [108]. The input to the first is the tabulation of G(s,b) at the five ISR energies by Amaldi and Schubert [127]. We transform to eikonal values according to Eq. (5.9), performing a natural cubic 60-node spline at each energy. Then we extract $\tilde{M}_{pp}$ by Eq. (5.14), using a double-precision 32-point Gaussian quadrature between Bessel-function zeros. The results for four ISR energies are shown in Fig. 5.1. We have not included the top ISR energy because the resulting MFF had violent oscillations, probably due to several questionable data points signaled in [126]. This numerical method can be trusted only up to $-t \cong 5$ GeV^2.

To do better, we fit the pp dcs measured at the ISR for $\sqrt{s}=52.8$ GeV [128] and at FNAL for $p_{lab}=400$ GeV/c and large $-t$ [129]. Taking data at very large $-t$ into consideration improves the numerical Fourier-Bessel transform. Generalizing a form used in Ref. [118], we set

$$f(s,t) = i\sum_{j=1}^{J} A_j e^{B_j t} \qquad (5.15)$$

with J=5. A_j and B_j as obtained by using the CERN-MINUIT fitting routine are listed in Table 5.1. The fit is shown in Fig. 5.2. We perform the Fourier-Bessel transform of the eikonal obtained from (5.15) and get an independent extraction of the pp MFF at (approximately) $\sqrt{s}=52$ GeV. The extracted MFFs at that value of s by both methods are compared in Fig. 5.3.

Note that Method 2, which should be reliable at large $-t$, reveals a most striking feature of the pp MFF: it has a zero at $Q^2 \cong 5.65$ GeV^2 and then remains negative. This had been observed before [120,130].

Let us now use Method 2 in order to extract the $\pi^- p$ MFF from the differential cross-section measured at FNAL ($p_{lab}=200$ GeV/c) [131]. We compute $d\sigma/dt$ at $t=0$ from the total cross-section given in Ref. [132]. With a four-exponential form for the scattering amplitude (J=4) we obtain the dashed curve in Fig. 5.4. The fit to the $\pi^- p$ differential cross-section is shown in Fig. 5.5 and the corresponding values of A_j and B_j are given in Table 5.1. We see that the occurrence of a zero in the MFF is confirmed - for this reaction at this energy, it is at

$Q^2 \simeq 8.5$ GeV^2. We may suspect at this point that the presence of the MFF zero has to do with the absence of further diffraction dips in our fits to the dcs. Indeed, let us replace our parametrization by the following form used by Lai et al. [133]:

$$f_{\pi p}(t) = \alpha_1 e^{\beta_1 t} + \alpha_2 e^{\beta_2 t} + \alpha_3 e^{\beta_3 t} J_0(-\gamma t) \qquad (5.16)$$

(their coefficients are reproduced in Table 5.2). This amounts to interpreting the data point at $-t=9$ GeV^2 as a second dip. The resulting extraction is almost identical to ours in the Q^2-range shown in Fig. 5.4 but stays positive up to $Q^2=20$ GeV .

The preceding results definitely suggest that MFFs explicitly depend upon s. However, as is apparent from Fig. 5.1, there is no clear trend in the s-dependence over the narrow range covered by the ISR. On the contrary, we may expect a well-defined change from the ISR to the S$\bar{p}$pS. Let us therefore proceed to the extraction of the $\bar{p}$p MFF corresponding to the data collected up to now by the UA4 collaboration at the CERN SppS [109]. Their elastic dcs data [134,135] are represented by the full dots in Fig. 5.6. We shall use the following parametrization of $f_0(t)$, based on the UA4 fits of Ref. [135]

$$\mathrm{Im}\, f_0(t) = \begin{cases} 12.65\, e^{7.6t} & 0 \le |t| \le 0.15 \\ 11.376\, e^{7.1t} & 0.15 \le |t| \le 0.21 \\ 10.79\, e^{6.7t} & 0.21 \le |t| \le 0.5 \end{cases} \qquad (5.17)$$

For $|t| \geqslant 0.5$ GeV^2 we take [119,126]

$$\mathrm{Im}\, f_0(t) = \mathrm{Re}\left[0.10725\, e^{i0}\left(e^{5.45(t-t_0)} + e^{i\varphi + 2.3(t-t_0)}\right)\right] \qquad (5.18)$$

with $-t = 0.81$ GeV^2, $\varphi = \pi - 0.39$ and $\theta = 0.13$. We calculate the corresponding (normalized) MFF as in Method 2 above. The results are represented by the dotted curve in Fig. 5.7. This extraction can only be trusted up to roughly 1 GeV^2 because the dcs has as yet only been measured up to $-t = 1.5$ GeV^2. We have verified by explicit computation that the MFF for $-t \lesssim 1$ GeV^2 is unsensitive to the changes in Eq. (5.18) which are required in order to fit the newest UA4 data (third paper under [135]).

To make a statement about the MFF at larger Q^2, and most importantly about the occurrence of a zero, we must thus rely on some prediction for the dcs at large $-t$. By Assumption 1 in Section 5.1, the pp and $\bar{p}p$ MFFs at the same (high) s must be identical, therefore we can perform a simultaneous fit to the measured S$\bar{p}$pS dcs and to the pp dcs at $\sqrt{s} = 52.8$ GeV, using the Short Range Expansion (SRE) ansatz [118,129,136] for G(s,b):

$$G(s,b) = P e^{-b^2/4B} \sum_{n=0}^{2} \delta_{2n} \left(\frac{\gamma b}{\sqrt{2B}} e^{1/2 - (\gamma b)^2/4B} \right)^{2n} \qquad (5.19)$$

This is an expansion of G(s,b) around a Gaussian form, in terms of the short-range variable ($b e^{-(\gamma b)^2/4B}$); the argument of the power series is chosen such that its maximal value be unity. Given the simplifying assumptions that γ is constant and $\delta_4 = \delta_2^2/4$ [136], a simultaneous fit to the dcs data at two c.m. energies determines a well-defined evolution of each of the three remaining parameters with the increase of s. Setting $y = \ln^2(s/s_0)$ with $s_0 = 100$ GeV one writes

$$\begin{aligned} P(y) &= \frac{b + cy}{1 + cy} \\ B(y) &= d + ey \\ \delta_2(y) &= f + gy \end{aligned} \qquad (5.20)$$

as discussed in the Bern talk of Ref. [136] and in the Syracuse talk of Ref. [119]. The MINUIT fit to a selected set of data shown in Fig. 5.6 is obtained for the parameter values listed in Table 5.3.

The errors on these parameters (corresponding to those of the fitting routine) induce errors in the corresponding MFFs. In Fig. 5.7, the full curve corresponds to the lowest value of B($\sqrt{s}$=546 GeV) compatible with the fit and the error bars show the effect of the uncertainty in the SRE parameters upon the extracted MFF. We have represented this curve (instead of the one corresponding to the central values of the parameters) because it coincides with the direct extraction (dotted curve) up to 1 GeV^2 and clearly shows our prediction for the MFF at large Q^2, corresponding to the dashed curve for the dcs in Fig. 5.6. We note that our predicted S$\bar{p}$pS MFF has a zero at $Q^2 \simeq 3.2$ GeV^2.

Finally, let us note that, once having adopted a parametrization such as (5.19,5.20) as a trustworthy representative of the data, we can generate the MFF at intermediate (as yet unmeasured) values of s. We can thus display the motion of the zero in the MFF from ISR to S$\bar{p}$pS energies. The result of this exercise is shown in Fig. 5.8b. Fig. 5.8a displays the normalization function F(s) defined in Eq. (5.14). Error bars are again induced by the parameter uncertainties listed in Table 5.3. Slightly larger error bars are obtained if we compare different versions of the SRE/BEL analysis: one which gives a detailed description of the ISR regime and yet another one which is especially designed for the analysis at very high energies (the SSC and beyond) since it explicitly satisfies unitarity at asymptotically large s by saturating the edge strength $\int_2(y)$ with an analytic form similar to that for P(y).

We find that this does not affect the conclusions we draw from Figures 5.8a and 5.8b, namely that F(s) is very well described by

$$F(s) \sim s^{\varepsilon} \quad , \quad \varepsilon \approx 0.105 \qquad (5.21)$$

and that the zero in the MFF decreases in a very specific way as s increases.

The question arises whether the decrease of the zero required by the SRE formalism also takes place at low s (in the ISR range and below), where the quality of the data is not sufficient to allow the extraction of a clear signal. We have performed an SRE extraction of the pp MFF at p_{lab}=400 GeV/c and have found the zero at $\approx$ 6.02 GeV^2. Together with our observation that the πp MFF at p_{lab}=200 GeV/c has its zero at 8.5 GeV^2, this tends to confirm that the MFF zero decreases with the increase of s also at lower energies. However, Fig. 5.1. seems to indicate that, in this region, the relevance of the motion of the MFF zero for the dcs is overshadowed by Regge effects.

5.3. MFF's IN THE TWO-SCALE PICTURE

We shall now try to understand these empirical facts starting from our two-scale picture of hadron structure. Let us assume that we stay below the deconfinement/chiral-symmetry restoration threshold for all s-values under study. It follows that the confinement mechanism acts upon valons in the same way at all s, so that the matter distributions of valons in their host hadrons only depend upon Q^2. We write [109,137]

$$M_{AB}(s,Q^2) = \int_0^1 dx_A \int_0^1 dx_B \left[\hat{\mathcal{K}}_A(x_A,Q^2)\,\hat{\mathcal{K}}_B(x_B,Q^2)\,\hat{V}(\hat{s},Q^2)\right] \qquad (5.22)$$

This is obviously a generalization of the Eq. (4.5) for charge form factors. The "reduced MFF" $\hat{V}(\hat{s},Q^2)$ describes the elastic scattering of two valons, one from each hadron, at a c.m energy squared of $\hat{s}=x_A x_B s$. The existence of a multiplicative valon-valon MFF must again be considered as a low-energy approximation which should break down when hard gluon exchanges between partons become important.

$\hat{K}_A$ stands for the matter distribution in hadron A in terms of its component valons and $\hat{K}_B$ denotes the corresponding distribution in hadron B. These are easily obtained from the distributions extracted from DIS or from CFF's, by weighing the contributions from various valon flavors by the number of such valons in the host hadron rather than by their charges. We shall use

$$\hat{K}_p(x,\vec{k})=\hat{K}_{\bar{p}}(x,\vec{k})=\tfrac{1}{3}\left[2L_U^p(x)T_U^p(\vec{k})+L_D^p(x)T_D^p(\vec{k})\right]_{\vec{k}=(1-x)\vec{Q}}$$

$$\hat{K}_\pi(x,\vec{k})=L^\pi(x)T^\pi(\vec{k})\Big|_{\vec{k}=(1-x)\vec{Q}} \qquad (5\cdot 23)$$

with the coefficients marked by an asterisk in Table 3.1.

While the $\hat{K}$'s are thus completely determined, we don't know much about the reduced MFF. From our model of the static parton distribution in a valon we may, however, expect that the scale Λ_χ should again play an essential role. We have seen in the preceding chapter how this scale determines the momentum scale at which a valon is fully grown - equivalently, the spatial size of the valon. It is also related to the momentum scale at which the notion of a valon form factor becomes inadequate. We shall therefore interpret the empirical zero in the MFF as a manifestation of Λ_χ and as a measure of the relative size of a valon within its host. In other words, as the s-dependent generalization of the resolution scale Q_0^2. It is natural that a scale of Q^2 should run with s; this corresponds to a "scaling" law between Q^2 and s which physically means that a given resolution with the gluon microscope can be achieved by varying either s or Q^2. The decrease of the position of the MFF zero with growing s is then intuitively understandable: the higher s is, the lower need Q^2 be to bring the complicated internal dynamics of the colliding valons into play.

If this interpretation is to make any sense in the context of Eq. (5.22), we must show that the relative size of a valon compared to its host does not depend on s. Let us take $-t$, the position of the single zero in the pp or $\bar{p}p$ elastic amplitude f(s,t), as an indication of the size of the colliding hadronic system at a given s. Then the radii of the VV and of the pp systems are in the ratio

$$R = \left(-t_o(s)/Q_o^2(s)\right)^{1/2} \qquad (5.24)$$

At $\sqrt{s}=52.8$ GeV, we have $-t_o \cong 1.3$ GeV^2 and $Q_o^2 \cong 5.65$ GeV^2 so $R \cong 0.48$; at the S$\bar{p}$pS, $-t_o \cong 0.8$ GeV^2 and $Q_o^2 \cong 3.2$ GeV^2 therefore $R \cong 0.5$. We conclude that the VV system stays roughly half the size of the pp system while both grow by a factor of $\simeq 1.7$ between ISR and SppS. These findings are qualitatively compatible with what one would expect from the increase of $\sigma_{tot}(s)$ or by using the forward slopes of the pp and VV amplitudes as an indication of the relative sizes. Equations (5.19) and (5.20) imply that the proton becomes Blacker, Edgier and Larger (or "BEL") as P, and B increase with s, respectively. The above discussion thus suggests that the evolution of the shape of the proton is driven by the evolution of the shape of its constituent quarks. The same exercise, applied to the πp system (see Figs. 5.4 and 5.5), reveals that the ratio is approximately 2/3 in that case. This is, of course, in agreement with the fact that the (Goldstone) pion is a very tightly bound state in which the constituent quark and antiquark overlap significantly so that the filling ratio is large.

Now let us note that the two-scale picture also requires the presence of a purely s-dependent factor in the MFF. As we have mentioned in Section 3.4, one can only define the color and the spin projection of a valon in the average, because they are perpetually changed by random emission and absorption of "wee" infrared gluons. Like in QED (see Section 2.2) there must be an infinite cloud of such wee gluons mixed in with any Fock states containing valons at any stage of their Q^2-evolution. It has been known for a long time [138] that wee gluons contribute significantly to the rise of the total cross-section with increasing s, so the collision of these clouds should have important effects on the MFF, but their contribution should not depend on Q^2.

The presence of a factor of the form

$$F(s) \sim s^{\epsilon} \qquad (5.25)$$

has long ago been argued to be a general consequence of field-theoretic models with soft infrared quanta [139]. In fact, these arguments underlie the s-dependence of "factorizable-eikonal" (FE-type) geometric models (Eq. (5.12)). The value of ϵ for QCD has not been calculated by field-theoretic considerations, but, as in all problems involving soft infrared quanta, one can only expect an effective value obtained from phenomenology.

This seems therefore a natural physical explanation of the function F(s) in the empirical MFFs, and Fig. 5.8a is a surprisingly good confirmation of Eq. (5.25) with $\epsilon \cong 0.105$. This value for ϵ is consistent with the estimates of FE modellers [120,123,139].

The two-scale picture thus implies that the factor $\hat{V}$ in Eq. (5.22) can further be written as

$$\hat{V}(\hat{s},Q^2) = F(s)\,\hat{W}(\hat{s},Q^2) \tag{5.26}$$

where F(s) is of the form (5.25) and $\hat{W}$ features an $\hat{s}$-dependent zero in Q^2.

5.4. MFFs IN THE VALON MODEL

The present status of nonperturbative QCD does not allow any direct derivation of W(s,t). We are therefore compelled to use certain simplistic guesses and assumptions in any attempt to go beyond the purely qualitative discussion of the preceding section. Observing that the simplest ansatz for a form factor which has a zero in Q^2, whose value also determines the effective size of the corresponding matter distribution (cf. Eq. (4.14)) is

$$\hat{W}(\hat{s},Q^2) = \frac{a^2(\hat{s})-Q^2}{a^2(\hat{s})+Q^2} \tag{5.27}$$

we employ this as a simple model for $\hat{W}$. Eq. (5.27) with s-independent parameter values has been written down originally by Bourrely et al. [119].

To test the valon-model description of MFFs at some fixed s for a given reaction, without knowing the function $a^2(\hat{s})$, we might approximate

$\hat{K}_H(x_H,Q^2) = \delta(x_H-\bar{x}_H)K_H(Q^2)$ with $\bar{x}_H$ appropriately defined for each hadron. Indeed, in this approximation Eq. (5.22) reduces to a factorized expression:

$$\tilde{M}_{AB}(Q^2) = K_A(Q^2)\, K_B(Q^2)\, W(Q^2) \qquad (5.28)$$

where

$$K_H(Q^2) = \int_0^1 dx_H\, \hat{K}_H(x_H, Q^2) \qquad (5.29)$$

For pp scattering at $\sqrt{s}$=52.8 GeV we use the appropriate valon distributions from Eq. (5.23) to generate K_p and, upon fixing a^2 to the observed Q_0^2 at that energy, we obtain the dashed-dotted curve in Fig. 5.3. We repeat this exercise for the S$\bar{p}$pS MFF (with a^2= 3.2 GeV^2) and obtain the dashed curve in Fig. 5.7. A result of the same quality is obtained for the πp MFF (this valon-model curve is not shown in Fig. 5.4). These approximations are quite good, considering that there is no free parameter (the coefficients in the t-distributions are independently determined and a^2 is constrained to coincide with the zero in the MFF). Obviously, one could improve them "esthetically" either by untying a^2 from the value of the zero to come closer to the positive portion of the MFF (we have done this at 52.8 GeV and obtained a close reproduction of the full curve in Fig. 5.3 for a^2=7 GeV^2) or by redetermining the coefficients in the valon distributions to give the best fit to the MFFs at all energies. However, such procedures would not bring us any closer to the solution of the real problem, which is the calculation of the true $\hat{W}(\hat{s},t)$ from nonperturbative QCD. In this interpretation, Fig. 5.8b displays the dependence of a^2 on s (not on $\hat{s}$) which corresponds to BEL phenomenology.

The factorized expression (5.28) is of course unable to describe the $\hat{s}$-dependence of the MFF or to correlate MFFs for different reactions. In particular, if we try to reproduce the valon-model prediction of the πp CFF from the pp CFF in the case of matter form factors, by computing

$$\tilde{M}_{\pi p} = \frac{K_\pi}{K_p} \tilde{M}_{pp} \tag{5.30}$$

we obtain the solid curve in Fig 5.4 which actually is a quite good approximation to the empirical dashed curve up to near the zero in the pp MFF (5.65 GeV^2 as opposed to 8.5 GeV^2 for the dashed πp MFF). To understand this result, note that Eq. (5.22) implies the existence of "equivalent energies" $\sqrt{\hat{s}}$ at which Eq. (5.28) could indeed be used to correlate the MFFs for reactions AB-->AB and CD-->CD. Fig. 5.4 indicates that, due to the shape of the valon distributions in pions and protons, $\sqrt{s} \simeq 19$ GeV is not too far from the πp energy which would be equivalent to a pp c.m. energy of 52.8 GeV. In fact, if we calculate the pp MFF by applying Eq. (5.30) to the empirical πp MFF, we obtain a curve which is nearly the median of the MFF's over the Q^2-range shown in Fig. 5.1.

We conclude that, even with the substantial simplifications forced upon us by our lack of knowledge of the nonperturbative valon-valon MFF, the valon model provides tantalizingly close approximations to the empirical MFFs.

5.5. DISCUSSION

We have shown that our two-scale picture of hadron structure, when suitably generalized to the dynamical excitations produced in hadron-hadron scattering, provides us with a qualitative understanding of the essential features of the MFF's extracted from pp, $\bar{p}p$ and πp elastic differential cross-sections at various values of s. The requirements imposed by the analysis of valon-valon elastic scattering are compatible with the "BEL" effect which has been convincingly shown to characterize all aspects of elastic hadron-hadron scattering from ISR to S$\bar{p}$pS and beyond [118,119,136]. The SRE analysis improves upon the performance of both geometrical scaling (GS) and FE models, whose s-dependences can be viewed as too restrictive particular cases of BEL behavior. Indeed, GS hadrons only become larger as s increases, while FE hadrons become excessively black at the expense of an insufficient size increase which causes too small an increase of the forward logarithmic slope of the dcs as a function of increasing s. We have seen that the two-scale picture also leads to an MFF which is reminiscent of FE models (the factor F(s)) but which at the same time features a scaling component embodied in the function $a^2(s)$. This scaling expresses the requirement that the confinement mechanism must act in the same way at all s, even though valons expand as s increases. Thus, the size of the overlapping valon-valon system relative to the overall hadron-hadron system appears to be s-independent for a given reaction (approximately 1/2 for pp, 2/3 for πp).

The relationship between the two-scale model and other geometric models of elastic hadron-hadron scattering can be seen by noting that the latter can be considered as particular cases of the generic form

$$M_{AB}(s,Q^2) = F(s)\, K_{AB}(Q^2)\, W(s,Q^2) \qquad (5.31)$$

which is the factorized approximation to our Eqs. (5.22) and (5.26).

The new "edgy" version of the Chou-Yang model parametrizes the eikonal as [122]

$$\Omega(s,b) = A(s)\left(\frac{s}{s_0}\right)^{Cb}\Omega_0(b) \qquad (5.32)$$

Upon Fourier-Bessel transformation, this will yield an expression of the form (5.31).

Chiu [124] writes

$$M(s,t) = iK\left(Ee^{-i\pi/2}\right)^{c}\exp\left[-B(\lambda^2-t)^{1/2}-\lambda\right]$$
$$B = b_0 + b_1\left[\ln(E/E_1) - i\pi/2\right]\ ;\ E_1 = 1400\,\mathrm{GeV}$$
$$(5.33)$$

with $E=s/2m_p$. His parametrization of $W(s,t)$ does not have a zero because it does not apply for $|t| \gtrsim 1.2$ GeV^2.

Glauber and Velasco [125] analyze the small-t S$\bar{p}$pS data using

$$\tilde{M}_{pp}(t) = G_p^2(t)\,\Phi(t) \qquad (5.34)$$

with G_p given by various parametrizations of the proton's electric form factor at small $|t|$. A future extension of their model to variable s and to large $-t$ would presumably also lead to the form (5.31). Indeed, if we too restrict our analysis to small $-t$ data, we see that, since our $a^2(s)$ increases from S$\bar{p}$pS to ISR, their equivalent parameter in $\Phi(t)$ has to follow suit, a fact which these authors preliminarily report. Their $\Phi(t)$ would thus become s-dependent, like the factor $W(s,Q^2)$ in Eq. (5.31).

Bourrely, Soffer and Wu (BSW) still use a purely FE-type ansatz [123]

$$M_{pp}(s,t) = \left(1-\frac{t}{m_1^2}\right)^{-2}\left(1-\frac{t}{m_2^2}\right)^{-2} S_0(s)\,\frac{a^2+t}{a^2-t} \qquad (5.35)$$

The presence of the MFF zero enables them to analyze the large Q^2 region but its lack of s-dependence leads to the aforementioned, generic FE problem with the forward logarithmic slope. However, it is interesting to note that the simultaneous BSW fit to ISR and S$\bar{p}$pS data reported in Ref. [123] requires $a^2 \simeq 3.8$ GeV^2, whereas their previous fit to ISR data alone required $a^2 \simeq 5.1$ GeV^2 [119].

We conclude that our model embodies the data-reproducing features of other models while explaining them in terms of fundamental characteristics of hadron structure. The hope is, of course, that we can establish valon-valon scattering as the nonperturbative dynamics behind BEL behavior. Recall our suggestion in Section 2.5 that one might obtain a scaling law between s and Q^2 by studying the deconfinement temperature for various values of the number of lattice sites in the timelike direction. In this context, it is interesting to compare Figure 3 in Kripfganz's report on the work of Kennedy et al. [58] to our Fig. 5.8b: the right tendency seems already to be seen in pure-glue lattice QCD.

Once $a^2(\hat{s})$ were known from many more such measurements, performed in full lattice QCD with dynamical fermions, one might try to use it in the simple $\hat{W}$ given by Eq. (5.27) to calculate the G corresponding to M(s,t) as given by Eq. (5.13). Hopefully this inelastic overlap function would then be describable by an SRE with parameters close to those presently imposed by phenomenology. A more ambitious project would be to calculate the "true" $\hat{W}(\hat{s},Q^2)$ by lattice QCD, generalizing the rigorous version of the computation of $\Sigma(p)$.

CHAPTER 6: INTERQUARK AND INTERHADRON POTENTIALS

6.1. THE $Q\bar{Q}$ POTENTIAL IN THE TWO-SCALE PICTURE

In the preceding two chapters we have used the valon model to explore the phenomenological implications of the two-scale picture for lepton-hadron and hadron-hadron elastic scattering. The valon model, however, has nothing to say about the confinement mechanism itself - confinement is imposed at an effective level by the parametrizations chosen for the valon distributions in their host hadrons. We recall from Sections 3.3. and 2.3. that the main problem concerning the confinement mechanism has to do with the importance of vacuum domain fluctuations at distance scales $> \Lambda_c^{-1}$. To apply the two-scale picture to this problem, we have to explicitly parametrize the effective theory of interacting valons and pions which describes hadron structure at resolutions lower than Λ_χ.

Bag models [20-22] and potential models [5,19] are two broad categories of phenomenological descriptions of this resolution region. As we have already mentioned, the potential picture differs from the "classical" bag models by the interpretation of Λ_c. In the latter type of models, confinement is "sharp" in that $1/\Lambda_c \approx 1$ fm is a cutoff on the possible hadron radii. On the other hand, unboundedly rising potentials allow for arbitrarily large rms radii of (excited) hadrons, so that Λ_c has a probabilistic interpretation. Color screening by dynamical quarks (Section 2.4.) can be expected to limit the possible bound-state radii in the potential model, while the inclusion of pions could in principle modify the characteristics of both models.

An important effort is being made in the literature to combine the bag model with the existence of Goldstone pions [21,22,24;18]. The problem is a complicated one and requires the use of ingenious analytical techniques. No definite conclusions about the confinement mechanism (the large-scale structure of QCD vacuum domains) have been reached as yet. The spectroscopy of all such models is only qualitative at present. On the other hand, we have seen in Section 2.4. that the $Q\bar{Q}$ potential can be relatively easily calculated from lattice QCD, both in the presence and in the absence of dynamical fermions. It is well-known that even flavor- and spin- independent potentials (flavor-dependent masses are parameters of such models) can give a surprisingly good description of quarkonium spectroscopy. As we have explicitly seen in the model described by the effective Lagrangian (2.131), which leads to the potential (2.135), such models automatically incorporate the effect of long-wavelength fluctuations. Therefore, it seems more straightforward to incorporate pion effects into the potential-model and to explore the phenomenological consequences of this modification.

Let us first reformulate the potential picture according to the two-scale idea [140]. $V(r)$ acts between flavor non-singlet "valence" current quarks. It should amount to an effective, low-resolution description of the flavor-independent structure of the valons formed around the parent valence quarks by χSB, of the color interactions between these constituent quarks and of their interactions with pions. If the flavors of the valence quarks are heavy enough ($f = c$, b) $V(r)$ can be used in the nonrelativistic Schrodinger equation to calculate hadron masses; for light flavors a relativistic wave equation would be required [141].

Thus, some of the effects of dynamical sea pairs - those related to their dressing up the valence quarks to form constituent quarks - are absorbed into the definition of the color string itself. On the other hand, dynamical pairs can also screen the valence quark and antiquark from each other and thereby lead to the saturation of V(r). In the language of fluctuating color strings, this phenomenon can be represented as a competition between stretching the string out further than a given r and the alternative of creating a valence quark-antiquark pair out of the vacuum, so that the original string is replaced by two strings of length r: one connecting the original quark to the new antiquark and the second one connecting the new quark to the original antiquark. If r is large enough the second alternative would become energetically more favourable and very long strings would be suppressed. Therefore V(r) would not increase indefinitely but reach a constant, finite limit for $r \to \infty$. We have introduced a possible parametrization of this effect in Eq. (2.153). Note that the Schwinger-model description of screening can also be viewed as a "decay law" which governs the suppression of long strings. We shall now try to incorporate pions into the model leading to Eq. (2.153).

We have interpreted the string fluctuation field $\vec{\xi}$ as an effective strong-coupling description of the structure and color interactions of constituent quarks. To implement our assumption that this effective theory is valid at resolutions lower than Λ_χ, the $\vec{\xi}$-field must also interact with pions.

Let us consider the fluctuating-string picture to hold in a certain reference frame where the two-dimensional transverse fluctuation vector $\vec{\xi}$ is defined. However, we postulate that the description of the hadron in terms of string fluctuations holds in any reference frame so that can be "extended" to a four-vector ξ_μ. On the other hand, pions are to be considered as structureless elementary fields U (they must not be replaced by their internal string-fluctuation field) and shall be defined as the Goldstone bosons of χSB. These requirements can be satisfied by considering $\vec{\xi}$ as a massless "gauge field" exchanged between sigma-model pions, in analogy with (pseudo)scalar electrodynamics (Eq. (2.85)):

$$L_{U\xi} = [(\partial_\mu - ig\xi_\mu)U^+][(\partial_\mu + ig\xi_\mu)U] \qquad (6.1)$$

Since $\langle U\rangle = -f_\pi$ in the chiral limit, where $f_\pi \cong 93$ MeV is the pion decay constant, the Higgs mechanism operates in the usual way and gives mass to the fluctuation field:

$$m = g f_\pi \qquad (6.2)$$

Radiative corrections à la Coleman-Weinberg will also contribute to the ξ mass as would the u and d current quark masses if we were to consider them. Let us denote the resultant ξ-mass by m_2.

Physically, it is known that $\vec{\xi}$ is to be interpreted as the Goldstone boson field corresponding to the spontaneous breakdown of the Euclidean symmetry enjoyed by the straight-string state [142]. In the present model, the pion would thus act as a Higgs field which gives mass to the would-be Goldstone mode.

The Coulomb term in the interquark potentials (2.135) and (2.153) was due to the masslessness of the $\vec{\xi}$-field. Now that ξ has become massive, the Coulomb term should be replaced by a Yukawa potential of range r_2. Our discussion thus suggests the following generalization of the screened potential (2.153):

$$V(r) = -\frac{\alpha}{r} e^{-r/r_2} + \sigma\left(1 - e^{-r/r_1}\right) \qquad (6.3)$$

Let us see if there are values of the parameters in Eq. (6.3) for which ψ and Υ spectroscopy can be reasonably described.

We use the potential (6.3) in the computer programme employed by Margolis, De Takacsy and Roskies [143] to solve the nonrelativistic Schrodinger equation for the n= 0,1,2,3, l=0 ψ and Υ masses. The parameters are estimated by fitting the calculated masses to the experimental values [144], using the CERN-MINUIT routine. The masses corresponding to the parameters listed in Table 6.1 are compared to experiment in Table 6.2.

The large values for σ and r_1 lead to a large effective string tension which is counterbalanced by a value of α a factor 1.7 larger than $\pi/12$. Since r_2 is also very large, the good reproduction of spectroscopic data means that our potential is close to the traditional potentials for the range of r probed by ψ and Υ spectroscopy (see Fig. 6.1). The fact that $r_2 > r_1$ is in agreement with Peskin's arguments that the Coulomb term should survive string breaking [145]. Equation (6.3) with the parameter values in Table 6.1 would imply that string breaking is a very slow process, the confining potential being felt out to interquark separations of the order of 3 fm (see Fig. 6.1).

The inclusion of pions and the determination of the screening parameters from spectroscopic data has radically modified the "JM potential" (2.153). A comparison of the potentials (2.153) and (2.135) (with the parameter values given in Table 6.3) to the empirical flavour-and spin-independent quark-antiquark potential between 0.1 and 1 fm (Fig. 6.2) confirms that our modification goes in the right direction: even though it neglects vacuum polarization effects, Stack's $SU(2)_c$ potential (2.135) resembles the empirical potentials better than the JM potential, which is seen to start flattening out at too low r - it takes too long to reach its asymptotic value. Clearly, the value of σ given by Joos and Montvay is unrealistically low.

We have thus formulated a potential-model of confinement which expresses the two-scale picture and which gives a reasonable reproduction of spectroscopic data. It only begins to differ from the conventional, unboundedly rising confining potentials at $Q\bar{Q}$ separations of the order of 3 fm. Such distance scales are clearly not experimentally accessible to spectroscopy; to do a lattice calculation at 3 fm would require a huge lattice, beyond present technical capabilities. It would therefore seem difficult to discriminate between our potential and any other potential which reproduces spectroscopy. There is, however, one aspect of potential-models which is extremely sensitive to the detailed shape of V(r) and which can therefore distinguish between various parametrizations (and possibly between the potential and the bag descriptions of confinement).

6.2. THE COLOR VAN DER WAALS PROBLEM

The Yukawa potential is a key concept in the theory of the strong interaction; it describes the force due to the exchange of an ordinary hadron of mass m. It falls off exponentially with the distance between the interacting particles, within a range of the order of the Compton wavelength of the exchanged hadron, $\lambda\!\!\!^{-} = \hbar/mc$. The maximum-range potential, with $\lambda \simeq$ 1.4 fm, is that due to the exchange of a pion, the lightest state in the hadron spectrum. Is there room for a strong interaction of a longer range? There is an experimental and a theoretical side to the answer of this question: there is room but no signal yet.

No experiments, up to now, have been done with the specific aim to search for such a strong, long-range interaction. Existing experiments, however, have been analyzed by a number of authors [146-148] to see whether there was any evidence for the presence of such a force. These efforts resulted in a set of upper limits for its strength. On the experimental side, then, the answer to our question is, indeed: there is room but no signal yet. This situation has prompted a group of experimentalists at SIN to plan a dedicated high-precision search experiment [149] in which they will study the energy levels of pionic atoms, correct for electromagnetic and meson-exchange effects and thus place improved upper bounds on the strong long-range π^+p interaction.

Theoretical considerations may be grouped into three categories: general principles of field theory, quantum chromodynamics (QCD) arguments for and against such a force. The usual general principles of quantum field theory seem to exclude the strong long-range interaction because it entails a singularity in the famous singularity-free Lehmann-Martin ellipse [150,151] – at zero square of momentum-transfer, t=0, in the case of a $1/R^N$ interhadron potential. The same general principles would correlate such a singularity with physical states whose mass spectrum extends down to zero (no Lehmann-Martin ellipse). Since the observed spectrum of hadrons does not do this, the discovery of a strong, long-range force between hadrons might profoundly affect the choice of what are considered to be the general principles of field theory (traditionally, Wightman's axioms). These considerations, at present, unfortunately allow no definite conclusion about the occurrence of a long-range force in QCD because it is not known yet whether QCD satisfies the usual axioms.

Quantum chromodynamic arguments in favor of the strong long-range force hold that, in analogy to the well-known Van der Waals force due to the exchange of two photons between two electrically neutral atoms, the exchange of two or more massless gluons can give rise to a strong, long-range force between two color-neutral hadrons. By analogy with electrodynamics, this is called the "Color Van der Waals (CVDW)" force. Such forces have been calculated from perturbative QCD [147,152,153] and from potential-models [146,154,155].

QCD arguments against the CVDW force typically maintain that the gluons are confined inside a hadron bag and cannot travel to another hadron far away. Somewhat similar to this, Greenberg and Hietarinta [156] extended the traditional interquark potential model by adding a particular version of the string concept: there is no strong long-range force between hadrons because the confining string stays within the hadron. Then there is the belief held by some that, although hadrons fundamentally interact through multiple-gluon exchange (and quark interchange), this interaction, at large distance, is equivalent to meson-exchange effects. Neither of these arguments, however, has been derived from general field theory or from QCD.

On the theoretical side, then, one sees that the apparent nonobservation of massless hadrons makes the occurence of the strong long-range force less trivial but nevertheless not impossible at present. So the answer to our initial question is, once again: there is room but no "signal" yet. It is clear, however, that either the existence or the nonexistence of CVDW forces has profound implications. Indeed, the issue is the detailed confinement mechanism, or, equivalently, the true large-scale structure of the QCD vacuum. CVDW forces exist if confinement is "soft" and allows virtual gluons to tunnel through the vacuum. They must be absent if vacuum domain walls are very rigid to long-range fluctuations. This is why CVDW forces are characteristic of potential models but are automatically eliminated in the bag picture.

As we have indicated above, there are two "traditional" methods for calculating CVDW forces: perturbative QCD applied to the exchange of two or more gluons and the use of the potential approach. Perturbative many-gluon exchange calculations can yield CVDW forces which fall off like $1/R^N$ with N large enough that existing experimental bounds [146,147,152] are not violated. However, the use of perturbative QCD at distance scales $R \gg 1$ fm seems impossible to justify.

The methods for deriving the CVDW potential U(R) between, say, two mesons, given the quark-antiquark potential V(r) as an input [146,154,155], assume the existence of a virtual color-octet intermediate state for each meson, in which the two octets combine to give an overall color singlet. Color sources located in different singlet mesons will thus interact by means of an octet potential $V_8(r)$, which is argued to be proportional to $-V(r)$.

In the case of the conventional confining potentials of the form

$V(r)=kr^a$ $(a>0)$, the corresponding color-octet potential is clearly unrealistic: it is unbounded below since it tends to $-\infty$ as $r \to \infty$. The CVDW potential one obtains if one uses the method in spite of this grave problem is of the form KR^{a-4} and strongly violates existing experimental bounds [146-148].

We have seen that color screening reduces the "softness" of confinement in the potential picture by limiting the possible radii of hadronic systems from above. Correspondingly, it is easy to see that the saturating JM potential does not lead to the problems encountered by unboundedly increasing potentials. Indeed, we note that the color-octet potential corresponding to Eq. (2.153) is bounded below by $-\sigma$ and yet it does not allow the formation of unphysical color-octet bound states because the finite-energy minimum is only reached at infinite separation. The same is true for our two-scale potential model (6.3). It is therefore interesting to calculate the CVDW potentials corresponding to the interquark potentials (2.153) and (6.3). A word of caution is, however, required concerning the applicability of the potential picture to multihadron systems. The concept of an interquark potential is phenomenologically justified for color-singlet hadrons only. There is no corresponding argument for the applicability of this concept to the virtual color exchange interactions between hadrons, even if these exist. The other argument for the interquark potential as a valid description of color-singlet hadrons is its calculability from lattice QCD; because of the large distance scales involved, lattice QCD can of course not be applied yet to the calculation of CVDW forces. Therefore, the traditional approach to the derivation of the CVDW potential from the interquark potential must be viewed as yet another simplistic approximation we have to make in order to estimate the consequences of our ideas about hadron structure. With these considerations in mind, we proceed to the calculation of the CVDW potential.

6.3. CALCULATING CVDW POTENTIALS

In the textbook problem of the classical, interatomic Van der Waals potential [157] , the input is the Coulomb potential. The interaction hamiltonian can be treated as a small perturbation at large R and the classical R^{-6} power law results from second-order perturbation theory. The atomic excitation energy serves as energy denominator. This procedure can obviously not apply to an unboundedly rising interquark potential. The standard treatment [146,154,155] , known as "modified" second-order perturbation theory, consists in replacing the atomic excitation energy by V(R), which is the dominant large-R term in this case. For the JM potential, the situation is intermediate between these two extremes. It is hence natural to still use modified perturbation theory, but with $V(R)-V(r_{q\bar{q}})$ as energy denominator. The following formula

$$U(R) = -K \frac{2\left(\frac{1}{r}V'\right)^2\Big|_{r=R} + V''^2\Big|_{r=R}}{V(R) - V(r_{q\bar{q}})} \qquad (6.4)$$

has been written down by Greenberg and Lipkin [154] to describe the CVDW potential between two mesons. They calculate the "absolute strength" $K=\langle r^2_{q\bar{q}}\rangle^2/162$ for stationary mesons and then argue that the effects of kinetic energy should rescale K to about 3K. Gavela et al. [146] use the same formula (6.4) for the large-R CVDW potential between two nucleons, but with $K=2\langle r^2_{\alpha}\rangle^2/3$, where r_{α} is the distance of a constituent quark from the center of mass of the nucleon.

The SIN experiment [149] will search for the π^{+}-p Van der Waals interaction. A first guess for the corresponding K would be the geometric mean of the meson-meson and baryon-baryon strengths (including the effects of kinetic energy according to [154]). With a realistic choice of $\langle r^2_{q\bar{q}}\rangle = \langle r^2_{Q}\rangle = 0.25\ fm^2$, one finds

$$K_{\pi p} \sim 1.2 \times 10^{-2}\ fm^4 \qquad (6.5)$$

We shall, however, treat K as a free parameter. For any given input potential V(r), comparing the result of (6.4) to existing experimental data places an upper bound on K. One can then check how this bound compares to the estimate (6.5).

One should not forget that modified perturbation theory only applies to the asymptotic large-R region. For the case of the linear interquark potential, Liu [155] has used a more general method to calculate an interhadron potential which is valid for all R. He finds the corrections to the asymptotic result to be small. We thus feel justified to proceed on the basis of formula (6.4).

To begin with, we compute U(R) for R between 1.5 fm and 100 fm, using (2.153) with the parameters α and σ listed in Table 6.3. Fig. 6.2 tells us that $V(r_{q\bar{q}})$, the value of the interquark potential corresponding to a typical separation of the constituent quark and antiquark in a meson ($r_{q\bar{q}} \approx 0.5$ fm), should be of the order of 200 MeV. Next, we investigate the asymptotic behaviour of U by dropping all exponentially damped terms in the numerator of (6.4) and by neglecting the Coulomb term in the denominator with respect to σ. This yields a London-type R^{-6} law

$$U^{nr}_{as} = \frac{-9K\alpha^2}{\sigma} R^{-6} \qquad (6.6)$$

We find that Eq. (6.6) is a very good approximation to (6.4) down to about 10 fm (see Fig. 6.3). The presence of the non-saturated screened interquark potential at "intermediate" distances (between 1.5 and 10 fm) gives rise to a stronger interhadron attraction than predicted by the R^{-6} law. Let us call 1.5 fm $\lesssim R \lesssim$ 10 fm the "near-force zone" and $R \gtrsim$ 10 fm the "far-force zone".

The rise of the interhadron attraction in the near-force zone requires an upper limit on the otherwise free parameter K, such as to avoid conflict with existing experimental data. Lyth [148] condenses the experimental bounds obtained up to June 1982 from accurate π^{+}-p scattering data and from pionic atom energy levels into an analytic parametrization of the upper limit line:

$$|U(R)|_{EL} = 0.025\, R^{-4.9} \qquad (6.7)$$

valid for interhadron separations ranging from 1.5 to 100 fm. This line is labeled "EL" in Fig. 6.3. We choose a maximal value of K such that the limit (6.7) be saturated by Eq.(6.4) at R=1.5 fm (see Table 6.3). This K_{max} =4.72x10^{-3} fm^{4} is seen to be a factor 2.54 lower than our apriori estimate (6.5). It yields the theoretical upper bounds shown in Fig. 6.3. The full curve labeled "R^{-6}" represents Eq.(6.4) for the JM potential: it saturates the Lyth bound at 1.5 fm and merges into the corresponding R^{-6} asymptote slightly above 10 fm.

In the classical interatomic case, the London R^{-6} law is valid up to values of R which are sufficiently large compared to the largest wavelength λ associated with electric dipole excitations of the atomic ground state - when $R \gg \lambda$, a R^{-7} law takes over [158]. Let us assume the wavelength of the color-singlet to color-octet transition in hadrons to be of the order of 1 fm [146]. We would then conclude that measurements of the interhadron attraction at distances of more than, say, 5 fm should detect the retarded force, not the one we calculated above.

All past discussions of the color Van der Waals force have assumed that the retarded asymptotic potential can be estimated from the nonretarded one by multiplication with λ/R, as is done in the classical interatomic problem. In our case, application of this rule would simply change the asymptotic interhadron potential (6.6) to

$$U_{as}^{ret}(R) = -K\frac{9\alpha^2\lambda}{6}R^{-7} \qquad (6.8)$$

and its effect on the complete eq. (6.4) is represented in Fig. 6.3 by the full curve labeled "R^{-7}". As a finishing touch, we might argue that the true intermediate-range potential would start off nonretarded and merge smoothly into the retarded curve. We have drawn the dashed curve in Fig. 6.3 as a possible example of such interpolation. Needless to say, the future complete theory of U(R) will have to include a rigorous treatment of retardation.

Let us now compute the CVDW potential corresponding to our potential (6.3). Fig. 6.4 shows the retarded U(R) between 2 and 100 fm predicted for the parameter values in Table 6.2 by setting the CVDW strength equal to 0.011 fm^4 in order to saturate the existing experimental upper bound at 2 fm. The agreement of this K_{max} with the expected value (6.5) is striking. In using Eq. (6.4), $V(r_{q\bar{q}}=0.5\ fm)$ has been computed directly from (6.3).

The JM interquark potential has two components: the Coulomb term and the parametrization of the approach to saturation. To see how each of these components influences the result for the CVDW potential, let us delete them one at a time and compute the corresponding U(R). First define a "fast-screening" (FS) potential:

$$V(r) = -\frac{\alpha}{r} + \begin{cases} \varkappa r & , r \leq r_\sigma \\ \sigma & , r > r_\sigma \end{cases} \qquad (6.9)$$

where r_σ is determined by the condition $\varkappa r_\sigma = \sigma$. If we use the values of α and $\varkappa$ corresponding to the empirical "Cornell" potential shown in Fig. 6.2 together with JM's σ, we obtain $r_\sigma = 0.8$ fm. Calculating the corresponding CVDW potential, we find that the asymptotic regime applies all the way down to 1.5 fm. As can be seen from Fig. 6.3, K_{max} is shifted to 0.49 fm^4.

Now let us delete the Coulomb term from V(r) beyond 1 fm:

$$V(r) = \begin{cases} -\frac{\alpha}{r} + \sigma\left(1-e^{-r/r_1}\right) & , r \leq 1 fm \\ \sigma\left(1-e^{-r/r_1}\right) & , r > 1 fm \end{cases} \qquad (6.10)$$

This "cut-off Coulomb" (CC) potential results in the rapid falloff indicated by the dash-dotted curve in Fig. 6.3. If screening were more abrupt, the Van der Waals potential would vanish still earlier. Only if a long-range Coulomb term is present can one expect a detectable Van der Waals force beyond $R \gtrsim 10$ fm. Therefore, we can explain the two characteristic regions of the CVDW potential in Fig. 6.3 in terms of the components of the input JM potential: screening controls the "near-force" and the Coulomb term controls the "far-force" (see Table 6.4).

This discussion now allows us to interpret the three regions in the

CVDW potential shown in Fig. 6.4 in terms of the parameters in our potential (6.3): the first is dominated by color screening (the parameter r_1) the second by the as yet nonvanishing Coulomb term and the third by the Yukawa-type vanishing of this term (the parameter r_2).

6.4. DISCUSSION

We have seen that potential models which take the color screening effects of dynamical quarks into account do not lead to unphysical potentials in the color-octet channel and can avoid conflict with existing upper limits on CVDW forces. The characteristics of these forces depend on the detailed screening mechanism and on the shape of the interquark potential at large distances (several fermi). In particular, the conjectured large-distance Coulomb term implies that the CVDW force extends out to large interhadron separations.

The potential (6.3) with the parameters listed in Table 6.1 is a definite prediction for the outcome of $SU(3)_c$ LQCD calculations with dynamical quarks at large values of r. It is a generalization of the standard Cornell-type parametrization to include the screening effect of dynamical current quarks and the effect of the interaction between pions and constituent quarks. The parameter values imposed by Ψ and Υ spectroscopy mean that these additional effects are only felt at interquark separations of about 3 fm. This slow saturation is a feature of the Schwinger-model description of color screening by vacuum polarization.

If our potential is correct, the experimentalists at SIN should detect a CVDW signal, because our prediction between 10 and 20 fm is quite close to the present experimental limit (Fig. 6.4). What could a negative result of the search mean? Obviously, our parametrizations of screening and of valon-pion interactions could be wrong. Another possibility is that the traditional potential-model approach for deriving the CVDW force is not valid. If one could eliminate both of these possibilities, this would indicate that potential models for color-singlet hadrons can only "mimic" real hadrons up to a certain point, while failing to describe the true confinement mechanism. This conclusion would then favor the bag picture.

Future progress in lattice QCD should be able to solve these problems. In addition to the investigation of the $Q\bar{Q}$ potential at distances larger than 1 fm, a promising approach seems to be the computation of the gluonic vacuum condensate or, equivalently, of the dynamical gluon mass [Section 3.3]. This would go beyond the limitations of model representations (potentials, bags...) and would amount to a rigorous theory of multihadron systems.

CHAPTER 7: SUMMARY AND OUTLOOK

7.1. SUMMARY OF THE TWO-SCALE PICTURE

We were led to a two-scale picture of hadron structure by examining the implications of the assumption that chiral-symmetry breaking by QCD can be described as dynamical quark mass generation. If this description is to be consistent, the breakdown of chiral symmetry must imply that not only baryons, but also constituent quarks are massive and are accompanied by massless Goldstone bosons (which are transmuted into pions in the real world of nonzero electroweak masses). This requires the existence of a separate scale Λ_χ, independent of the confinement scale Λ_c ($\Lambda_c^{-1} \sim 1$ fm is the characteristic hadron size) so that $\Lambda_\chi \gg \Lambda_c$ (see Section 3.2).

At scales between Λ_c and Λ_χ, QCD gives rise to an effective theory of pions interacting with confined constituent quarks. In terms of the Mandelstam variable $-t=Q^2$, which can be physically represented as the resolution of a picture of hadron structure seen by means of an "electroweak gauge boson microscope", the existence of Λ_χ is expressed by a scale Q_0^2 which characterizes the size of a constituent quark. The "valon model" is used to determine the effective distribution of constituent quarks (="valons") within a given hadron from deep inelastic scattering or from low-Q^2 charge form factor data. These distributions presumably incorporate the effect of confinement as well as that of the interaction of valons with pions.

To elucidate the confinement mechanism, that is, the large-scale structure of the QCD vacuum, the pion–valon interactions must be explicitly taken into account, since pions dominate the non-electromagnetic interactions between hadrons. We have studied this effect within the potential picture of confinement and have been led to a test of the validity of the latter picture as a description of large-distance hadron physics in terms of the ensuing color Van der Waals forces.

At scales higher than Λ_χ, corresponding to hadron structure as explored at resolutions higher than Q_o^2, QCD generates a certain distribution of partons within the valon. This distribution is the same for all valons and is independent of the confinement problem. In terms of transverse coordinates (Section 4.1), the factorizability of the longitudinal momentum-fraction ("Feynman x") distributions of partons in the hadron into a parton-in-valon and a valon-in-hadron term is explicitly compatible with perturbative QCD. This is not true for the transverse (geometric) distributions, which must therefore be calculated nonperturbatively. Since our two-scale picture is based on dynamical quark mass generation, we use the only available nonperturbative parametrization of this mechanism to generate the transverse distribution of partons in the valon. By calculating hadronic charge form factors and the pion decay constant, we show that this approach gives good phenomenological results.

In hadron-hadron elastic scattering at high c.m. energies $\sqrt{s}$, the scale Λ_χ manifests itself by the occurrence of a zero in the valon-valon scattering amplitude ("matter form factor") as a function of Q^2. The position of the zero is found to decrease with growing s in such a way that the valon-valon system always stays approximately one-half the size of the proton-(anti)proton system. For the pion-proton system, this ratio is about 2/3, in agreement with the fact that the pion is a very tightly bound system. Physically, the colliding valons become larger with the increase of s whereas the confinement mechanism acts upon them in the same way at all s. The existence of "wee" infrared soft gluons radiated by colored fermions at all stages of their Q^2-evolution is manifested in the function $F(s) \sim s^{\epsilon}$ in the matter form factor.

7.2. SUMMARY OF RESULTS

The application of the phenomenological valon model to the study of hadronic charge form factors has been completed by the formulation of our microscopic model of the transverse distribution of charged partons in a valon. The resulting proton CFF reproduces the data up to $Q^2 \approx 10$ GeV^2 while the deviation observed for higher Q^2 expresses the fact that radiative contributions have been neglected in the simple nonperturbative model for the dynamical quark mass which we have used.

In the field of high-energy elastic hadron-hadron scattering, our application of the two-scale picture has led to a qualitative dynamical interpretation of the observed trends in the differential cross-sections of pp, $\bar{p}$p and πp scattering at various c.m. energies. Valon-valon elastic scattering emerges as a promising candidate for the dynamical mechanism behind the BEL effect.

By incorporating the interaction of valons with pions into an expression for the $Q\bar{Q}$ potential which is favored by recent studies in lattice QCD, we have obtained a new potential-model for the confinement of valons in hadrons which gives a good reproduction of ψ and Υ s-wave energy levels while offering a definite prediction for the large-distance region which is as yet unexplored by hadron spectroscopy and by lattice QCD calculations. This potential, in conjunction with the traditional formalism for the calculation of the color Van der Waals potential from the interquark potential, implies the existence of long-range virtual color-exchange forces which should be observable in the dedicated high-precision search experiment [149]. If this prediction fails to materialize, whereas the prediction for the interquark potential is independently confirmed, one would conclude that the standard potential picture fails to describe either the dynamics of multihadron interactions or the true nature of the confinement mechanism itself. In particular, bag models of confinement naturally suppress CVDW forces. In the terminology of Section 2.3, this experiment might thus help to decide whether hadrons are "type I" or "type II" color superconductors.

7.3. CONCLUSIONS AND OUTLOOK

Our attempt to relate results of calculations in nonperturbatve QCD to static and dynamic hadron structure as manifested in various types of experiments has been quite successful, in that the outcome is consistent with phenomenology and generally improves upon the performance of existing models in the respective fields while offering a fundamental interpretation of the problems under study. Therefore, it seems worthwhile to pursue this line of research on a more rigorous and systematic basis.

The main limitation of our work is the use of simple guesses for key nonperturbative quantities. The distributions of partons and valons within hadrons, their dynamical excitations in the course of hadron-hadron collisions at various c.m. energies as well as the large-scale structure of the QCD vacuum should all be calculated directly from the QCD Lagrangian, without the use of other assumptions, of supplementary constructs or of effective theories. As we reviewed at length in Section 2.4., lattice QCD appears to offer realistic hopes of achieving these goals in a not-too-remote future.

The study of quark and gluon propagators in full lattice QCD at zero field-temperature should, by the arguments of Section 3.3, yield the true $\Sigma(p)$ and elucidate the exact confinement mechanism. One would have to define these quantities in an optimal fashion (with respect to the approach to the continuum limit and to computational requirements), to measure their dependence on the inverse coupling and would need to know the nonperturbative Callan-Symanzik function to obtain the momentum-dependent quark and gluon masses. It should also be possible to calculate the longitudinal distributions of partons in hadrons by using lattice QCD to evolve known perturbative distributions down to intermediate and low Q^2. Hopefully, the valon picture would (to some approximation) emerge at a scale Q_0^2 determined by the "true" $\Sigma(p)$. The next step would be to do these calculations at finite field-temperature, mimicking the dependence of hadron structure upon the c.m. energy in multihadron collisions.

One lattice QCD calculation which one could do much more easily is the study of the dependence of the deconfinement/chiral-symmetry restoration transition in full lattice QCD upon the number of sites in the timelike lattice direction (Section 2.5). As we have remarked in Section 5.4, the "scaling law" between s and t which would thus be established might be of immediate help in understanding valon-valon elastic scattering. Also, with the advent of parallel processors, of supercomputers, of the fifth generation..., one may hope for a calculation of the $Q\bar{Q}$ potential at sufficiently large distances to test our potential (6.3), even before the huge computing power which is being developed for the benefit of lattice gauge theories can be brought to bear upon the rather ambitious program outlined in the previous paragraph.

APPENDIX A: CONVENTIONS

1. Units.

The system of units used throughout this work is defined from SI by setting the speed of light in vacuum ($c=3x10^{8}$ m/s) and the reduced Planck's constant ($\hbar = 1.05x10^{-34}$ J.s) to (dimensionless) unity. In these units,

$$[L] = [T] = [M]^{-1} \qquad (A.1)$$

Mass is measured in MeV (1eV= $1.6x10^{-19}$ J) and length in fm (1fm=10^{-15} m). The following conversion relation holds true:

$$1 = \hbar c \cong 197.3 \quad MeV \cdot fm \qquad (A.2)$$

Scattering cross-sections are measured in mb. The following conversion relation holds true:

$$1 = (\hbar c)^2 \cong 0.389 \ GeV^2 \cdot mb \qquad (A.3)$$

2. Special Relativity.

Minkowski space-time is defined by the constant diagonal metric tensor:

$$g_M^{\mu\nu} = \begin{pmatrix} g_M^{00} & & & \\ & g_M^{11} & & \\ & & g_M^{22} & \\ & & & g_M^{33} \end{pmatrix}$$

$$g_M^{00} = -g_M^{11} = -g_M^{22} = -g_M^{33} \qquad (A.4)$$

A contravariant Minkowski 4-vector has components:

$$x_M^{\mu} = (x^0, x^1, x^2, x^3) \qquad (A\cdot 5a)$$

and the corresponding covariant 4-vector is given by:

$$x_{\mu}^{M} = (x^0, -x^1, -x^2, -x^3) \qquad (A\cdot 5b)$$

Euclidean space-time is defined by the constant diagonal metric tensor:

$$g_E^{\mu\nu} = \begin{pmatrix} g_E^{11} & & & \\ & g_E^{22} & & \\ & & g_E^{33} & \\ & & & g_E^{44} \end{pmatrix}$$

$$g_E^{11} = g_E^{22} = g_E^{33} = g_E^{44} = 1 \qquad (A\cdot 6)$$

Note that $x^4 = ix^0$ is real. The corresponding Euclidean momentum space is defined such that:

$$k_4^E x_4^E = k_M^0 x_M^0 \qquad (A\cdot 7)$$

Hence,

$$k_E^2 = -k_M^2 \ ; \ d^4k_M = i d^4 k_E \qquad (A\cdot 8)$$

Lorentz invariance in Minkowski space translates into O(4) invariance in Euclidean space. A real scalar field defined on Minkowski space-time can be continued into a real scalar field defined on Euclidean space-time. The corresponding functional integrals for the vacuum-to-vacuum amplitude are related by:

$$S_E[\phi] \equiv \int d^4x_E \, L[\phi(x_E)] = -iS_M[\phi] \qquad (A\cdot 9)$$

Derivatives with respect to space time shall be denoted by $\partial_\mu = \partial/\partial x^\mu$, $\partial^\mu = \partial/\partial x_\mu$. 4-indices are denoted by Greek lower-case letters while 2-indices and 3-indices are denoted by the Latin letters i,j,k... . Summation over repeated indices is implied unless explicitly stated otherwise.

Dirac matrices are 4x4 matrices with the following properties

$$(\gamma^0)^\dagger = \gamma^0 \qquad ; \ (\gamma^0)^2 = 1$$
$$(\gamma^i)^\dagger = -\gamma^i \qquad ; \ (\gamma^i)^{\dagger 2} = -1 \qquad (i=1,2,3) \tag{A.10}$$

where the dagger denotes hermitian conjugation. γ_5 is defined by

$$\gamma_5 = -i\gamma^0\gamma^1\gamma^2\gamma^3 \quad ; \quad (\gamma_5)^2 = 1 \tag{A.11}$$

Spinor indices are denoted by $\alpha, \beta, \ldots$. We shall use the notation $\not\partial = \gamma_\mu \partial^\mu = \gamma^\mu \partial_\mu$.

3. Internal Symmetries.

The Pauli matrices are:

$$\tau_1 = \begin{pmatrix} 0 & 1 \\ 1 & 0 \end{pmatrix} \quad ; \quad \tau_2 = \begin{pmatrix} 0 & -i \\ i & 0 \end{pmatrix} \ ;$$
$$\tau_3 = \begin{pmatrix} 1 & 0 \\ 0 & -1 \end{pmatrix} \tag{A.12}$$

The Gell-Mann matrices are

$$\lambda_1 = \begin{pmatrix} 0 & 1 & 0 \\ 1 & 0 & 0 \\ 0 & 0 & 0 \end{pmatrix} ; \quad \lambda_2 = \begin{pmatrix} 0 & -i & 0 \\ i & 0 & 0 \\ 0 & 0 & 0 \end{pmatrix} ; \quad \lambda_3 = \begin{pmatrix} 1 & 0 & 0 \\ 0 & -1 & 0 \\ 0 & 0 & 0 \end{pmatrix} ;$$

$$\lambda_4 = \begin{pmatrix} 0 & 0 & 1 \\ 0 & 0 & 0 \\ 1 & 0 & 0 \end{pmatrix} ; \quad \lambda_5 = \begin{pmatrix} 0 & 0 & -i \\ 0 & 0 & 0 \\ i & 0 & 0 \end{pmatrix} ; \quad \lambda_6 = \begin{pmatrix} 0 & 0 & 0 \\ 0 & 0 & 1 \\ 0 & 1 & 0 \end{pmatrix} ;$$

$$\lambda_7 = \begin{pmatrix} 0 & 0 & 0 \\ 0 & 0 & -i \\ 0 & i & 0 \end{pmatrix} ; \quad \lambda_8 = \frac{1}{\sqrt{3}} \begin{pmatrix} 1 & 0 & 0 \\ 0 & 1 & 0 \\ 0 & 0 & -2 \end{pmatrix} \tag{A.13}$$

Internal-symmetry indices are denoted by a,b,c,... . We shall represent the generators of SU(3) as $T^a = (1/2)\lambda^a$ (see Appendix B). Vectors in internal-symmetry spaces are denoted by arrows (two-dimensional spatial vectors are also denoted by arrows: no confusion is possible since the contexts are clearly separated). All "local" notations specific to a given argument or calculation are defined in the corresponding portion of text.

APPENDIX B: QCD AS A GAUGE THEORY

1. Maxwell's equations without matter fields can be derived from the following Lagrangian density:

$$L^{0}_{em} = -\frac{1}{4} F_{\mu\nu}(x) F^{\mu\nu}(x) \qquad (B.1)$$

where $F_{\mu\nu}(x)$ is the electromagnetic field tensor obtained from the vector potential $A_\mu(x)$ which represents the spin-1 photon field:

$$F_{\mu\nu}(x) = \partial_\mu A_\nu(x) - \partial_\nu A_\mu(x) \qquad (B.2)$$

This object is invariant under the "gauge transformations" of the vector potential

$$A_\mu(x) \longrightarrow A_\mu(x) + \partial_\mu \varepsilon(x) \qquad (B.3)$$

where $\varepsilon(x)$ is an arbitrary function of space-time. Thus the Lagrangian of free electromagnetism is invariant under a one-parameter group of "local" (space-time dependent) transformations.

2. In coupling charged matter fields to the photon field, it is desirable to keep this invariance property intact. Consider a Dirac field with electric charge $-e$ and mass m. It is straightforward to check that the Lagrangian density

$$L^{int}_{em} = \bar{\psi}\left[i\gamma^\mu(\partial_\mu - ieA_\mu(x)) - m\right]\psi \qquad (B.4)$$

is invariant under the simultaneous transformations

$$A_\mu(x) \longrightarrow A_\mu(x) - \frac{1}{e}\partial_\mu \varepsilon(x) \qquad (B.5a)$$

$$\psi(x) \longrightarrow e^{ie\varepsilon(x)}\psi(x) \qquad (B.5b)$$

induced by $\varepsilon(x)$ on the photon and the lepton fields. Eq. (B.4) describes the "minimal gauge-invariant coupling" of photons to charged leptons. The full Lagrangian density of classical electrodynamics is given by the sum of (B.1) and (B.4). From this one derives the equations of electromagnetism with sources

$$\partial_\mu F^{\mu\nu} = j^\nu$$
$$\partial_\mu F^{\nu\lambda} + \partial_\lambda F^{\mu\nu} + \partial_\nu F^{\lambda\mu} = 0 \qquad (B.6)$$

where $j^\nu = e\bar{\psi}\gamma^\nu\psi$ is the electric current density. Quantum electrodynamics is obtained from the classical Lagrangian density by adding a gauge-fixing term. We conclude that the requirement of invariance under the local U(1) group of gauge transformations affecting matter fields as in Eq. (B.5b) completely determines electrodynamics.

3. We have seen in the main text that quarks are Dirac fermions transforming in the fundamental representation of the local color group $SU(3)_c$ and that gluons are spin-1 vectors transforming in the adjoint representation of the same group. QCD is defined by the requirement that quarks couple to gluons in the minimal gauge-invariant way. A local $SU(3)_c$ transformation

$$U(x) = \exp\left[\frac{ig}{2}\sum_{a=1}^{8} \lambda_a \varepsilon^a(x)\right] \equiv \exp\left[ig\,\vec{T}\cdot\vec{\varepsilon}(x)\right] \quad (B.7)$$

where λ_a (a=1,...8) are the Gell-Mann matrices (A.13), transforms a three-component spinor $\psi=(q_{red}, q_{yellow}, q_{blue})$ representing one flavor of colored quarks into the spinor $U\psi$. Arrows indicate vectors in SU(3) group space. The group generators T_a (a=1,2,...8 is the color index) satisfy the Lie commutation relations

$$[T_a, T_b] = i f_{abc} T^c \qquad (B.8)$$

where f_{abc} are the structure constants of $SU(3)_c$. The main difference between $SU(N\geq 2)$ and $U(1)$ gauge theories is that $[T_a, T_b]\neq 0$ whereas the generator of $U(1)$ commutes with itself (the latter group is "abelian" whereas the former are "nonabelian"). This observation allows us to generalize the transformation law of the gauge field from the abelian Eq. (B.5a) to

$$\vec{A}_\mu(x) \to \vec{A}_\mu(x) - \frac{1}{g}\partial_\mu \vec{\epsilon}(x) + \vec{\epsilon}(x)\times\vec{A}_\mu(x) \qquad (B.9)$$

(the vector product in group space is induced by Eq. (B.8)). The field strength tensor is

$$\vec{F}_{\mu\nu}(x) = \partial_\mu \vec{A}_\nu(x) - \partial_\nu \vec{A}_\mu(x) + g\vec{A}_\mu(x)\times\vec{A}_\nu(x) \qquad (B.10)$$

Correspondingly, the "covariant derivative" of electrodynamics

$$D_\mu \equiv \partial_\mu - ieA_\mu \qquad (B.4')$$

generalizes to

$$D_\mu = \partial_\mu - ig\vec{A}_\mu\cdot\vec{T} \qquad (B.11)$$

where g is the color coupling constant.

With these properties, the classical chromodynamic Lagrangian density for a given quark flavor, written by analogy to Eqs. (B.1) and (B.4)

$$L_{CD} = -\frac{1}{4}\vec{F}_{\mu\nu}\cdot\vec{F}^{\mu\nu} + \bar{\psi}\left[i\gamma^\mu D_\mu - m_f\right]\psi \qquad (B.12)$$

is indeed $SU(3)_c$ gauge-invariant. Since the covariant derivative is diagonal in flavor space, the fermion Lagrangian for N_f flavors is just the sum of N_f fermion terms differing only in their masses. The unrenormalized quantum Lagrangian density is obtained from Eq. (B.11) upon adding a gauge-fixing term and some prescription to preserve unitarity in all gauges (a popular way to do this is to add a "Fadeev-Popov ghost" term in troublesome gauges).

REFERENCES AND FOOTNOTES

[1] S. Weinberg, Phys. Rev. Lett. 19 (1967) 1264; A. Salam, in "Elementary Particle Theory: Relativistic Groups and Analyticity" (Nobel Symposium 8), ed. N. Svartholm (Almqvist and Wiskell, Stockholm 1968); S.L. Glashow, Nucl. Phys. 22 (1961) 579; S.L. Glashow, J. Iliopoulos and L. Maiani, Phys. Rev. D2 (1970) 1285; G. Arnison et al., Phys. Lett. 122B (1983) 103 and 126B (1983) 398.

[2] H. Georgi and S.L. Glashow, Phys. Rev. Lett. 32 (1974) 438; H. Georgi, H.R. Quinn and S. Weinberg, Phys. Rev. Lett. 33 (1974) 451; P. Fayet and S. Ferrara, Phys. Reports 32C (1977) 249; P. van Nieuwenhuizen, Phys. Reports 68C (1981) 189; A. Zee, "Unity of Forces in the Universe" (World Scientific, Singapore, 1982).

[3] M. Gell-Mann, Phys. Rev. 125 (1962) 1067; Y. Ne'eman, Nucl. Phys. 26 (1961) 222.

[4] M. Gell-Mann, Phys. Lett. 8 (1964) 214; G. Zweig, CERN-TH 401 (1964) and CERN-TH 412 (1964) (unpublished).

[5] J.J.J. Kokkedee, The Quark Model (Benjamin, New York, 1969); A. De Rujula, H. Georgi and S.L. Glashow, Phys. Rev. D12 (1975) 147.

[6] S.L. Glashow, J. Iliopoulos and L. Maiani, Phys. Rev. D2 (1970) 181 and Phys. Rev. D3 (1971) 1043; S.W. Herb et al., Phys. Rev. Lett. 39 (1977) 252.

[7] M. Breidenbach et al., Phys. Lett. 23 (1969) 935; R.P. Feynman, in Proc. of the 3rd Int. Conf. on High Energy Collisions, Stony Brook, Sept. 1969; J.D. Bjorken and E.A. Paschos, Phys. Rev. 185 (1969) 1975.

[8] H. Fritzsch, M. Gell-Mann and H. Leutwyler, Phys.Lett. 47B (1973) 365; W. Marciano and H. Pagels, Phys. Rep. 36C (1978) 137.

[9] The following work implies that this decay rate is proportional to the number of colors: S.L. Adler, Phys. Rev. 177 (1969) 2426.

[10] G. Ross, in Proc. of the 21st Scottish Univ. Summer School in Physics, Edinburgh 1981 (SUSSP Press 1981) p.1.

[11] S.D. Drell, D.J. Levy and T.M. Yan, Phys. Rev. 187 (1969) 2159.

[12] F. Dydak, in Proc. of the Int. Symp. on Lepton and Photon Inter. at High Energies, Cornell University Aug. 1983.

[13] S. Weinberg, Phys. Rev. Lett. 31 (1973) 494; D.V. Nanopoulos, Nuovo Cim. Letters 8 (1973) 873.

[14] Y. Nambu, Phys. Rev. Lett. 4 (1960) 380; J. Goldstone, Nuovo Cim. 19 (1961) 154.

[15] H. Nishijima, Nuovo Cim. 11 (1959) 698; F. Gursey, Nuovo Cim. 16 (1960) 230; M. Gell-Mann and M. Levy, Nuovo Cim. 16 (1960) 705.

[16] H. Pagels, Phys. Reports 16C (1975) 219; S.L. Adler and W. Dashen, "Current Algebras" (Benjamin, N.Y. 1968)

[17] S. Weinberg, Phys. Rev. 166 (1967) 1568; S. Coleman, J. Wess and B. Zumino, Phys. Rev. 177 (1969) 2239; G. Moore and P. Nelson, Phys. Rev. Lett. 53 (1984) 1519.

[18] T.H.R. Skyrme, Nucl. Phys. 31 (1962) 556 and J. Math. Phys. 12 (1971) 1735; E. Witten, Nucl. Phys. B223 (1983) 422 and 433; A.P. Balandacharan, Syracuse preprint 4222-288 (June 1984).

[19] K. Gottfried, Hadronic Spectroscopy, in Proceedings of the EPS Conference on High Energy Physics, Brighton (July 1983), J. Guy and C. Costain eds. (1984) 743;
P.M. Tuts, Experimental Results in Heavy Quarkonia, in Proceedings of the International Symposium on Lepton and Photon Interactions at High Energies, Cornell Univ. (Sept. 1983), D.G. Cassel and D.L. Kreinick eds. (1984) 284;
W. Buchmuller, preprint CERN-TH 3938, July 1984.

[20] A. Chodos et al., Phys. Rev. D9 (1974) 3471; K. Johnson, Acta Phys. Pol. B6 (1975) 865; P. Hasenfratz and J. Kuti, Phys. Reports 40C (1978) 75.

[21] A.W. Thomas, in "Advances in Nuclear Physics" Vol. 13 (Plenum, N.Y. 1984) p.1.

[22] G.E. Brown and M. Rho, Phys. Lett. 82B (1979) 177; H.K. Lee and V. Vento, CERN-TH 3994 (Sept. 1984).

[23] A. Manokhar and H. Georgi, Nucl. Phys. B234 (1984) 189.

[24] M. Rho, A.S. Goldhaber and G.E. Brown, Phys. Rev. Lett. 51 (1983) 747; J. Goldstone and R.L. Jaffe, Phys. Rev. Lett. 51 (1983) 1518.

[25] G. Altarelli, R.K. Ellis and G. Martinelli, Nucl. Phys. B143 (1978) 521, Erratum Nucl. Phys. B146 (1978); Nucl. Phys. B157 (1979) 461.

[26] G. 't Hooft and M. Veltman, Nucl. Phys. B44 (1972) 189.

[27] E.C.G. Stueckelberg and A. Petermann, Helv. Phys. Acta 26 (1953) 499; M. Gell-Mann and F.E. Low, Phys. Rev. 95 (1974) 1300.

[28] H.D. Politzer, Phys. Rev. Lett. 30 (1973) 1346; D.J. Gross and F.A. Wilczek, Phys. Rev. Lett. 30 (1973) 1343.

[29] W. Cashwell, Phys. Rev. Lett. 33 (1974) 244; D.R.T. Jones, Nucl. Phys. B75 (1974) 531.

[30] R.M. Barnett, M. Dine and L. McLerran, Phys. Rev. D22 (1980) 594.

[31] K.G. Wilson, Phys. Rev. 179 (1969) 1499; B.L. Ioffe, Phys. Lett. 30B (1969) 123; R.A. Brandt and G. Preparata, Nucl. Phys. B27 (1971) 541; Y. Frishman, Ann. Phys. (N.Y.) 66 (1971) 373.

[32] D.J. Gross and F.A. Wilczek, Phys. Rev. D8 (1973) 3633 and D9 (1974) 980; H. Georgi and H.D. Politzer, Phys. Rev. D9 (1974) 416; D. Bailin, A. Love and D.V. Nanopoulos, Lett. Nuovo Cim. 9 (1974) 501.

[33] G. Altarelli and G. Parisi, Nucl. Phys. B126 (1977) 298.

[34] D.W. Duke and R.G. Roberts, Phys. Lett. 85B (1979) 289 and Nucl. Phys. B166 (1980) 243.

[35] M.A. Shifman, A.I. Vainshtain and V.I. Zakharov, Nucl. Phys. B 147 (1979) 385, 448, 519; L.J. Reinders, H.R. Rubinstein and S. Yazaki, Nucl. Phys. B186 (1981) 109 and CERN-TH 4079/84 (1984); S.N. Nikolaev and A.V. Radyushkin, Nucl. Phys. B213 (1983) 285.

[36] B.L. Ioffe, ITEP preprint 150 (1984).

9

[37] R.P. Feynman and A.R. Hibbs, "Quantum Mechanics and Path Integrals" (McGraw-Hill, N.Y. 1965); P. Ramond, "Field Theory A Modern Primer" (Benjamin, Reading (Mass.) 1981).
In many texts (e.g. in Ramond's book) W[J] denotes the vacuum- to- vacuum functional and Z[J] the generating functional for connected Green's functions. We interchange these symbols to conform with the convention preferred in lattice gauge theories.

[38] G. Jona-Lasinio, Nuovo Cim. 34 (1964) 1790;
S. Coleman, in "Laws of Hadronic Matter", Proceedings of the Erice Summer School 1974 (Academic Press, N.Y. 1975).

[39] R. Jackiw, Phys. Rev. D9 (1974) 1686.

[40] S. Coleman and E. Weinberg, Phys. Rev. D7 (1973) 1888.

[41] S.G. Matinyan and G.K. Savvidy, Nucl. Phys. B156 (1979) 1;
M.J. Duff and M. Ramon-Medrano, Phys. Rev. D12 (1976) 3357;
H. Pagels and E. Tomboulis, Nucl. Phys. B143 (1978) 485.

[42] N.K. Nielsen and P. Olesen, Nucl. Phys. B144 (1978) 376 and Phys. Lett. 79B (1978) 304.

[43] N.K. Nielsen and P. Olesen, Nucl. Phys. B160 (1979) 380;
J. Ambjørn and P. Olesen, Nucl. Phys. B170 (1980) 60 and 265.

[44] G.C. Callan, R. Dashen and D. Gross, Phys. Lett. 66B (1977) 375; J.M. Cornwall, Nucl. Phys. B157 (1979) 392.

[45] V.P. Nair and C. Rosenzweig, Phys. Lett. 131B (1983) 434 and Phys. Lett. 135B (1984) 450.

[46] J.M. Cornwall, R. Jackiw and E. Tomboulis, Phys. Rev. D10 (1974) 2428.

[47] F.A. Berezin, "The Method of Second Quantization" (Academic Press, N.Y., 1966).

[48] M. Peskin, in Proc. of the Les Houches Summer School in Theoretical Physics Aug. 1982 (North Holland, Amsterdam, 1984).

[49] C.N. Yang and R.L. Mills, Phys. Rev. 96 (1954) 1605.

[50] F. Wegner, J. Math. Phys. 12 (1971) 2259.

[51] K.G. Wilson, Phys. Rev. D14 (1974) 2455 and Phys. Reports 23C (1975) 331.

[52] A.M. Polyakov, Phys. Lett. 59B (1975) 79 and 82.

[53] B. Berg, S. Meyer and I. Montvay, Nucl. Phys. B235[FS11] (1984) 149.

[54] J.-M. Drouffe and J.-B. Zuber, Phys. Reports 102C (1984) 1.

[55] B. Berg, A. Billoire and C. Rebbi, Ann. Phys. (N.Y.) 142 (1982) 185; M. Creutz, L. Jacobs and C. Rebbi, Phys. Reports 95C (1983) 201.

[56] K. Binder, in "Phase Transitions and Critical Phenomena", Vol. 5B (Academic Press, N.Y. 1976); C. Rebbi, "Lattice Gauge Theories and Monte Carlo Simulations" (World Scientific, Singapore 1983).

[57] C. Lang and C. Rebbi, Phys. Lett. 115B (1982) 137; A. Hasenfratz, P. Hasenfratz, U. Heller and F. Karsch, CERN-TH 3842 (1984).

[58] J. Kripfganz, in Proc. of the 22nd EPS Conf. on High Energy Physics, Leipzig 1984.

[59] J. Ambjørn, P. Olesen and C. Peterson, Phys. Lett. 142B (1984) 410.

[60] J. Kogut, Rep. Mod. Phys. 55 (1983) 775.

[61] M. Lüscher, Nucl. Phys. B180[FS 2] (1981) 317; J.D. Stack and M. Stone, Phys. Lett. 100B (1981) 365.

[62] J.D. Stack, Phys. Rev. D27 (1983) 412; S. Otto and J.D. Stack,

Phys. Rev. Lett. 52 (1984)

[63] D. Barkai, K.J.M. Moriarty and C. Rebbi, Phys. Rev. D30 (1984) 1293 and 2201.

[64] A.D. Linde, Rep. Prog. Phys. 42 (1979) 389; M. Jacob and Tran Thanh Van, eds., Phys. Reports 88C (1982) 321.

[65] A.M. Polyakov, Phys. Lett. 72B (1978) 477; L. Susskind, Phys. Rev. D20 (1979) 2610.

[66] B. Svetitsky and L.G. Yaffe, Nucl. Phys. B210[FS 6] (1982) 423; for a rigorous proof of finite field-temperature deconfinement in SU(N) lattice gauge theories, see C. Borgs and E. Seiler, Comm. Math. Phys. 91 (1983) 329.

[67] L. McLerran and B. Svetitsky, Phys. Lett 98B (1981) 195; K. Szlachanyi, Phys. Lett. 98B (1981) 199; T. Celik, J. Engels and H. Satz, Z. Phys. C22 (1983) 301; A.D. Kennedy, J.Kuti, S. Meyer and B.J. Pendleton, preprint UCSDF-10P10-234 (1984).

[68] J.S. Bell and R. Jackiw, Nuovo Cim. A60 (1969) 47; S.L. Adler and W.A. Bardeen, Phys. Rev. 182 (1969) 1517; S.L. Adler, in "Lectures on Elementary Particles and Quantum Field Theory", Vol. 1 (M.I.T. Press, Cambridge, MA, 1970).

[69] A. Belavin, A.Polyakov, A. Schwartz and Y. Tyupkin, Phys.

Lett. 59B (1975) 85; G. 't Hooft, Phys. Rev. Lett. 37 (1976) 8; S. Coleman, in "The Whys of Subnuclear Physics", Proc. of the Erice Summer School 1978 (Plenum, N.Y. 1979).

[70] E. deGroot, Zakopane Lectures 1984, preprint BI-TP 26/84.

[71] J. Kogut and L. Susskind, Phys. Rev. D11 (1975) 395; L. Susskind, Phys. Rev. D16 (1977) 3031.

[72] N. Kawamoto and J. Smit, Nucl. Phys. B192 (1981) 100.

[73] K.G. Wilson, in "New Phenomena in Subnuclear Physics", Proc. of the Erice Summer School 1976 (Plenum, N.Y. 1977).

[74] S. Drell, M. Weinstein and S. Yankielowicz, Phys. Rev. D14 (1976) 1627.

[75] H.B. Nielsen and M. Ninomiya, Nucl. Phys. B185 (1981) 20 and B193 (1981) 173.

[76] H. Hamber and G. Parisi, Phys. Rev. Lett. 47 (1981) 1792; D. Weingarten, Phys. Lett. 109B (1982) 57.

[77] J. Kogut et al., Nucl. Phys. B225[FS 9] (1983) 326.

[78] H. Lipps, G. Martinelli, R. Petronzio and F. Rapuano, Phys. Lett. 126B (1983) 250; K. Bowler et al., Nucl. Phys. B 220

[FS 8] (1983) 137; C. Bernard, T. Draper and K. Olynik, Phys. Rev. D27 (1983) 227; R. Gupta and A. Patel, Phys. Lett. 124B (1983) 94.

[79] J. Kogut et al., Phys. Rev. Lett. 50 (1983) 393 and 51 (1983) 869; T. Celik, J. Engels and H. Satz, Phys. Lett. 129B (1983) 323; F. Fucito and B. Svetitsky, Phys. Lett. 131B (1983) 165.

[80] E. Marinari, G. Parisi and C. Rebbi, Phys. Rev. Lett, 47 (1981) 1795 and references under [76].

[81] T. Banks and A. Ukawa, Nucl. Phys. B225[FS 9] (1983) 145; T.A. De Grand and C. De Tar, Nucl. Phys B225[FS 9] (1983) 590.

[82] P. Hasenfratz, F. Karsch and I.O. Stamatescu, Phys. Lett. 133B (1983) 221.

[83] W. Fischler and R. Roskies, Phys. Lett. 145B (1984) 99.

[84] T. Celik, J. Engels and H. Satz, Phys. Lett. 133B (1983) 427; J. Polonyi et al., Phys. Rev. Lett. 53 (1984) 644; R.V. Gavai, M. Lev and B. Petersson, Phys. Lett. 140B (1984) 397; F. Fucito and S. Solomon, Phys. Lett. 140B (1984) 387.

[85] E. Tomboulis and L.G. Yaffe, Phys. Rev. Lett. 52 (1984) 2115.

[86] P.H. Damgaard, N. Kawamoto and K. Shigemoto, Phys. Rev. Lett.

53 (1984) 2211; A. Gocksch and M. Ogilvie, Phys. Lett. 141B (1984) 407.

[87] H. Joos and I. Montvay, Nucl. Phys. B225[FS 9] (1983) 565.

[88] P. Becher, Ann. Phys. (N.Y.) 146 (1983) 223 and references therein.

[89] I. Montvay, Phys. Lett. 139B (1984) 70; W. Langguth and I. Montvay, Phys. Lett. 145B (1984) 261.

[90] J. Kogut, Rev. Mod. Phys. 51 (1979) 659.

[91] H.D. Politzer, Nucl. Phys. B117 (1977) 397; T.I. Larsson, SLAC-PUB 3457, Sept. 1984.

[92] J. M. Cornwall, Phys. Rev. D22 (1980) 1452.

[93] M.D. Scadron, Ann. Phys. (N.Y.) 148 (1983) 257.

[94] M. Nicolescu, S. Sanielevici and P. Valin, McGill report (1984), to appear in Phys. Rev. D.

[95] G. 't Hooft, in "Recent Developments in Gauge Theories" (Plenum, N.Y., 1980).

[96] Y. Frishman et al., Nucl. Phys. B177 (1981) 157; S. Coleman and

B. Grossman, Nucl. Phys. B203 (1982) 205.

[97] S. Adler and W.A. Bardeen, Phys. Rev. 182 (1969) 1517.

[98] E.V. Shuryak, Nucl. Phys. B203 (1982) 93 and 140.

[99] J.M. Cornwall, Nucl. Phys. B157 (1979) 352 and Phys. Rev. D26 (1982) 1453; J.M. Cornwall and A. Soni, Phys. Lett. 120B (1983) 431; R. Akhoury, Nucl. Phys. B234 (1984) 533.

[100] R.C. Hwa, Phys. Rev. D22 (1980) 759 and 1593; R.C. Hwa, in Proceedings of the Europhysics Study Conference, Eriče 1981 (World Scientific, Singapore, 1981).

[101] T. Kanki, Prog. Theor. Phys. 56 (1976) 56; N. Cabibbo and R. Petronzio, Nucl. Phys. B137 (1978) 395; V.V. Anisovich, Yu.M. Shabelsky and V.M. Shekhter, Nucl. Phys. B133 (1978) 447.

[102] R.C. Hwa and M.S. Zahir, Phys. Rev. D23 (1981) 2539 and D25 (1982) 2455.

[103] R.C. Hwa and M.S. Zahir, Z. Phys. C20 (1983) 27.

[104] L. Gatignon et al., Z. Phys. C16 (1983) 229 and work quoted in Ref. [106] below.

[105] R.C. Hwa and C.S. Lam, Phys. Rev. D26 (1982) 2338.

[106] R.C. Hwa, in Proc. of the 13th Int'l Conf. on Multiparticle Dynamics, Volendam 1982 (World Scientific, Singapore, 1983).

[107] R.C. Hwa, Phys. Rev. Lett. 50 (1983) 305.

[108] S. Sanielevici and P. Valin, Phys. Rev. D29 (1984) 52.

[109] S. Sanielevici and P. Valin, Phys. Rev. D32 (1985) 586.

[110] D.E. Soper, Phys. Rev. D15 (1977) 1141.

[111] S.D. Drell and T.M. Yan, Phys. Rev. Lett. 24 (1970) 181; G.B. West, Phys. Rev. Lett. 24 (1970) 1206.

[112] G.P. Lepage and S.J. Brodsky, Phys. Lett. 87B (1979) 359, Phys. Rev. Lett. 43 (1979) 545 and Phys. Rev. D22 (1980) 2157; A. Duncan and A.H. Mueller, Phys. Rev. D21 (1980) 1636.

[113] N. Isgur and C. Llewellyn-Smith, Phys. Rev. Lett. 52 (1984) 1080.

[114] O. Dumbrajs et al., Nucl. Phys. B216 (1983) 277.

[115] G. Altarelli, G. Parisi and R. Petronzio, Phys. Lett. 76B (1978) 351 and 356; R.K. Ellis, G. Martinelli and R. Petronzio, Phys. Lett. 104B (1981) 45; R.R. Horgan and P.N. Scharbach, Nucl. Phys. B181 (1981) 421.

[116] See, for instance, the following review articles:
G. Alberi and G. Goggi, Phys. Reports 74C (1981) 1;
A. Castaldi and G. Sanguinetti, CERN EP 85-36 (1985).

[117] T.T. Chou and C.N. Yang, Phys. Rev. 170 (1968) 5.

[118] R. Henzi and P. Valin, Nucl. Phys. B148 (1979) 513.

[119] P. Valin, in Proc. of the 6th Montreal-Rochester-Toronto-Syracuse High Energy Theory Meeting (Syracuse, May 1984) p.68.

[120] C. Bourrely, J. Soffer and T.T. Wu, Phys. Rev. D19 (1979) 3249.

[121] H. Miettinen and G. Thomas, Nucl. Phys. B166 (1980) 365.

[122] T.T. Chou and C.N. Yang, Phys. Lett. 128B (1983) 457.

[123] C. Bourrely, J. Soffer and T.T. Wu, Nucl. Phys. B247 (1984) 15.

[124] C. Chiu, Phys. Lett. 142B (1984) 309.

[125] R.J. Glauber and J. Velasco, Phys. Lett. 147B (1984) 380.

[126] P. Valin, Nucl. Phys. B219 (1983) 215 and
Z. Phys. C25 (1984) 259.

[127] U. Amaldi and K.R. Schubert, Nucl. Phys. B166 (1980) 301.

[128] K.R. Schubert, in "Landolt–Börnstein: Numerical Data and Functional Relationships in Science and Technology",Group I, Vol. 1 (Springer, Berlin 1979).

[129] S. Conetti et al., Phys. Rev. Lett. 41 (1978) 924.

[130] V. Franco, Phys. Rev. D11 (1975) 1837.

[131] A. Schiz et al., Phys. Rev. D24 (1981) 26; W.F. Baker et al., Phys. Rev. Lett.47 (1981) 1683.

[132] A.S. Carroll et al., Phys. Lett. 80B (1979) 423.

[133] C.H. Lai, S.Y. Lo and K.K. Phua, Report NUS-HEP-82001 (unpubl.)

[134] F. Cervelli, Invited Talk at the 4th Topical Workshop on $\bar{p}p$ Collider Physics (Bern, 1984).

[135] M. Bozzo et al., Phys. Lett. 142B (1984) 385 and 392; Phys. Lett. 155B (1985) 197.

[136] R. Henzi and P. Valin, Phys. Lett. 132B (1983) 443 and Phys. Lett. 149B (1984) 239; R. Henzi, in Proc. of the 4th Topical Workshop on $\bar{p}p$ Collider Physics (Bern, 1984) 314.

[137] S. Sanielevici, in Proc. of the 6th Montreal-Rochester-Syracuse-Toronto High Energy Theory Meeting (Syracuse, May 1984) p.43.

[138] L. Van Hove, Acta Phys. Pol. B7 (1976) 339 and Nucl. Phys. B122 (1977) 525; H.I. Miettinen and J. Pumplin, Phys. Rev. D18 (1978) 1696.

[139] H. Cheng and T.T. Wu, Phys. Rev. Lett. 24 (1970) 1456; H. Cheng, J.K Walker and T.T. Wu, Phys. Lett. 44B (1973) 97.

[140] R. Henzi and S. Sanielevici, McGill report June 1985, submitted to Nucl. Phys. B. Part of the discussion on color Van der Waals forces can be found in the Contributed Paper 676 to the 22nd EPS Conference on High Energy Physics, Leipzig 1984 (by the same authors).

[141] For a recent assessment of this traditional idea, see e.g. D.B. Lichtenberg and W. Namgung, Indiana preprint IUHET 95 (1984).

[142] D.J. Wallace, in Proceedings of the 21st Scottish Universities Summer School in Physics (SUSSP Press 1981) p. 459.

[143] B. Margolis, R. Roskies and N. De Takacsy, in Proc. of the 4th European Antiproton Symposium, ed. by A. Friedman (Ed. du CNRS, Strasbourg 1978), Vol. 2 p. 455.

[144] Particle Data Group: C.G. Wohl et al., Rev. Mod. Phys. 56 (1984) S1.

[145] M. Peskin, Phys. Lett. 94B (1980) 161.

[146] M.B. Gavela et al., Phys.Lett. 82B (1979) 431.

[147] G. Feinberg and J. Sucher, Phys. Rev. D20 (1979) 1717.

[148] D.H. Lyth, Z.Phys. C15 (1982) 177.

[149] W. Beer et al., Proposal for an Experiment at S.I.N. , No. R-82-10.1 (1982)

[150] H. Lehmann, Nuovo Cimento 10 (1958) 579 and Fortschr. d. Phys. 6 (1959) 159.

[151] A. Martin, Nuovo Cimento 42 (1966) 930.

[152] R.S. Willey, Phys. Rev. D18 (1978) 270;
Y. Fuji and K. Mima, Phys. Lett. 79B (1978) 138.

[153] P.M. Fishbane and M.T. Grisaru, Phys. Lett. 74B (1978) 98;
T. Appelquist and W. Fischler, Phys. Lett. 77B (1978) 138;
L. Bracci, G. Fiorentini and R. Tripiccione, Nucl. Phys. B217 (1983) 215.

[154] O.W. Greenberg and H.J. Lipkin, Nucl. Phys. A370 (1981) 349.

[155] K.F. Liu, Phys.Lett. 131B (1983) 195.

[156] O.W. Greenberg and J. Hietarinta, Phys. Lett. 86B (1979) 309.

[157] F. London, Z. Phys. 63 (1930) 245;
L. Schiff, Quantum Mechanics, 2nd edition
(McGraw-Hill 1955) 176.

[158] H.B.G. Casimir and D. Polder, Phys.Rev. 73 (1948) 360;
G. Feinberg and J. Sucher, Phys.Rev. A2 (1970) 2395.

TABLES

Table 3.1: Coefficients of the distributions of valons in protons and pions, as extracted by two different methods. The coefficients are defined by $L_V^H(x)=A_V^H\, x^{B_V^H}(1-x)^{C_V^H}$ and $T_V^H(\vec{k})=\exp(-D_V^H\, k^2)$, where $H=p,\pi$ and $V=U,D$. Asterisks denote the values which we employ in the study of hadronic matter form factors (see Eq. (5.23).

	Deep Inelastic Scattering [102]		:	Hadron Charge Form Factors [105]	
A_U^p	7.98	*	:	10.74	
B_U^p	0.65	*	:	0.9	
C_U^p	2.	*	:	2.	
D_U^p			:	6.1	*
A_D^p	6.01	*	:	4.63	
B_D^p	0.35	*	:	0.1	
C_D^p	2.3	*	:	2.8	
D_D^p			:	3.	*
A^π			:	1.77	*
B^π			:	0.3	*
C^π			:	0.3	*
D^π			:	6.	*

Table 5.1: Parameters for fits to the pp and πp differential cross-sections. A_j is in $(mb)^{1/2}\,GeV^{-1}$, B_j in GeV^{-2}.

	pp		π^-p	
j	A_j	B_j	A_j	B_j
1	0.60666	15.042	1.8075	6.4557
2	3.2310	6.6985	1.2652	2.8597
3	1.6289	3.8590	0.03529	1.0190
4	-0.03443	1.0353	-0.00426	0.42799
5	-0.0008	0.38062		

Table 5.2: Parameters for the fit to the πp dcs as reported in Ref. [133]. All parameters are in GeV^{-2}.

α_1	2.863	β_1	6.120
α_2	2.038	β_2	2.886
α_3	0.01265	β_3	0.4467
μ	0.6237		

Table 5.3: Parameters used for the fit shown in Fig. 3.6. d and e are in GeV^{-2}.

b	0.912 ± 0.004	c	0.026 ± 0.006
d	6.530 ± 0.211	e	0.045 ± 0.008
f	0.118 ± 0.0026	g	0.0009 ± 0.0001

Table 6.1: Parameters in Equation (6.3) which lead to the predicted ψ and Υ masses listed in Table 6.2.

σ	3076.2	MeV
α	88.55	MeV.fm
r_1	2.675	fm
r_2	12.11	fm

Table 6.2: Properties of ψ and Υ s-states as calculated from the potential (6.3) with the parameter values given in Table 6.1. Masses are listed in MeV; in brackets we show ratios of leptonic widths of the excited states with respect to the ground state of the respective $Q\bar{Q}$ system. The c and b current quark masses were also treated as parameters: for the predictions below, their values are m_c= 1304.7 MeV and m_b= 4722.4 MeV. Experimental values are from Ref. [144].

n	Experiment	Prediction
0	3097	3096
1	3686 (0.46)	3683 (0.45)
2	4030 (0.16)	4077 (0.22)
3	4415 (0.11)	4379 (0.09)
0	9460	9463
1	10025 (0.44)	10013 (0.40)
2	10355 (0.32)	10342 (0.28)
3	10575 (0.24)	10596 (0.25)

Table 6.3: Parameters of the CVDW potentials shown in Fig. 6.3.

Parameter	Value used	Units
α	32.3	MeV.fm
σ	0.6	GeV
r	0.8	fm
K	$K_{max}=4.72*10^{-3}$	fm^{4}
$V(r_{q\bar{q}})$	0.2	GeV
λ	1	fm

Table 6.4: Relationships between the components of the V(r) input and the retarded CVDW force.
The near-force is taken to include all exponentially damped terms in the derivative of Eq. (6.4).

Interquark V	CVDW Force	
	Near-Force	Far-Force
JM, Eq. (2.153)	stronger than R^{-8}	R^{-8}
FS, Eq. (6.9)	R^{-8}	R^{-8}
CC, Eq. (6.10)	stronger than R^{-8}	absent

FIGURE CAPTIONS

Figure 2.1: Feynman diagrams up to order α_s for $e^+e^- \to \bar{q}q$ annihilation. The photon carries $E^2=Q^2$; the quark four-momenta are p_μ and p'_μ.

Figure 2.2: Feynman diagrams up to order α_s for $e^+e^- \to \bar{q}qg$.

Figure 2.3: Feynman graphs of order α_s^2 in e^+e^- annihilation.

Figure 2.4: Quark self-energy subgraph.

Figure 2.5: Inelastic lepton-hadron scattering $lH \to l'X$. X stands for any final-state hadrons produced in the collision. The process is "deep inelastic" if the c.m. energy is large.

Figure 2.6: Parton-model interpretation of deep inelastic scattering. The electroweak gauge boson (photon, W or Z) interacts with a single quark-parton which carries a fraction x of the proton's longitudinal light-cone momentum.

Figure 2.7: Feynman diagrams up to order α_s for photon-quark scattering.

Figure 2.8: Contour used for computing moments of $T(x,Q^2)$.

Figure 2.9: The effective potential of the theory Eq. (2.70) in the absence (A) and in the presence (B) of spontaneous symmetry breaking.

Figure 2.10: J in the second diagram must be adjusted to cancel the contribution of the first diagram to the effective action...

Figure 2.11: ...which leaves only two-particle irreducible diagrams in the sum D.

Figure 2.12: "Hypercubic" 3x3 lattice in $d=2$ dimensions. a is the "lattice spacing". n, $n+\mu$,... are the "sites", μ,ν,... are the "links" and the closed contour is a "plaquette".

Figure 2.13: To take the continuum limit of lattice QCD is

a) to make any physical length measured in units of a diverge;

b) to resolve smaller and smaller distance scales inside a hadron (indicated by the circle inscribed into the lattice).

A coarser lattice corresponds to stronger QCD coupling.

Figure 2.14: a) A "Wilson loop", used to compute the static potential in a heavy $Q\bar{Q}$ system on the lattice. r is measured in the "space" direction $\vec{x}$ and T in the "time" direction.

b) A "Wilson-Polyakov line", used as the order parameter of the deconfinement phase transition at finite field-temperature ($\vec{x}$ is fixed). Here $n_t=4$.

Figure 2.15: The "triangle graph" which spoils the conservation of the flavor-singlet axial current J_μ formed out of colored fermions.

Figure 3.1: The nonperturbative self-energy of a colored fermion can be visualized as the sum of all Feynman diagrams having all possible gluons exchanged along the internal line which represents the fermion propagator.

Figure 3.2: The function $\Sigma(p)$ for three values of the parameter p_o (see Eqs. (3.8), (3.16)). The full curve is for p_o=600 MeV, the dash-dotted curve for p_o=400 MeV and the dash-double-dotted curve for p_o=800 MeV. The origin of these parameter values is explained in Section 4.3. For comparison, the dashed curve represents a Gaussian chosen to be numerically close to the other curves. Its $\sqrt{\langle \vec{p}_T^{\,2} \rangle}$ would have to be $\simeq$2.6 GeV.

Figure 3.3: Images of a proton seen by an "electroweak gauge boson microscope" at increasing resolution Q^2 (indicated by the boxes and arrows). The interior of a constituent quark appears as an ordered distribution of partons for

moderate Q^2; at high Q^2 the partons appear uncorrelated.

Figure 3.4: Downward Q^2-evolution of a "u" current quark into the "U" constituent quark in a proton.

Figure 3.5: Downward Q^2-evolution of a "protopion" into an on-shell pion.

Figure 4.1: Schematic diagram for the pion CFF at high Q^2 (from Ref. [105]). The photon interacts with a current quark which can exchange hard gluons with the spectator partons.

Figure 4.2: The pion CFF at low Q^2 (following Ref. [105]). The photon interacts with a valon (antivalon) which does not exchange hard gluons with the spectator antivalon (resp. valon).

Figure 4.3: Our computed proton charge form factor (full curve) as compared to the standard dipole approximation (dots). No best fit was attempted.

Figure 5.1: The pp matter form factor from overlap data at four ISR energies. Dotted curve at $\sqrt{s}$=23.5 GeV, dashed curve at $\sqrt{s}$=30.7 GeV, dash-dotted curve at $\sqrt{s}$=44.7 GeV and solid curve at $\sqrt{s}$=52.8 GeV.

Figure 5.2: Five-exponential fit to the pp differential cross-section.

Data are from the ISR at $\sqrt{s}$=52.8 GeV and from Fermilab at p_{lab}=400 GeV and large −t. Typical error bars are shown.

Figure 5.3: pp matter form factors by various methods at $\sqrt{s}$=52.8 GeV with $Q^2 \lesssim 5.3$ GeV^2. The points reproduce the solid curve of Fig. 5.1. Solid curve: extraction by method 2. The dashed curve represents K_p^2. The dash-dotted curve represents $K_p^2(a^2-Q^2)/(a^2+Q^2)$ with a^2=5.65 GeV^2 .

Figure 5.4: The $\pi^- p$ matter form factor. Solid curve: prediction from the pp matter form factor extracted at $\sqrt{s}$=52.8 GeV. Dashed curve: direct extraction from Fermilab data at p_{lab}=200 GeV.

Figure 5.5: Four-exponential fit to the $\pi^- p$ differential cross-section. Data from Fermilab at p_{lab}=200 GeV. Typical error bars are shown.

Figure 5.6: Simultaneous SRE fit to the pp differential cross-section at $\sqrt{s}$=52.8 GeV and to the $\bar{p}p$ differential cross-section at $\sqrt{s}$=546 GeV. ISR data are represented by open dots and S$\bar{p}$pS data by full dots. The full curve is the fit to the ISR data and the dashed curve is the fit to the UA4 data (up to −t=1.5 GeV^2). Beyond −t=1.5 GeV^2, the dashed curve is a prediction. Typical error bars are shown.

Figure 5.7: Various $\bar{p}p$ MFFs at $\sqrt{s}$=546 GeV. Dots represent the extraction from UA4 dcs data. The full curve corresponds to the smallest value of the SRE parameter B compatible with the fit in Fig. 5.6. The error bars are induced by the errors listed in Table 5.3. The dashed curve represents $K_P^2(a^2-Q^2)/(a^2+Q^2)$ with a^2=3.2 GeV^2.

Figure 5.8: F(s) (Fig. 5.8a) and a^2(s) (Fig. 5.8b) according to the SRE fit in Fig. 5.6. Error bars are induced by the errors listed in Table 5.3. The straight line in Fig. 5.8a corresponds to $\varepsilon \simeq 0.105$ in Eq. (5.21).

Figure 6.1: The potential (6.3). The full curve represents $m_c V(r)/\hbar^2$ with the parameter values in Table 6.1. The dashed curve is obtained from the "empirical" potential shown in Fig. 6.2. m_c has the value quoted in the caption of Table 6.2. This once, $\hbar$=197.3 (dimensionless: compare to Eq. (A.2)). In these units, the asymptotic value of the full curve is at $m_c\sigma/\hbar \simeq$ 103 MeV^2.

Figure 6.2: Various $q\bar{q}$ potentials. The full curve represents the standard empirical potentials following Refs. [19]. Shaded areas represent the dispersion of the various potentials which coincide between 0.1 fm and 1 fm. The dashed curve represents Eq. (2.135) and the

dashed-dotted curve, which below ≈0.3 fm coincides with the dashed curve, represents Eq. (2.153). The full line labeled "σ" indicates the asymptotic value of the JM potential, as quoted in Table 6.3.

Figure 6.3: Various upper bounds on the strength of the colour Van der Waals potential. The full line labeled "EL" reproduces Eq. (6.7). The solid curves labeled "R^{-6}" and "R^{-7}" correspond to the nonretarded resp. retarded potentials discussed in the text. The dashed curve shows a possible interpolation between the nonretarded and retarded regimes. Dots stress the asymptotic character of the straight lines which represent Eqs. (6.6) and (6.8). The line representing Eq. (6.8) has been continued down to 1.5 fm to illustrate the effect of replacing the JM potential (2.153) by the FS potential (6.9). The dash-dotted curve indicates the CVDW potential which corresponds to the CC interquark potential, Eq. (6.10)

Figure 6.4: The retarded CVDW potential corresponding to the interquark potential in Fig. 6.1. The line labeled "EL" is the same as in Fig. 6.3.
The full curve is the upper limit on the predicted CVDW potential, corresponding to a maximal strength parameter K_{max} = 0.011 fm^4 .

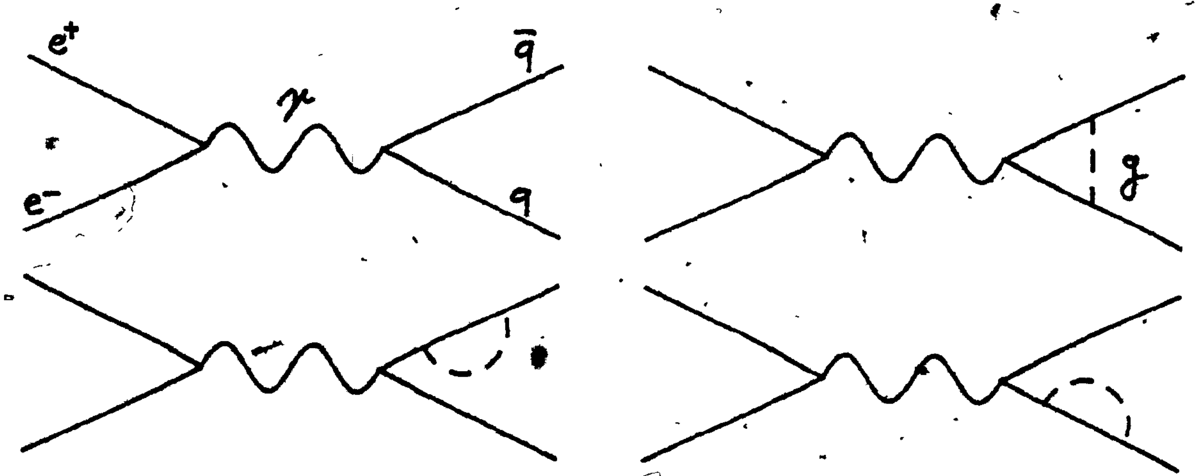

FIG. 2.1

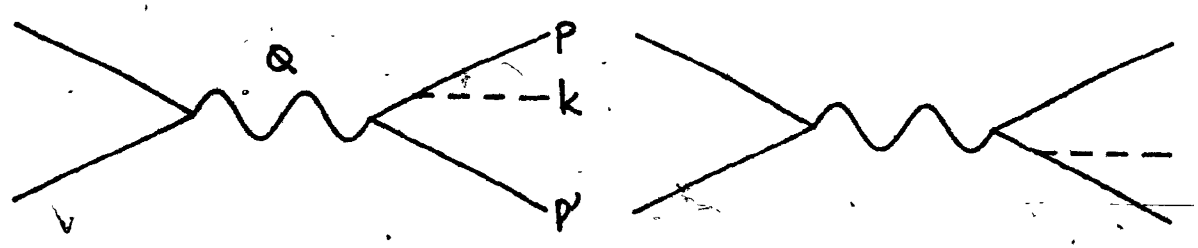

FIG. 2.2

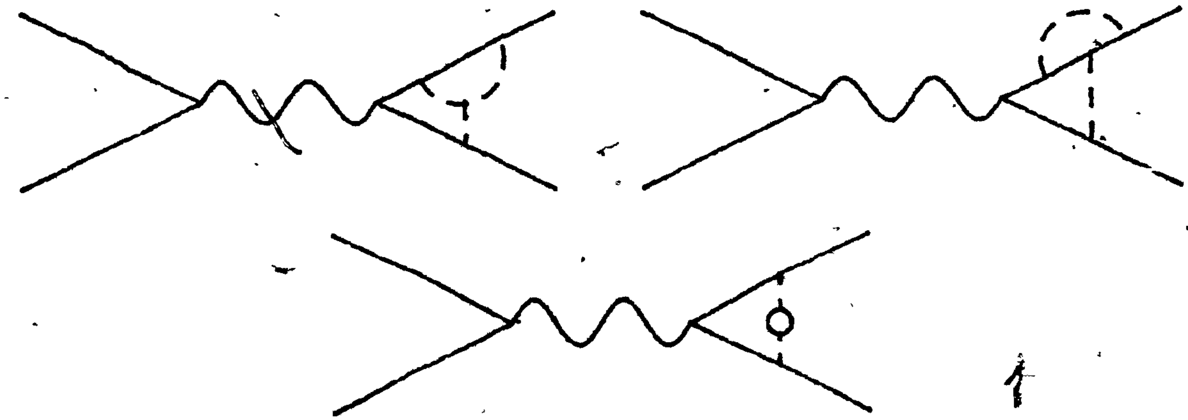

FIG. 2.3

FIG. 2.4

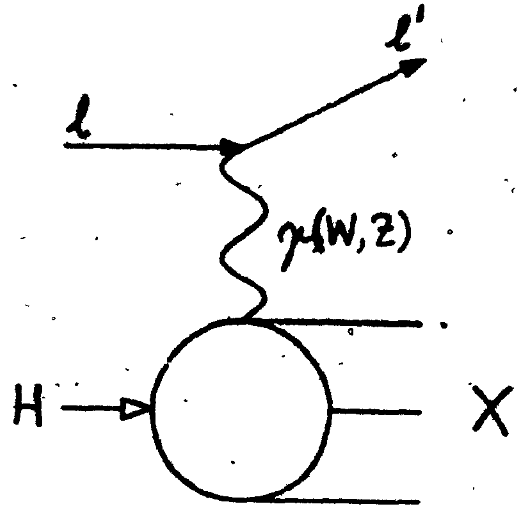

FIG. 2.5

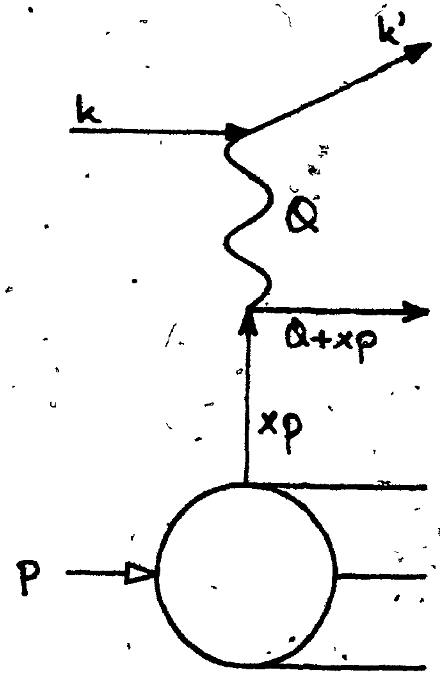

FIG. 2.6

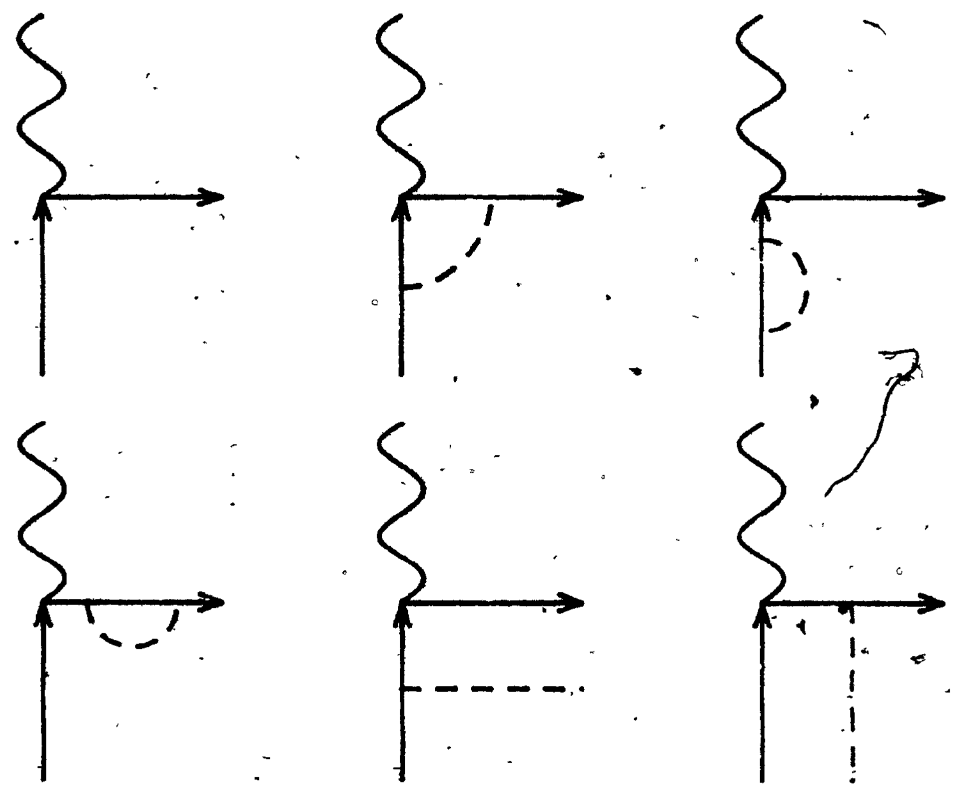

FIG. 2.7

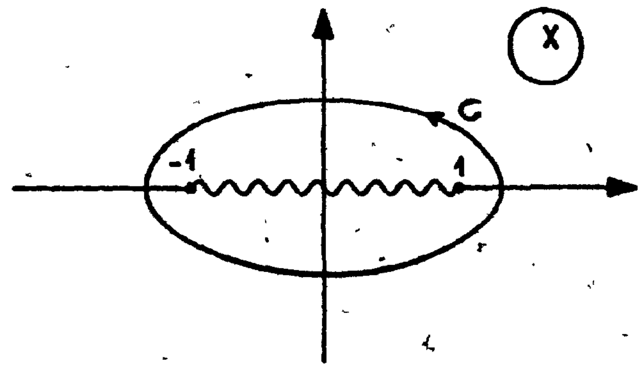

FIG. 2.8

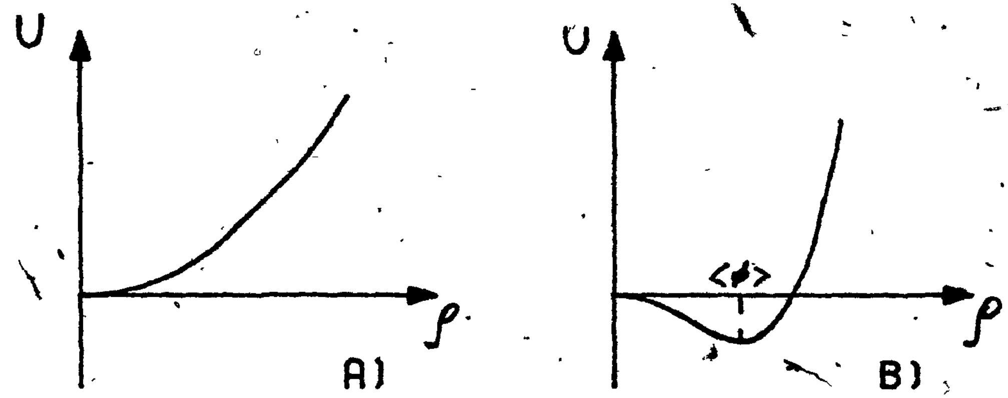

FIG. 2.9

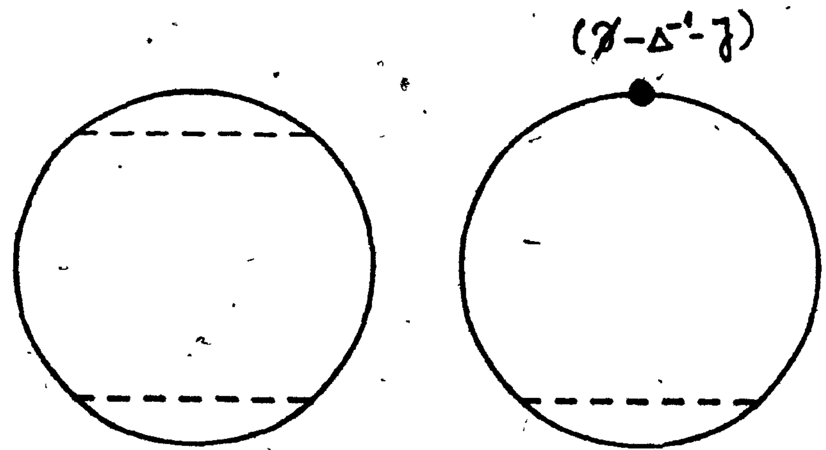

FIG. 2.10

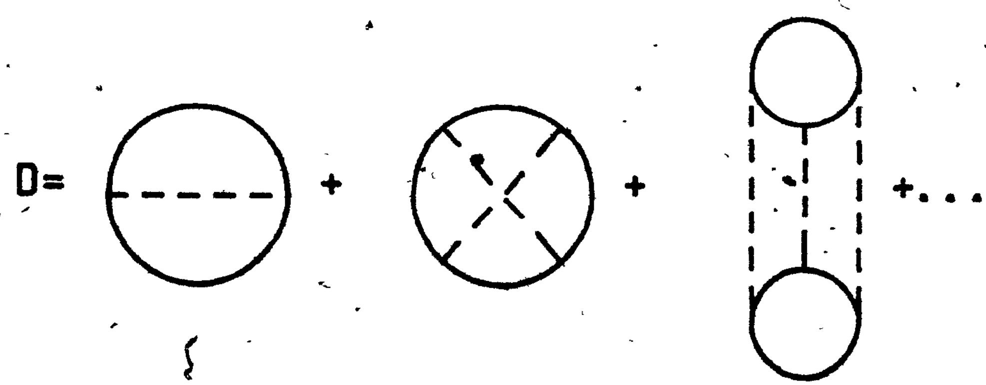

FIG. 2.11

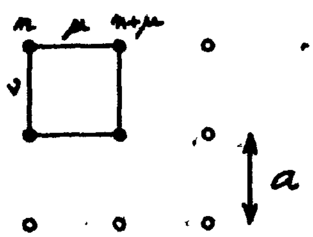

FIG. 2.12

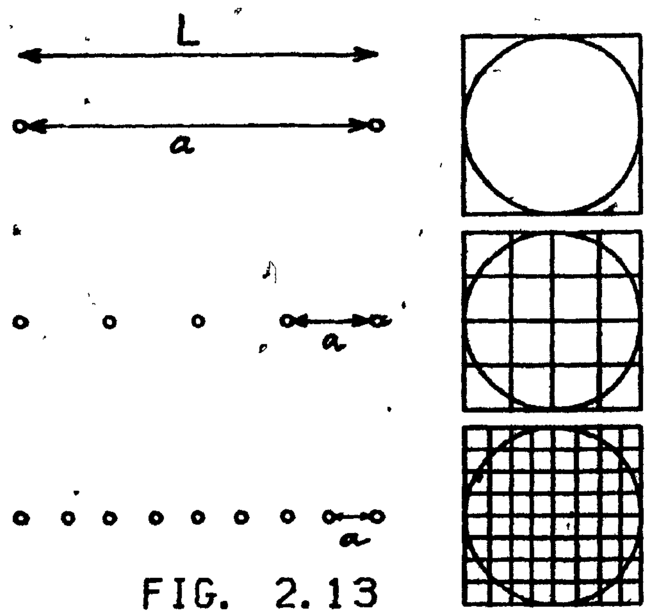

FIG. 2.13

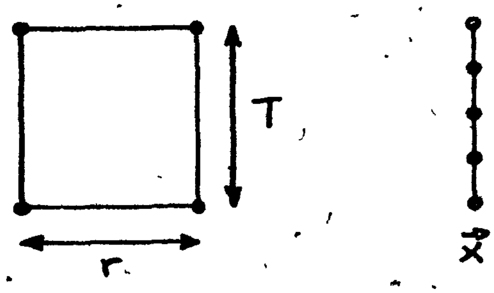

FIG. 2.14

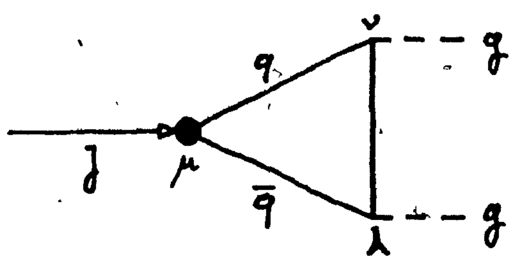

FIG. 2.15

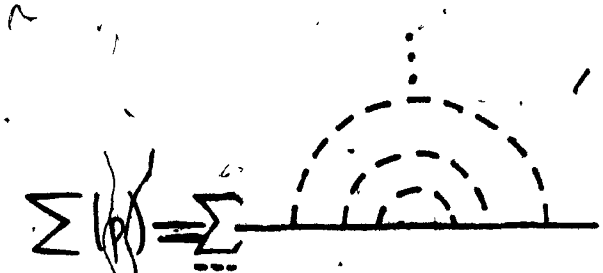

FIG. 3.1

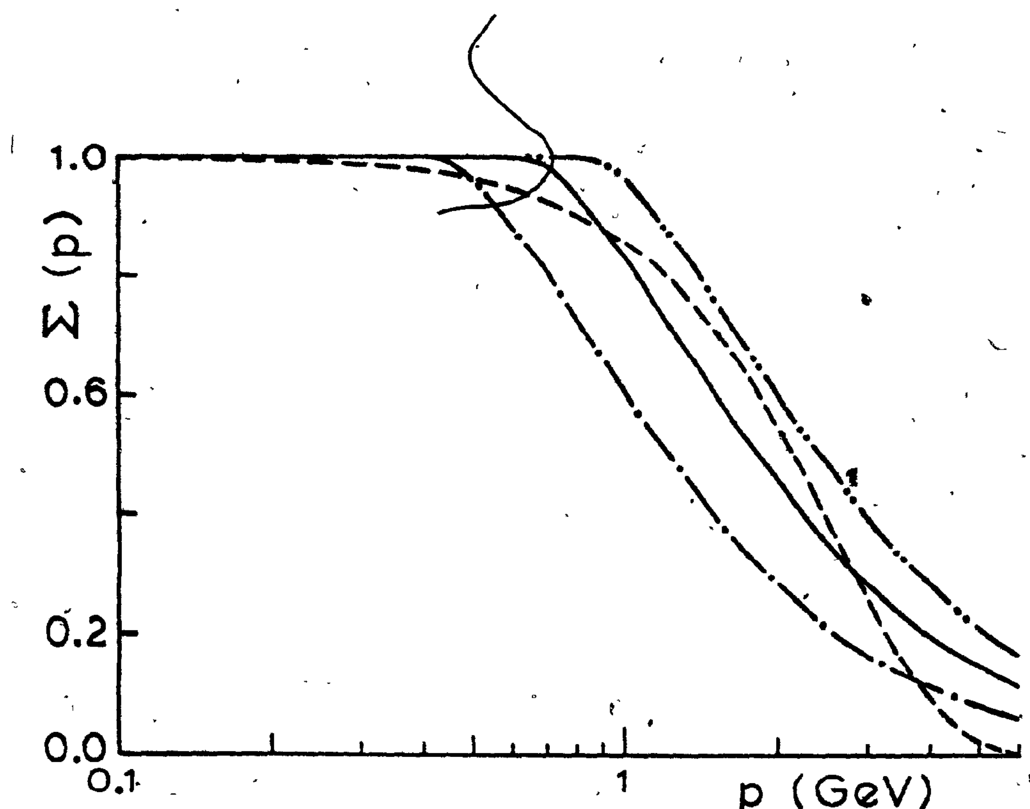

FIG. 3.2.

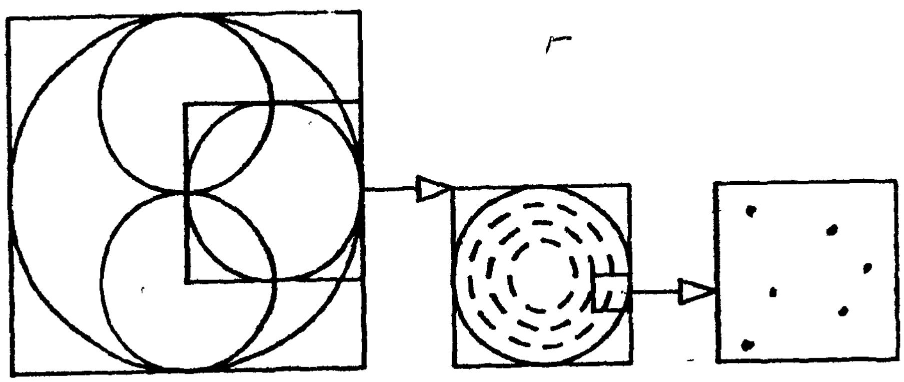

FIG. 3.3

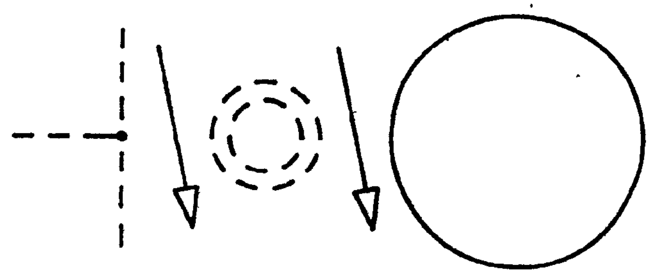

FIG. 3.4

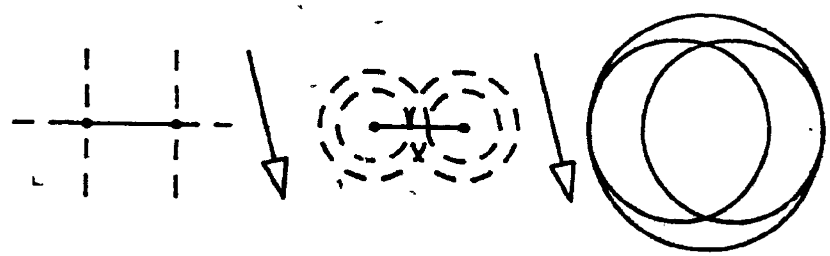

FIG. 3.5

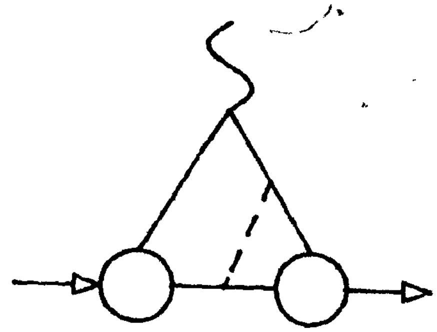

FIG. 4.1

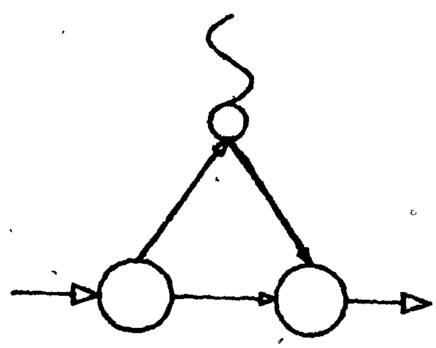

FIG. 4.2

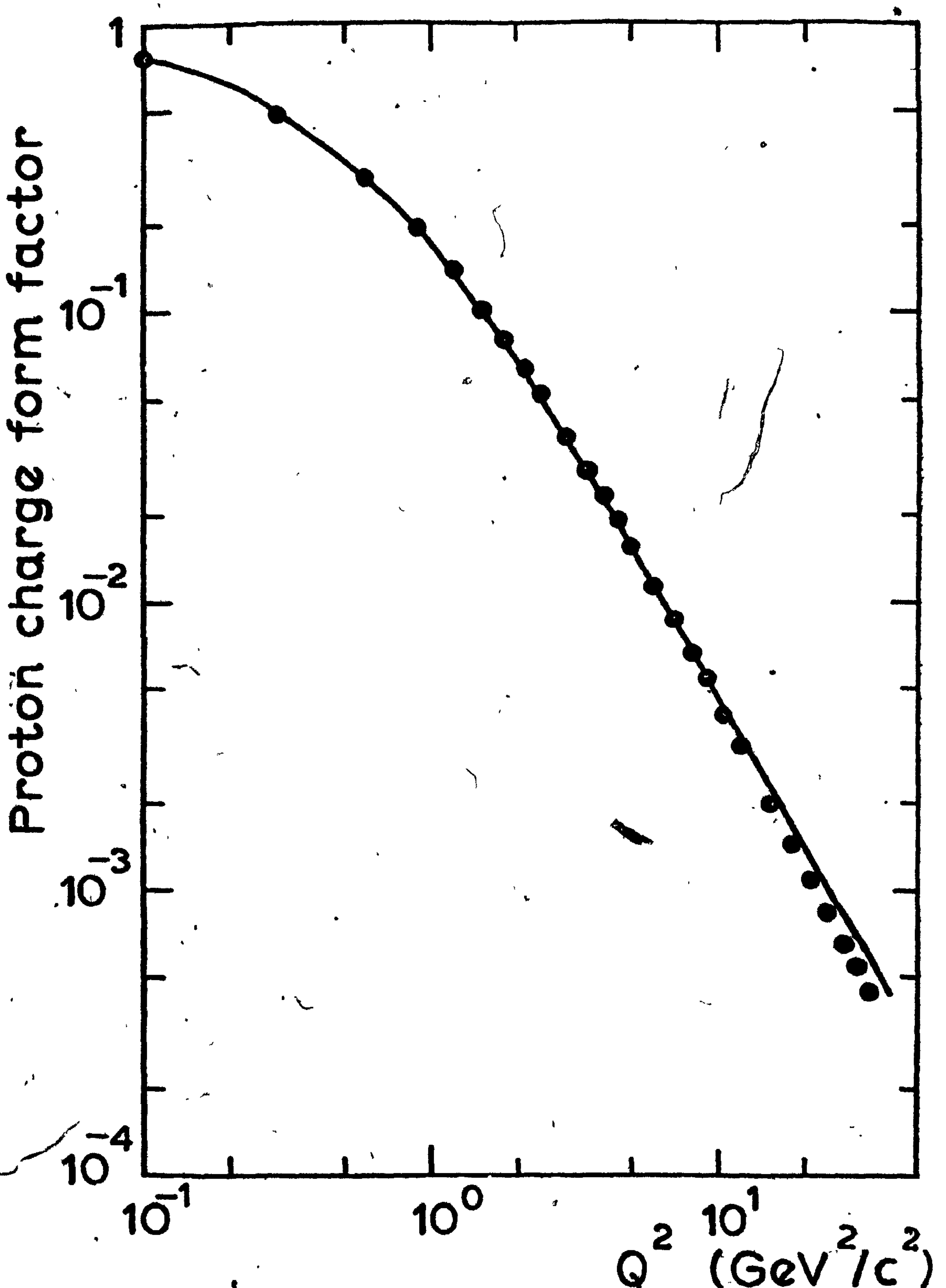

Proton charge form factor
1
10⁻¹
10⁻²
10⁻³
10⁻⁴
10⁻¹
10⁰
10¹
Q² (GeV²/c²)

FIG. 4.3.

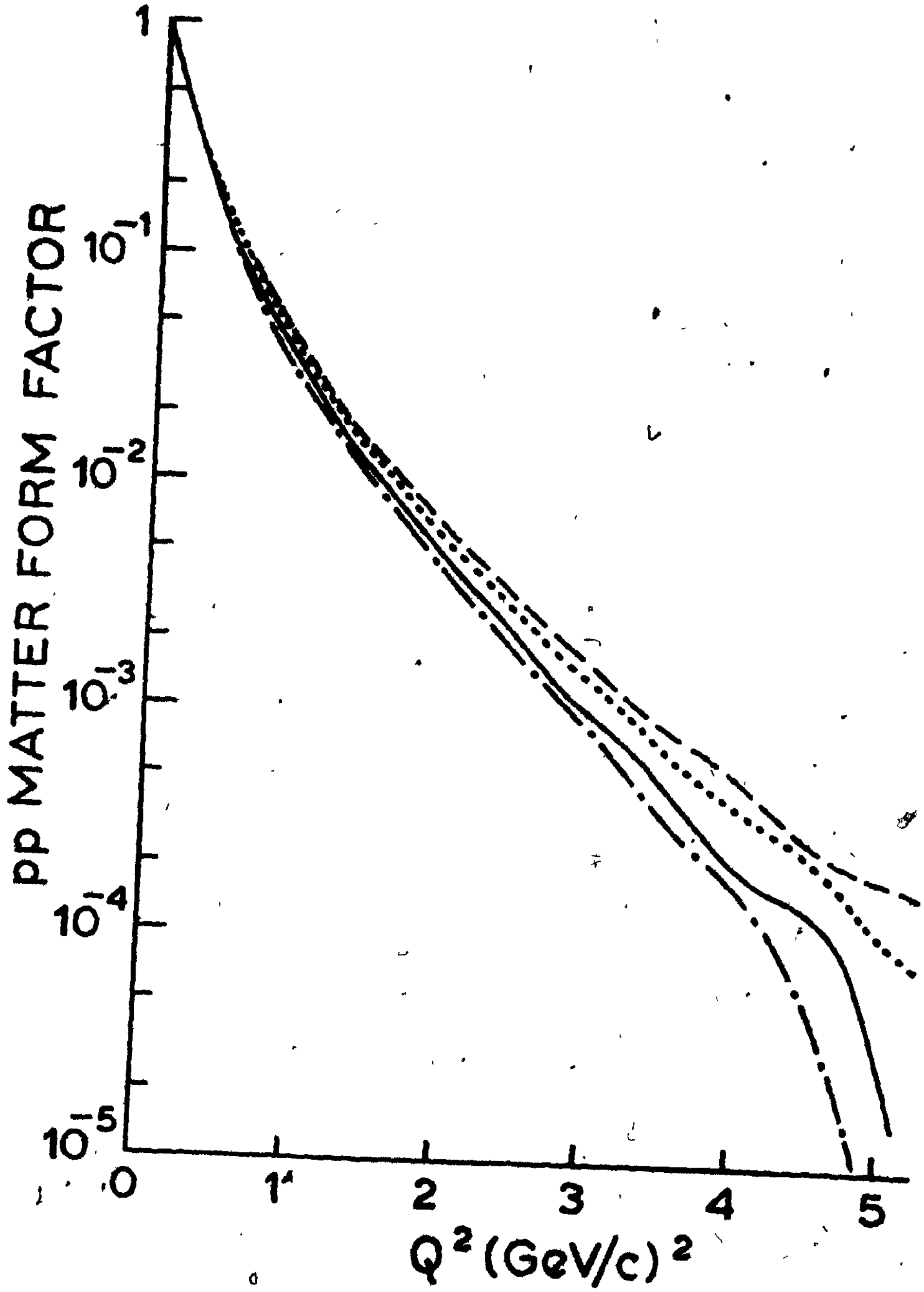

FIG. 5. 1.

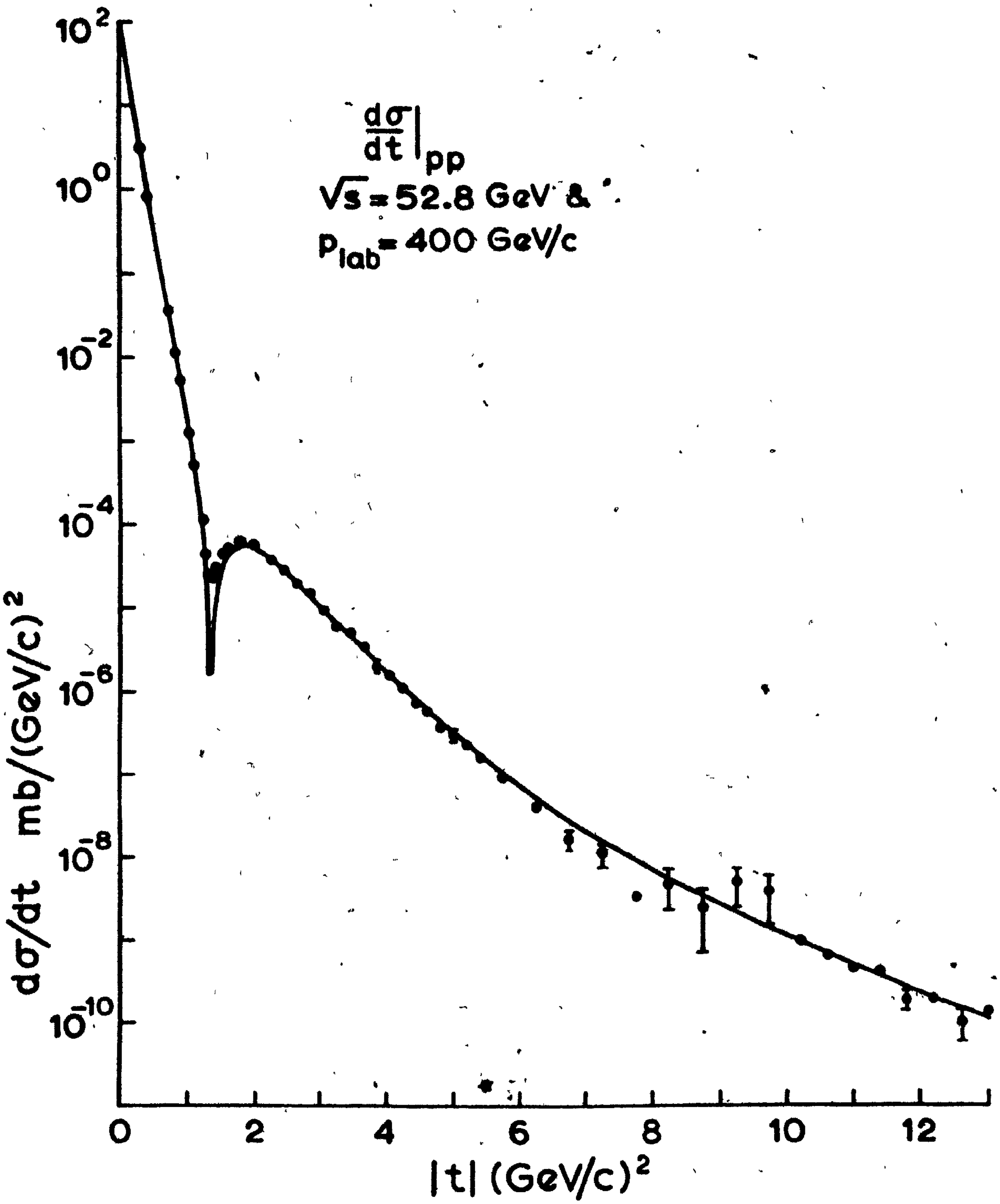

$\frac{d\sigma}{dt}\big|_{pp}$
$\sqrt{s} = 52.8$ GeV &
$p_{lab} = 400$ GeV/c
10^{2}
10^{0}
10^{-2}
10^{-4}
10^{-6}
10^{-8}
10^{-10}
$d\sigma/dt$ mb/(GeV/c)^2
0
2
4
6
8
10
12
$|t|$ (GeV/c)^2

FIG. 5. 2.

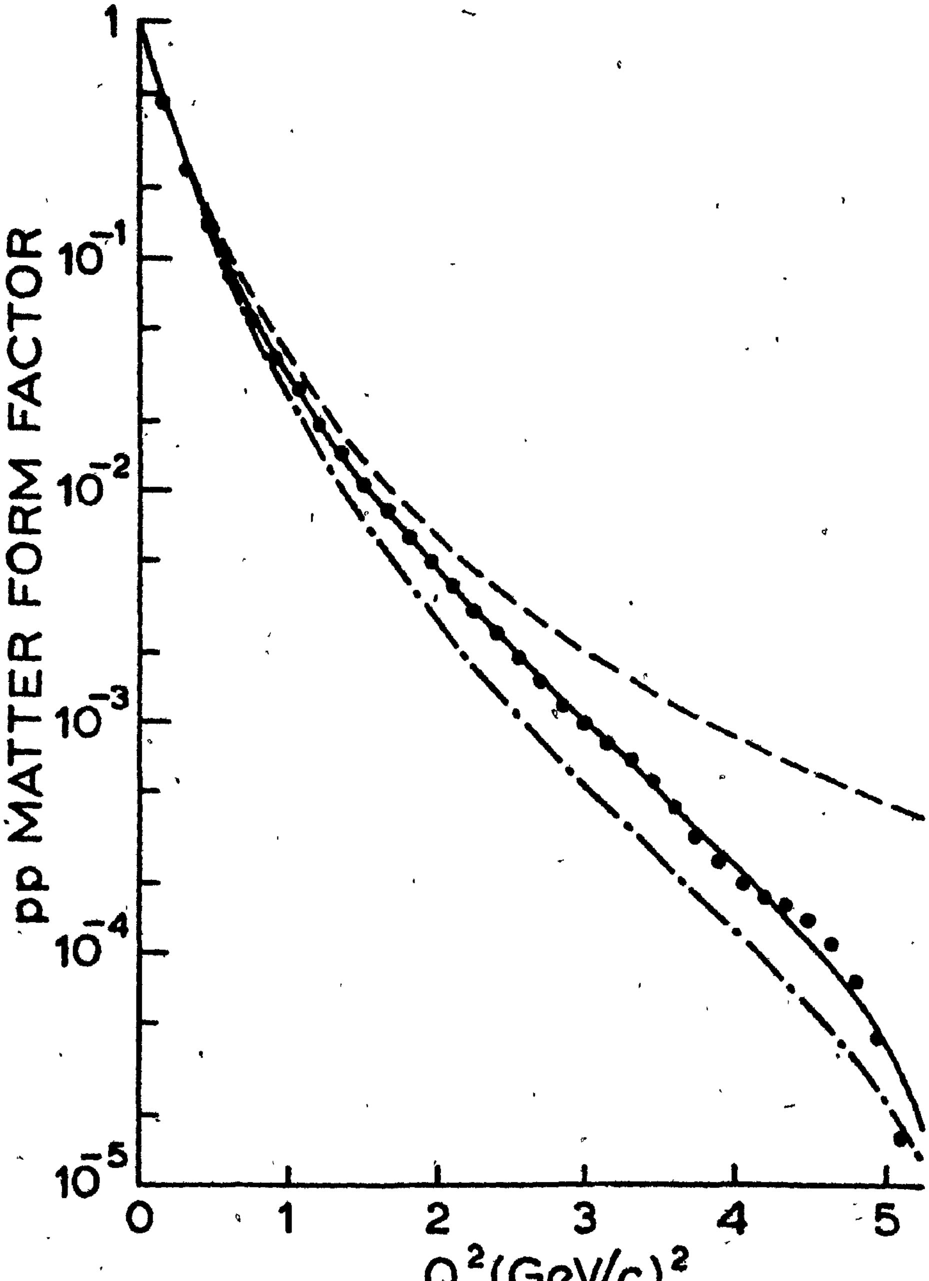

FIG. 5.3.

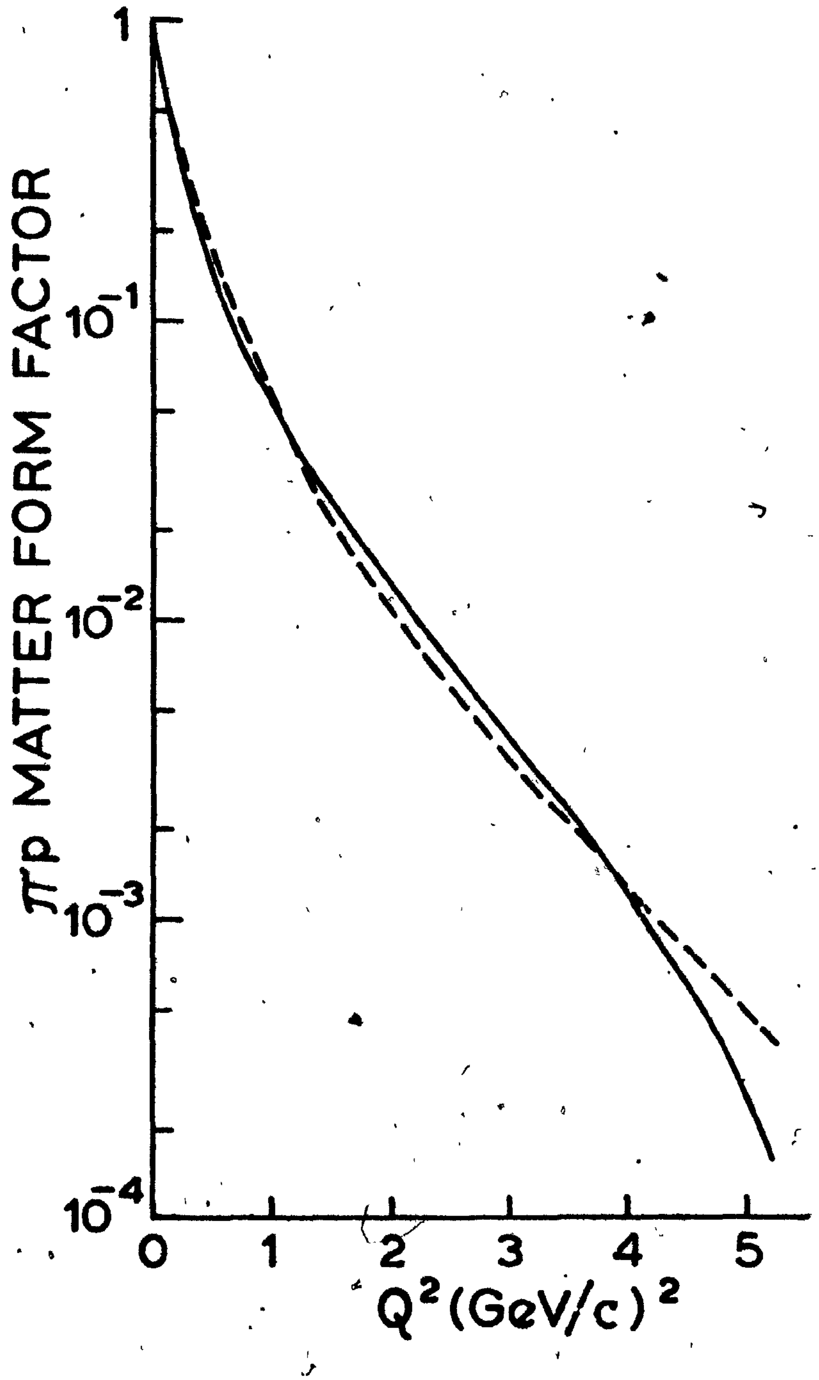

FIG. 5.4.

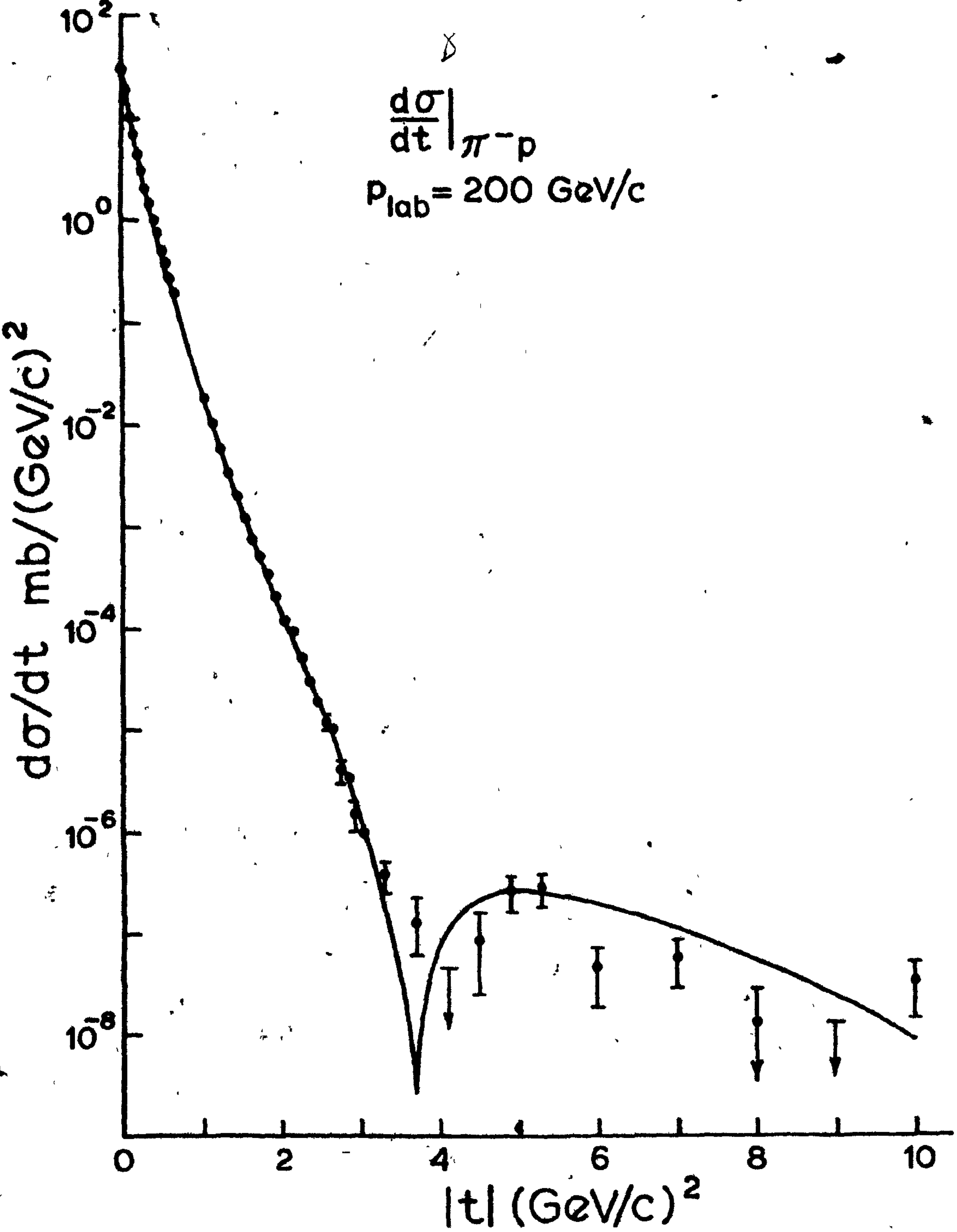

$\frac{d\sigma}{dt}\Big|_{\pi^- p}$
p_{lab} = 200 GeV/c
$d\sigma/dt$ mb/(GeV/c)^2
10^2
10^0
10^{-2}
10^{-4}
10^{-6}
10^{-8}
0
2
4
6
8
10
|t| (GeV/c)^2

FIG. 5.5.

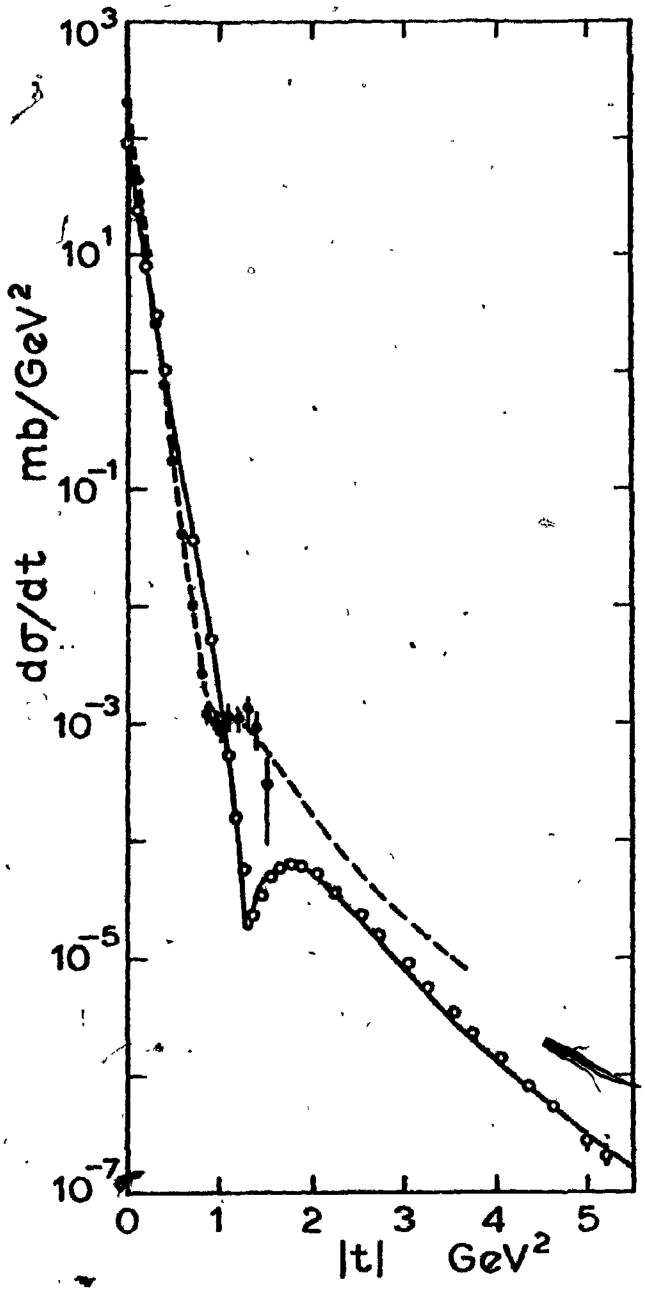

FIG. 5.6.

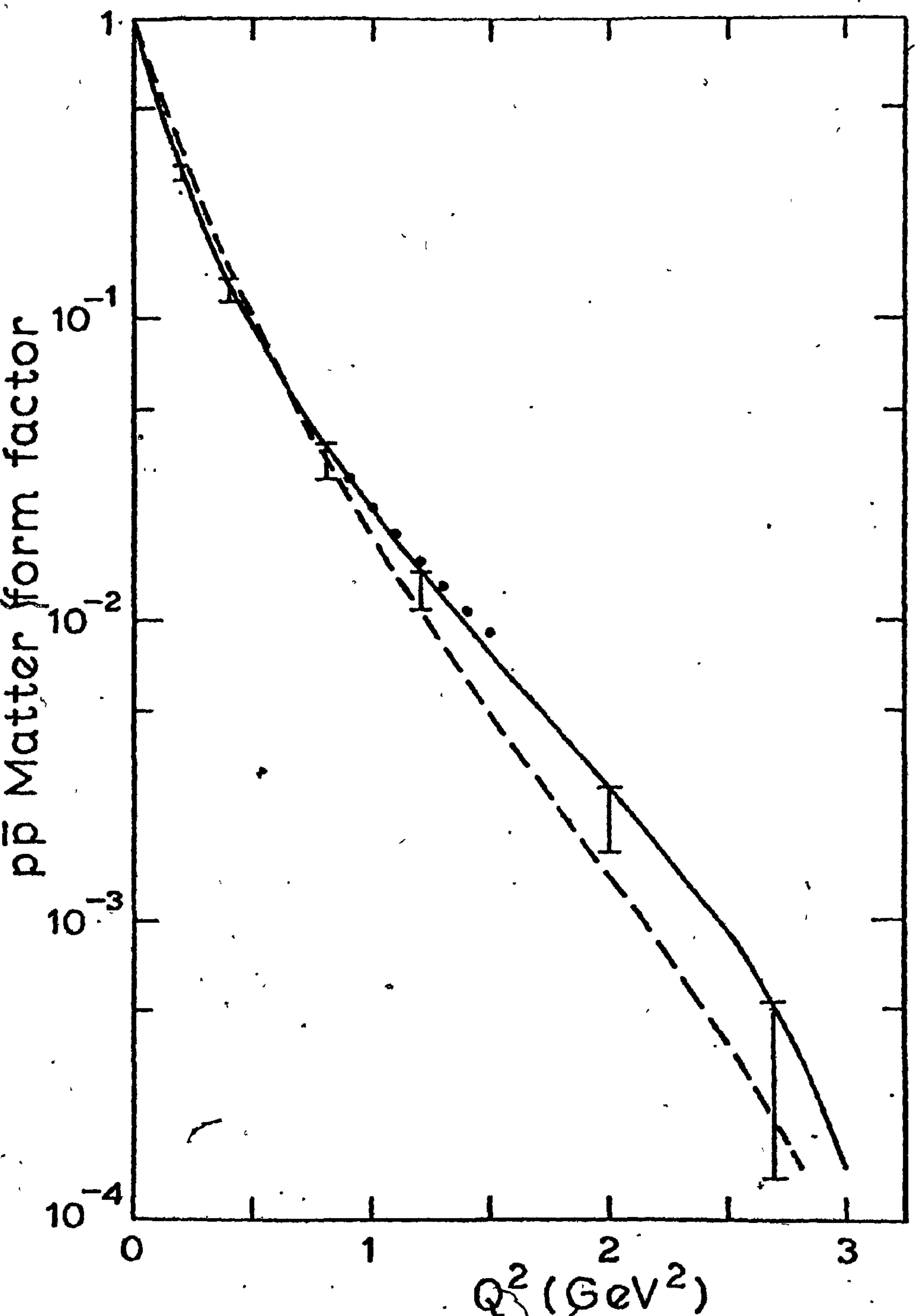

FIG. 5. 7.

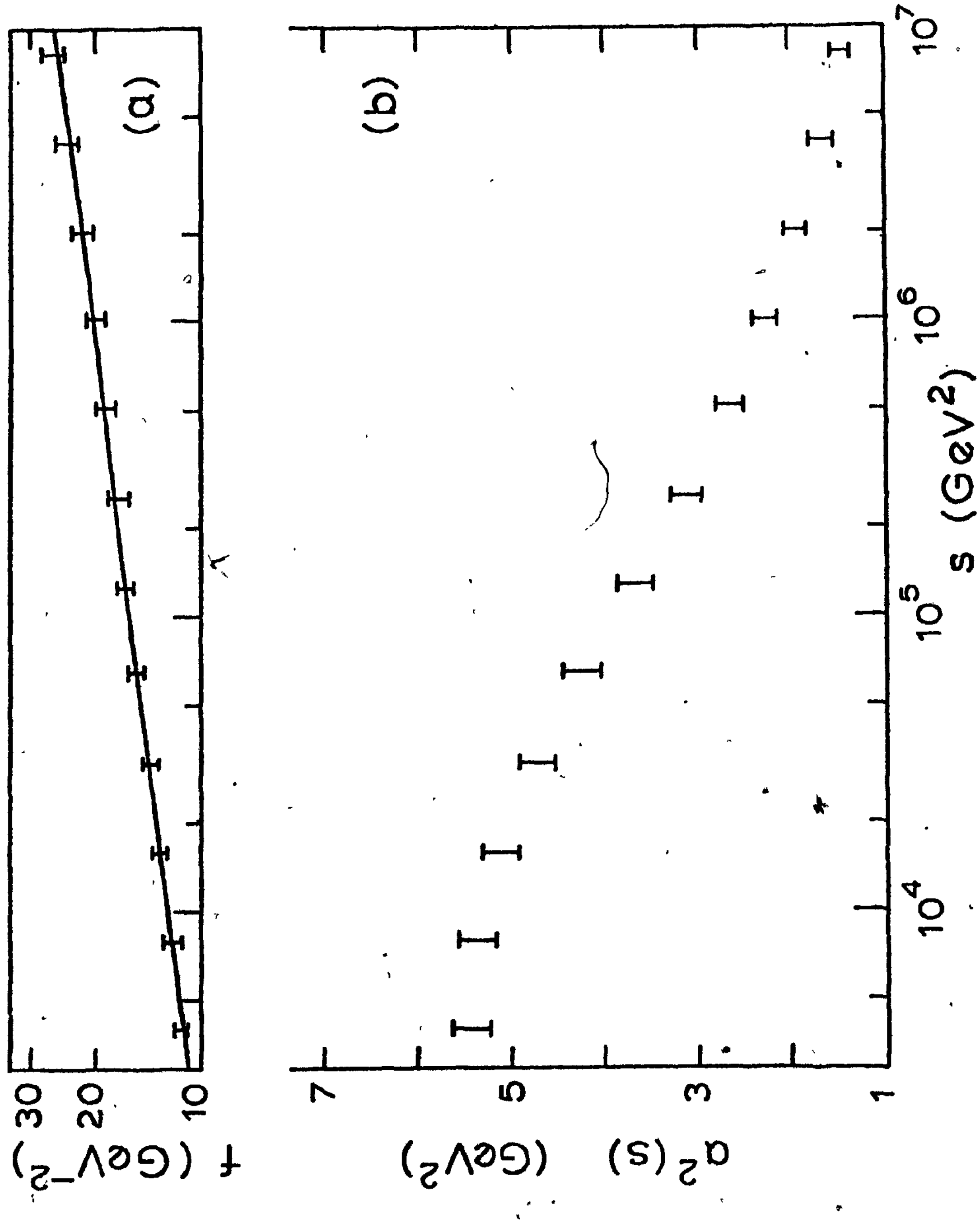

FiG. 5.8.

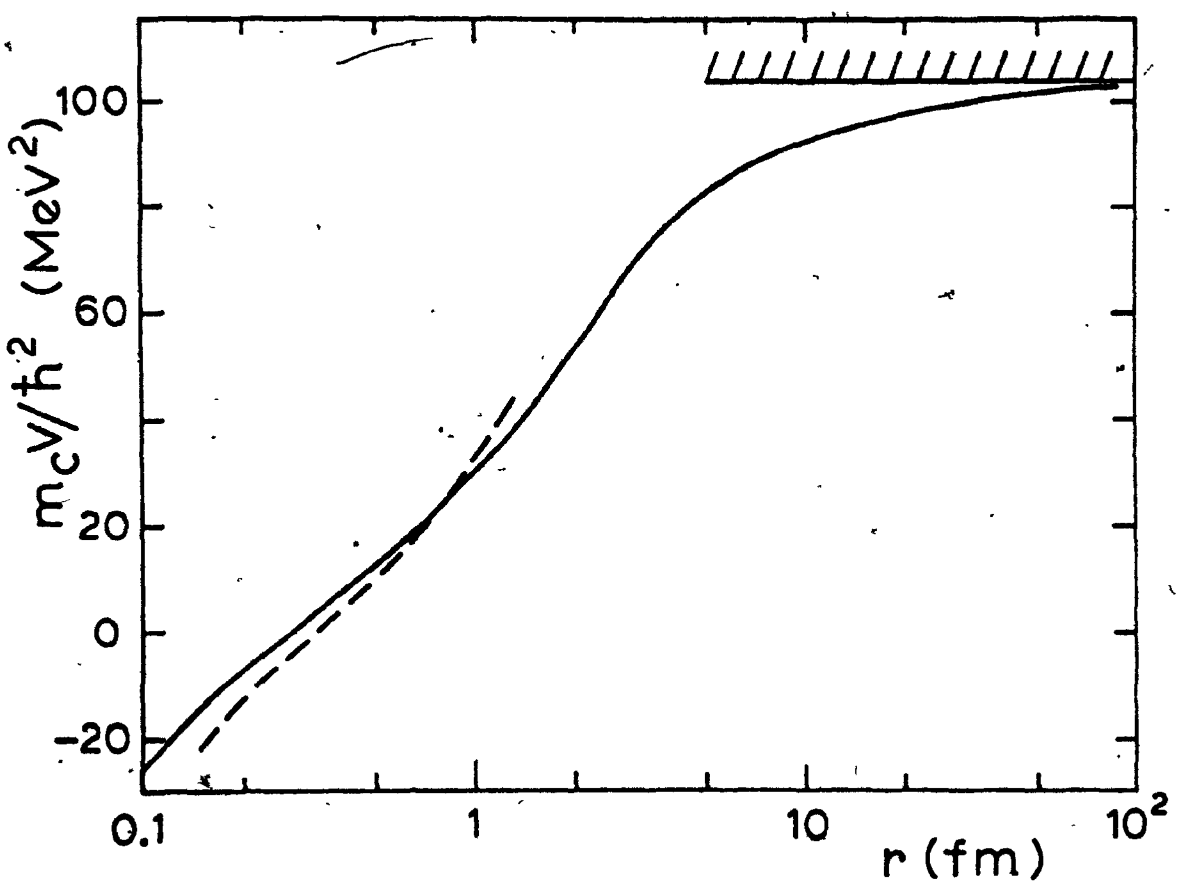

FIG. 6.1.

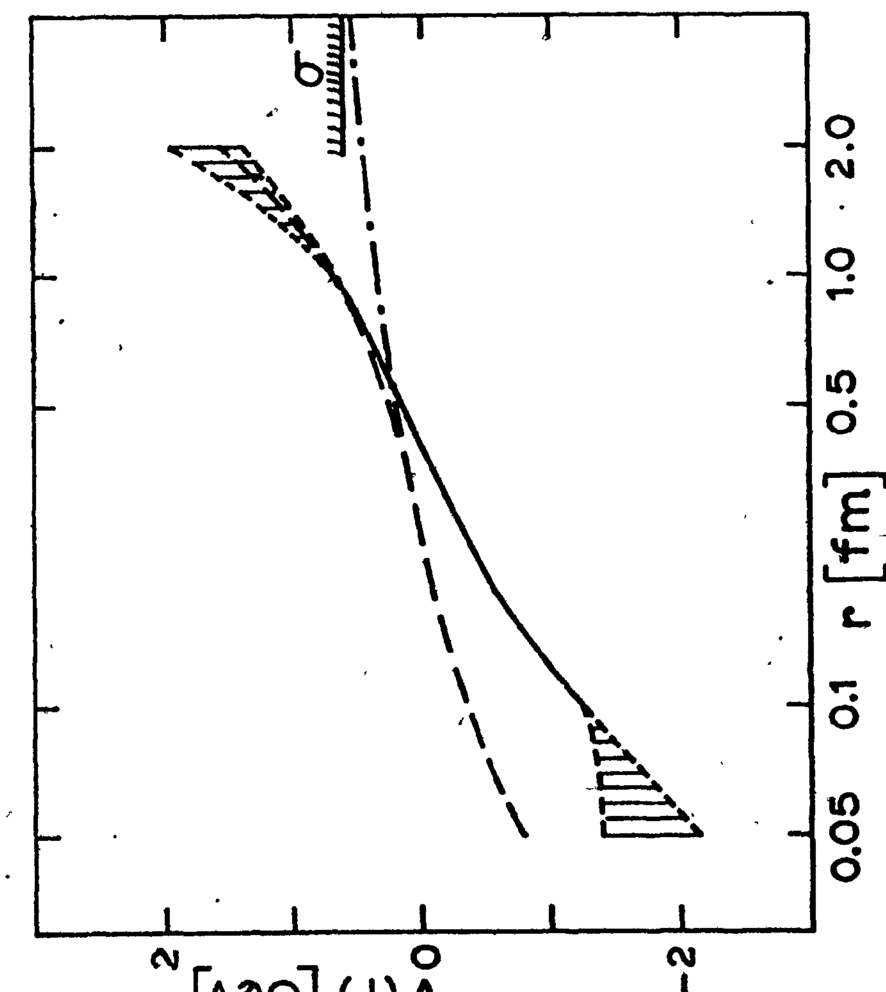

FIG. 6.2.

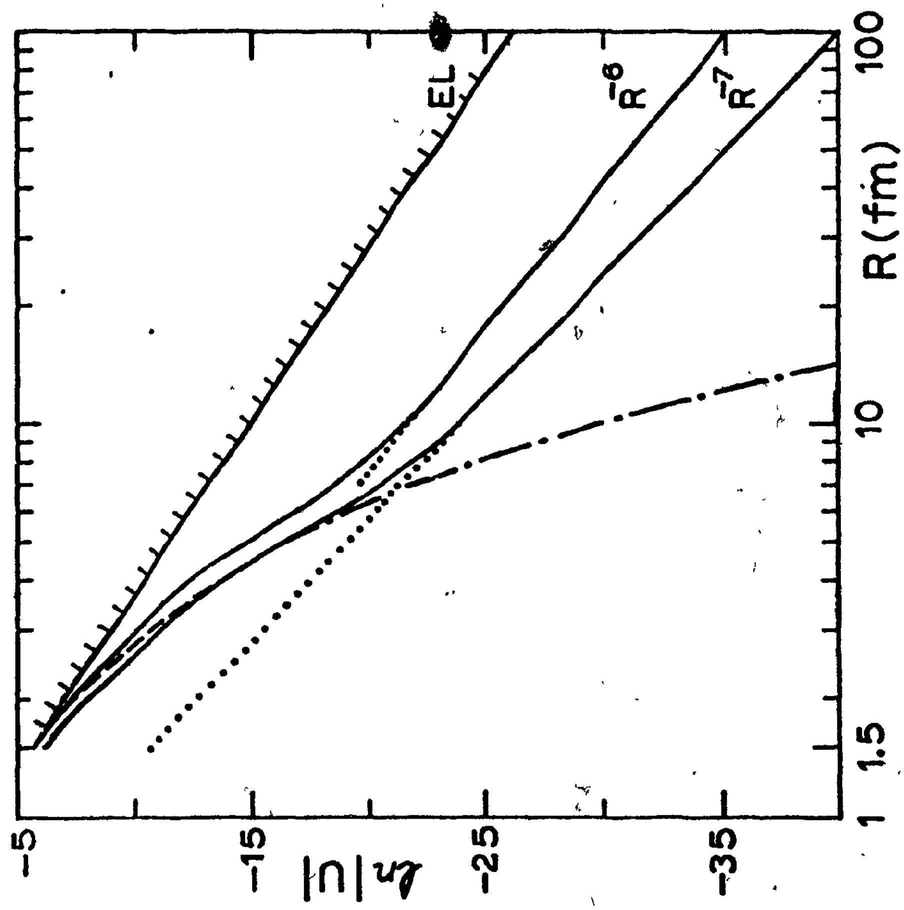

FIG. 6.3.

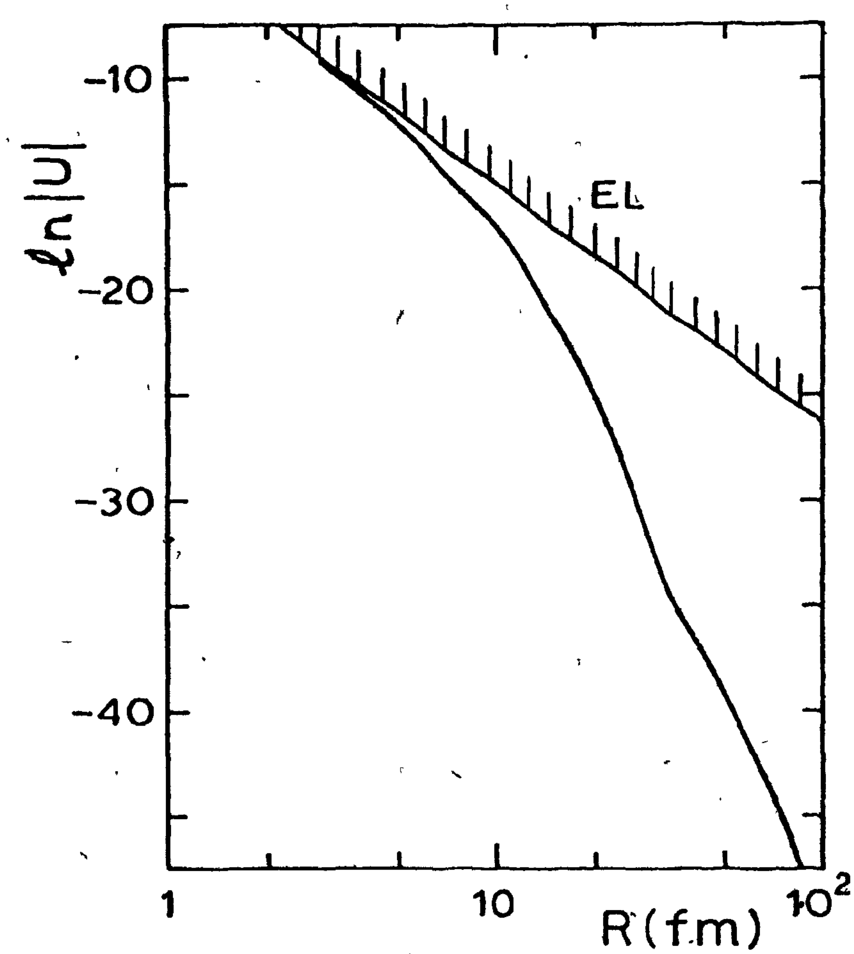

FiG. 6.4.

[37] R.P. Feynman and A.R. Hibbs, "Quantum Mechanics and Path Integrals" (McGraw-Hill, N.Y. 1965); P. Ramond, "Field Theory A Modern Primer" (Benjamin, Reading (Mass.) 1981).
In many texts (e.g. in Ramond's book) W[J] denotes the vacuum- to- vacuum functional and Z[J] the generating functional for connected Green's functions. We interchange these symbols to conform with the convention preferred in lattice gauge theories.

[38] G. Jona-Lasinio, Nuovo Cim. 34 (1964) 1790;
S. Coleman, in "Laws of Hadronic Matter", Proceedings of the Erice Summer School 1974 (Academic Press, N.Y. 1975).

[39] R. Jackiw, Phys. Rev. D9 (1974) 1686.

[40] S. Coleman and E. Weinberg, Phys. Rev. D7 (1973) 1888.

[41] S.G. Matinyan and G.K. Savvidy, Nucl. Phys. B156 (1979) 1;
M.J. Duff and M. Ramon-Medrano, Phys. Rev. D12 (1976) 3357;
H. Pagels and E. Tomboulis, Nucl. Phys. B143 (1978) 485.

[42] N.K. Nielsen and P. Olesen, Nucl. Phys. B144 (1978) 376 and Phys. Lett. 79B (1978) 304.

[43] N.K. Nielsen and P. Olesen, Nucl. Phys. B160 (1979) 380;
J. Ambjørn and P. Olesen, Nucl. Phys. B170 (1980) 60 and 265.